Genetic and biochemical characterization of YrkF, a novel two-domain sulfurtransferase in *Bacillus subtilis*

Jeremy Hunt

Thesis submitted to the faculty of

Virginia Polytechnic Institute and State University

in partial fulfillment of the requirements for the degree of

Master of Science

In

Biochemistry

Timothy J. Larson, Chair

Dennis R. Dean

Brenda J. Winkel

August 11, 2004

Blacksburg, Virginia

Keywords: YrkF, rhodanese, Ccd1, persulfide sulfur, disulfide cross-linking

Genetic and biochemical characterization of YrkF, a novel two-domain sulfurtransferase in *Bacillus subtilis*

Jeremy Hunt

Timothy J. Larson, Chair

Department of Biochemistry

ABSTRACT

Sulfur-containing compounds such as thiamin, biotin, molybdopterin, lipoic acid, and [Fe-S] clusters are essential for life. Sulfurtransferases are present in eukaryotes, eubacteria, and archaea and are believed to play important roles in mobilizing sulfur necessary for biosynthesis of these compounds and for normal cellular functions. The rhodanese homology domain is a ubiquitous structural module containing a characteristic active site cysteine residue. Some proteins containing a rhodanese domain display thiosulfate:cyanide sulfurtransferase activity *in vitro*. However, the physiological functions of rhodaneses remain largely unknown.

YrkF, the first rhodanese to be characterized from *Bacillus subtilis*, is a unique protein containing two domains, an N-terminal Ccd1 domain and a C-terminal rhodanese domain. Ccd1 (conserved cysteine domain 1) is a ubiquitous structural module characterized by a Cys-Pro-X-Pro sequence motif. Thus, YrkF contains two cysteine residues (Cys^{15} and Cys^{149}), one in each domain.

Biochemical, genetic, and bioinformatic approaches were used in order to characterize YrkF. First, YrkF was overexpressed and assayed for rhodanese activity to show that the protein is a functional rhodanese. A variant protein, $YrkF^{C15A}$, containing a cysteine to alanine substitution in the Ccd1 domain was created to determine if the Ccd1 cysteine is essential for rhodanese activity. The variant protein was overexpressed and rhodanese assays showed that $YrkF^{C15A}$ is also a functional rhodanese.

Inherent structural and catalytic differences were observed when comparing YrkF and $YrkF^{C15A}$, which may reflect the importance of the Ccd1 cysteine residue to normal enzymatic function and structural stability. Initial kinetic studies identified differences in activity between YrkF and $YrkF^{C15A}$. Cross-linking experiments showed a propensity for the formation of inter- and intramolecular disulfide bonds between the two cysteine residues and indicated that Cys^{15} and Cys^{149} are located near one another in the 3-dimensional structure of the protein. Analysis of the proteins by mass spectrometry suggested YrkF contains a stable persulfide sulfur, whereas $YrkF^{C15A}$ showed no evidence of a stable persulfide sulfur and was prone to oxidation and other active site modifications. A homology model of YrkF was created using structures of a rhodanese homolog and a Ccd1 homolog as templates. The model was used to predict the structure of YrkF based on the results of the cross-linking experiments. A strain containing a *yrkF* chromosomal deletion could be constructed, indicating YrkF is not essential for survival. Phenotypic analysis of the *yrkF* mutant revealed that YrkF is not needed for biosynthesis of sulfur-containing cofactors (thiamin, biotin, molybdopterin, or lipoic acid) or amino acids. The characterization of YrkF could lead to the discovery of novel physiological roles for rhodaneses and may give insight into possible roles for the Ccd1 module.

TABLE OF CONTENTS

LIST OF FIGURES

LIST OF TABLES

ACKNOWLEDGMENTS

I would like to extend my sincere gratitude to my advisor, Dr. Timothy J. Larson. From the day that I joined his lab, Dr. Larson has been completely dedicated to helping me obtain the goals I set out to achieve. Throughout my time here his guidance and kindness have given me the knowledge and confidence to successfully complete my studies. I am very grateful for the opportunity that was given to me because the education I received from my experience in his lab will stay with me always.

My graduate committee members, Dr. Dennis Dean and Dr. Brenda Winkel, have been equally important to my education. I would like to thank them for their suggestions and advice for improvements to my research. Their continual support and challenge of me to evaluate my research in greater depths have been a great learning experience.

I would also like to thank Janet Donahue. I do not think any of this would have been possible without her sincere compassionate for my wellbeing both personally and professionally. She has been a great example of how to conduct oneself in the most professional manner.

I also want to extend my thanks to the entire biochemistry department. Dr. John Hess and Dr. E. M. Gregory have been great educators and have been very supportive. I am also very grateful for all the help Dr. David Bevan has provided me in regards to my homology modeling and Keith Rays help with mass spectrometry.

Finally I would like to thank all of my friends and family. Your support and sincere friendship have made this all worthwhile. My hard work and dedication is merely a reflection of my parent's undying love for me. My work here is dedicated to them …Thank you.

CHAPTER ONE

Introduction

1.1. Chemistry of sulfur

Sulfur, the eighth most abundant element in the human body on a molar and absolute weight basis, is an essential element for life due in large part to its chemical versatility (1, 2). Some of the unique chemical properties of sulfur can be attributed to the availability of *d*-orbital electrons in its bonding. This feature of sulfur allows it to form long chains and therefore exist in many different allotropes (1, 3). Elemental sulfur is typically found in rings composed of eight sulfur atoms (S_8), which is the most stable allotrope (1). In fact, sulfur is never found as a single atom due to its tendency to readily form bonds with other atoms (2). The S–S bond is highly reactive to heat and radiation, but biologically-important processes typically involve bimolecular nucleophilic (S_N2) reactions with the S–S bond (3). Another characteristic of sulfur that can be attributed to the availability of *d* orbital bonding is its ability to exist in various valencies and oxidation states. Sulfur has valencies of 2, 4, and 6 and oxidation states of –2, 0, +2, +4, and +6 (3). The number of oxidation states available to sulfur allows it to form many oxyanions, including sulfate, sulfite and thiosulfate (3). These oxyanions are biologically active and play significant roles in cellular metabolism (1).

Sulfur is a critical component of proteins and coenzymes such as thiamin, biotin, molybdopterin, coenzyme A, and lipoic acid. Sulfur is found in protein and protein complexes as thiols (cysteine), as disulfides (cystine), thioethers (methionine), or as a constituent of iron-sulfur clusters (2, 4). The chemical activity of sulfhydryl groups and disulfides in proteins is essential to the activity of many enzymes. It has been reported

that nearly 40% of proteins lose activity when chemical reagents bind sulfhydryl groups, and disulfide bridges are important in the formation of the tertiary and quaternary structures of some proteins (1). Many human diseases can be attributed to deficiencies in enzymes involved in sulfur metabolism (5). Significant areas of research focus on trafficking of sulfur via sulfurtransferases and elucidating the pathways in which sulfur is incorporated into biologically-important molecules. Discoveries in these areas of research may lead to more efficient methods of vitamin production and the development of antimicrobial agents targeting essential pathways involved in sulfur metabolism.

1.2. Sulfane sulfur

1.2.1. Biological significance

Sulfur-containing compounds such as polysulfides (R-S-S_n, n > 2), thiosulfate (SSO_3^{2-}), polythionates ($^{2-}O_3S$-S_n-SO_3^{2-}), persulfides (R-S-S^-), and elemental sulfur (S_8) contain the highly-reactive, biologically-important sulfane sulfur atom (S^0) (Figure 1.1) (2, 6, 7). Sulfane sulfur atoms are sulfur atoms covalently bound in chains to other sulfur atoms and have an apparent oxidation state of 0. Though sulfane sulfur has a valence of 0 or –1, they are often incorrectly termed "zero valence sulfur" (7). S^0 readily reacts with cyanide and is frequently referred to as "cyanolyzable sulfur" (6, 7). S^0 is the form of sulfur that is believed to be incorporated into many biological compounds, including biotin, thiamin, and thiol-modified tRNA (2).

It has also been suggested that S^0 plays a significant role in cellular regulation (7), carcinogenesis (7, 8), and as an antioxidant (6). The generation of S^0 by known metabolic pathways such as the desulfydration of cyst(e)ine by cystathionase and the

conservation of S^0 carrier proteins in many species gives evidence that supports S^0 as an important component of cellular regulatory processes (7). Moreover, many of the regulatory effects observed *in vitro* occur at low concentrations of S^0 and this evidence further support its role in cellular regulation (6, 7). It is believed that the covalent modification of sulfhydryl groups in proteins by S^0 can lead to either their activation or inactivation (6, 7). Evidence has also shown that many neoplastic cell lines have no cystathionase activity, which in turn decreases the production of S^0 for the sulfane sulfur pool (7, 9). The proliferation of these carcinogenic cells is thought to occur due the uncontrolled activity of certain proteins that would normally have been inactivated in the presence of S^0 (7). Other studies have documented the ability of diallyl disulfides to inhibit the proliferation of human cancer cell lines in culture (8). The double bond characteristic of diallyl disulfides allows for tautomerization and the formation of a thiosulfoxide containing a S^0, which serves as a source of S^0 for cellular regulation (Figure 1.1) (6, 8).

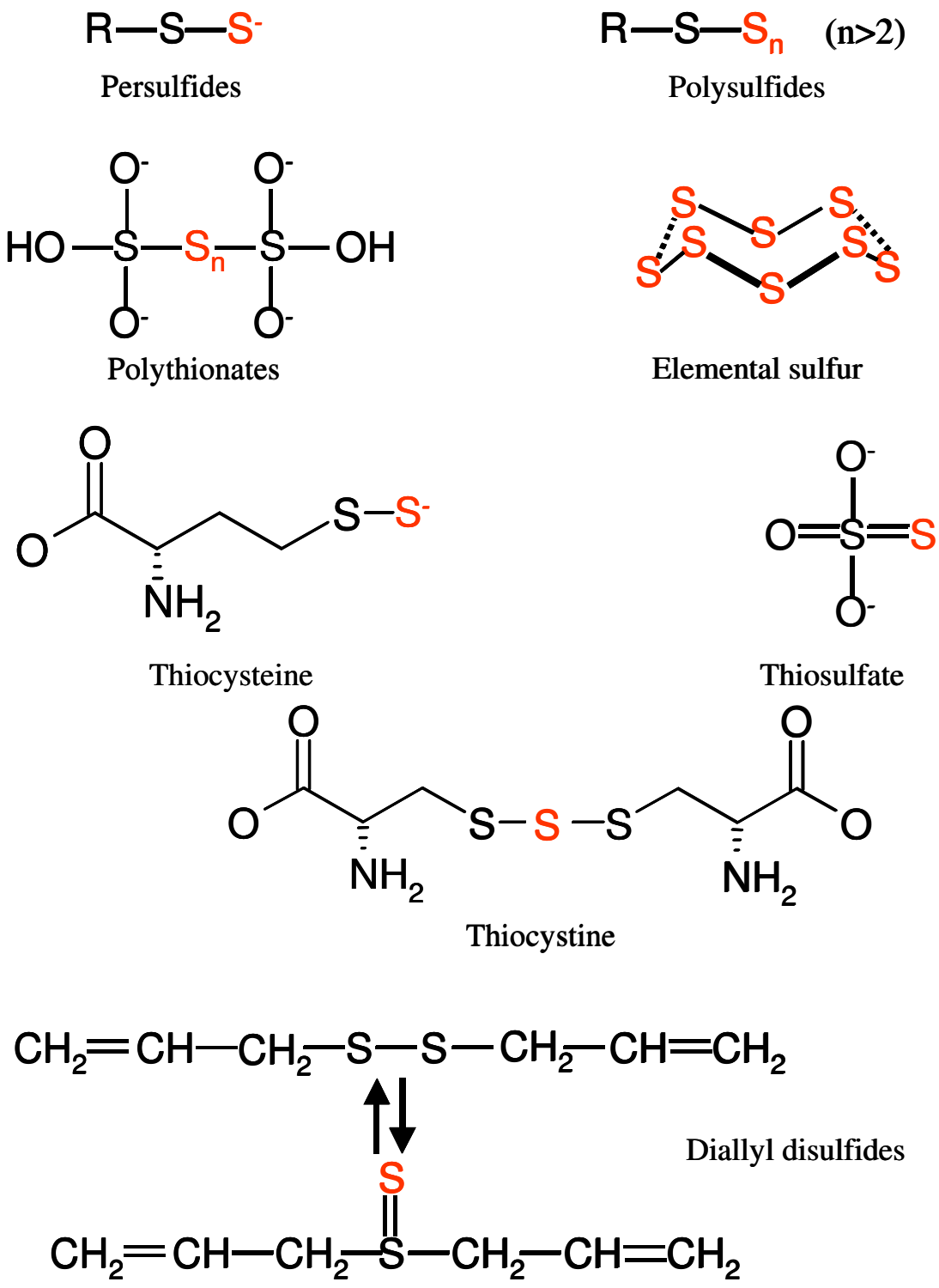

FIG. 1.1. Sulfane sulfur-containing compounds.

The sulfane sulfur atom(s) in each compound is highlighted in red.

1.2.2. S^0 carrier proteins

Many enzymes have been characterized as sulfane sulfur carrier proteins. Examples of proteins that have been well studied include 3-mercaptopyruvate sulfurtransferases, rhodaneses, and cystathionase. These proteins are distributed throughout life and allow for the transport of the highly reactive S^0 atom around the cell by forming stable protein-sulfur complexes (7). Mercaptopyruvate sulfurtransferases catalyze the transfer of sulfur from 3-mercaptopyruvate to cyanide, sulfite, or sulfonates and sulfhydryl groups of proteins *in vitro*, generating a persulfide intermediate (6, 7). Rhodaneses are ubiquitous proteins that are characterized by their *in vitro* transfer of the sulfane sulfur from thiosulfate to cyanide generating thiocyanate and sulfite (10). Cystathionase catalyzes the reactions (1 and 2) listed below:

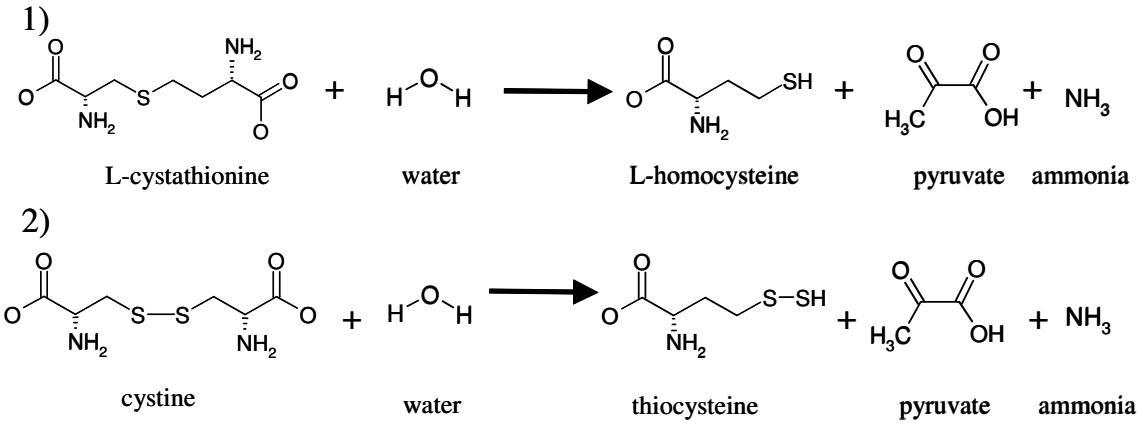

These reactions catalyzed by cystathionase are involved in cysteine and sulfur metabolism and may be important in the generation and maintenance of the sulfane sulfur pool in the cell (7). All three enzymes carry S^0 as cysteine persulfides or a persulfide derivative. Cystathionase has been shown to carry S^0 in a stable trisulfide between two cysteine residues (7). Szczepkowski and Wood showed that cystathionase and rhodanese

could be coupled *in vitro* to form an enzyme system that can transfer sulfur from cysteine to cyanide, sulfite, or other compounds (11). In one pathway for the desulfuration of cysteine, cysteine is spontaneously converted to cystine, which is then utilized by cystathionase in the generation of thiocysteine (reaction 2). Thiocysteine can then be converted to the more stable thiocystine (6). Thiocystine is a substrate for rhodanese and transfers its persulfide sulfur to the rhodanese active site cysteine (11, 12). Thiocysteine has actually been shown to be a more efficient substrate for rhodanese than thiosulfate (12). This evidence suggests that the two enzymes are coupled in a transsulfuration system that utilizes thiocystine generated from cysteine as an intermediate source of sulfane sulfur (11).

1.2.3. Cysteine desulfurase

Labeling studies have revealed that L-cysteine is the source of sulfur that is incorporated into a number of important vitamins and macromolecules, including biotin, thiamin, molybdopterin, lipoic acid, thionucleosides of tRNA, and [Fe-S] clusters (13). It is currently believed that sulfur mobilization in the cell is initiated by the homodimeric enzyme cysteine desulfurase, which represents another example of a S^0 carrier protein (13). Cysteine desulfurase is a pyridoxal 5'-phosphate (PLP)-dependent enzyme that catalyzes the conversion of L-cysteine to L-alanine and in turn generates sulfane sulfur in the form of an enzyme-bound cysteine persulfide (13). The sulfane sulfur atom is then incorporated into essential sulfur-containing compounds through pathways that are not yet fully elucidated.

Cysteine desulfurases were first studied in the nitrogen fixation (*nif*) gene cluster of *Azotobacter vinelandii* (13, 14). *nifS* encodes the homodimeric, PLP-dependent NifS cysteine desulfurase that is involved in the synthesis of [Fe-S] clusters specifically for the nitrogenase enzyme. The desulfuration of L-cysteine catalyzed by NifS generates of an enzyme-bound cysteine persulfide, which serves as the ultimate sulfur source for the specific [Fe-S] clusters essential for the activity of nitrogenase (15-17). *A. vinelandii* encodes a protein homologous to NifS named IscS (18). IscS is a cysteine desulfurase involved in the maturation of [Fe-S] clusters within proteins that are part of general cellular processes and is known to be essential as knockouts of the gene are lethal (17, 18). *Escherichia coli* contains three enzymes that exhibit cysteine desulfurase activity, IscS, CsdA/CSD, and CsdB/SufS (19-21). IscS of *E. coli* is 40 % identical in sequence to *A. vinelandii* NifS, whereas CsdA/CSD and CsdB/SufS are less than 30 % identical.

Cysteine desulfurases have been divided into two groups (I and II) based on the amino acid sequence surrounding the conserved active site cysteine residue (13, 20). Those with a consensus sequence similar to NifS and IscS of *A. vinelandii* and *E. coli* IscS (SSGSACTS) are characterized as group I cysteine desulfurases. Cysteine desulfurases with a consensus sequence similar to CsdA/CSD and CsdB/SufS of *E. coli* (RxGHHCA) are characterized as group II (13).

Cysteine desulfurases contain a specific cysteine residue that is essential for activity (15). The mechanism for cysteine desulfuration is initiated when the cysteine substrate forms a Schiff base with PLP. The sulfur atom of the substrate cysteine is subsequently transferred to the active site cysteine residue. Thus, the enzyme generates L-alanine and contains an active site cysteine persulfide intermediate (22). In the case of

IscS from *E. coli*, the persulfide sulfur can be released as either sulfane sulfur (S^0) or as sulfide (S^{2-}) (in reducing conditions), and can serve as a sulfur source for a variety of cofactors and thiolated tRNAs (23-27).

The structures of NifS/IscS paralogs, *Thermotoga maritima* NifS, *E. coli* CsdB/SufS, and recently *E. coli* IscS, have been solved (27-30). The overall structures of the cysteine desulfurases are very similar including the active site pocket containing the PLP cofactor. However, the structure of the loop containing the conserved active site cysteine varies in the enzymes (27-30). The region of NifS from *T. maritima* that contains the catalytic cysteine was disordered and the electron density of the loop could not be mapped (27, 30). The disordered refraction data observed in the region containing the catalytic cysteine suggested the loop was highly flexible. Consequently, this would allow the enzyme to catalyze the desulfuration of cysteine as well as transfer the persulfide sulfur to other proteins (27, 30).

The catalytic cysteine of *E. coli* IscS was determined to be located at least 17 Å from the PLP cofactor (27). Due to the large distance between this cysteine and PLP, a large conformational change would have to occur for IscS to catalyze the desulfuration of cysteine. Therefore, it was suggested that the active site loop containing cysteine in *E. coli* IscS was also highly flexible (27).

In contrast, the catalytic cysteine of CsdB is located deep within the enzyme in the active site pocket containing the PLP cofactor and shielded from solvent (27-29). The cysteine residue is not part of a flexible loop region and is held in place near the PLP cofactor. However, the 7 Å separating the catalytic cysteine residue from the PLP cofactor is thought to be too large a distance to allow efficient catalysis of the

desulfuration of cysteine (28, 31). It has been hypothesized that the lower cysteine desulfurase activity associated with SufS may be a consequence of the differences in structures and may indicate different catalytic mechanisms for the various NifS homologs (27). Recent studies now show that the cysteine desulfurase activity of SufS can be stimulated by binding of a protein encoded within the same operon, SufE (31, 32) (see section 1.4.1).

1.3. Sulfurtransferases

1.3.1. Thiosulfate:cyanide sulfurtransferase (rhodanese)

In 1933 an enzyme was characterized that catalyzed the transfer of sulfur from thiosulfate to cyanide, forming thiocyanate. The enzyme was named rhodanese from the German word for thiocyanate, *Rhodanid*, by Lang (33). Rhodanese (thiosulfate: cyanide sulfurtransferase EC 2.8.1.1) has become one of the better-characterized sulfurtransferases. The rhodanese homology domain is a ubiquitous structural module found in a variety of proteins (34, 35) (Figure 1.2). It was originally proposed that rhodaneses were involved in the detoxification of cyanide because these enzymes convert cyanide to the less toxic thiocyanate and were found at high concentrations in mitochondria (36). However, since rhodaneses are known to be ubiquitous enzymes and to be associated with a variety of functional domains, it has been suggested that they are involved in a wide range of cellular functions (34, 35) (Figure 1.2).

The rhodanese homology domain is comprised of an active site fold, containing a conserved cysteine residue, flanked by two structural motifs, CH2A and CH2B (37). Proteins containing the rhodanese module are found in a variety of different domain

architectures (34, 35) (Figure 1.2). Several well-characterized rhodaneses are comprised of a functional rhodanese domain fused to a structurally identical, non-functional rhodanese domain (34, 35, 38). Rhodaneses have also been isolated as single-domain proteins and have been found as modules associated with proteins of a variety of functions (39) (Figure 1.2).

The 297 amino acid rhodanese from *Bos taurus* is the best-characterized of the rhodaneses (40, 41). Bovine rhodanese catalyzes the transfer of sulfane sulfur from thiosulfate to cyanide via a double-displacement (ping-pong) mechanism involving the formation of a cysteine persulfide at the active site (Figure 1.3). Crystallographic studies reveal that bovine rhodanese is comprised of two domains of identical α/β topology (42, 43). Though there is limited sequence identity between the two domains, both display a structure consisting of a central five-stranded β-sheet surrounded by α-helices. The N-terminal domain is not catalytically active, whereas the active site Cys^{247} is located in the C-terminal domain. Cys^{247} can accept a sulfur from thiosulfate, forming a persulfide intermediate, and the enzyme cycles between this form and a sulfur-free form during its catalytic mechanism (43). The two forms of the enzyme (sulfur-free and persulfide) have no significant structural differences (44). However, the persulfide form of rhodanese is more resistant to oxidation (45).

Azotobacter vinelandii RhdA is a well-characterized example of a bacterial rhodanese. RhdA is similar to bovine rhodanese in that it contains a functional (C-terminal) and non-functional (N-terminal) domain. The amino acid composition of the active site loop is a major point of difference between RhdA and bovine rhodanese. The active site sequence of RhdA is CQTHHR, whereas the sequence for bovine rhodanese is

CRKGVT (35). In fact, the amino acid composition of the active site loop varies considerably among rhodanese homologs (Figure 1.4 A). However, the amino acid composition does not appear to affect the mechanism of sulfur transfer as RhdA also displays a ping-pong catalytic mechanism (46).

The crystal structure of RhdA has features similar to those of bovine rhodanese as well (35). RhdA is comprised of two identical rhodanese domains consisting of a central β core flanked by α helical structures, which are connected by a 17 amino acid linker peptide. The catalytic Cys^{230} is located in the C-terminal domain within a six amino acid active-site loop. This loop forms a "cradle-like" shape that creates a shallow pocket near the surface of the protein and houses a stable persulfide sulfur (35). Unlike bovine rhodanese, RhdA is isolated containing a stable active site persulfide even when purified in the absence of thiosulfate. The six main chain amide groups of the active site loop point towards the persulfide sulfur and may serve to stabilize this form of the enzyme. Soaking the native form of RhdA in cyanide removes the persulfide sulfur, which changes the conformation of the catalytic Cys^{230} as well as Trp^{195} and partially inactivates the enzyme (35). These results suggest that the native, active form of the enzyme contains an active-site persulfide that accepts the sulfur from thiosulfate (35). This would lead to a catalytic mechanism in which a polysulfide was formed on the active-site cysteine and would be consistent with a previously hypothesized mechanism for bovine rhodanese (47).

Until recently the rhodanese fold had not been observed in any other proteins. However, the catalytic domains of the cell-cycle control phosphatases Cdc25A and Cdc25B are found to contain a 3-dimensional structure identical to rhodaneses (34, 37).

The location of the conserved catalytic cysteine residue in both rhodanese and Cdc25A/B is also conserved (34). The active site loop of the Cdc25 phosphatase enzymes consists of seven amino acids, compared to six amino acids for rhodaneses, most likely to accommodate the larger phosphorous atom (34).

Though the first rhodaneses characterized consisted of two identical domains, the elucidation of entire genomes from a variety of organisms has revealed that rhodaneses can be found in a number of different domain architectures. The presence of single-domain rhodanese homologs supports the hypothesis that the duplication of an ancestral rhodanese gene gave rise to the two-domain rhodaneses (10, 34, 39). Rhodaneses such as GlpE (10) and PspE (48) of *E. coli* demonstrate that a second N-terminal domain is not necessary for catalysis. Therefore, a single-domain rhodanese module in a protein may play an important role in the activity of the enzyme. This assertion is supported by known examples, including YbbB (49) and ThiI of *E. coli* (50) and human MOCS3 (51) where it has been shown that the rhodanese domain of each protein is necessary for their respective activities.

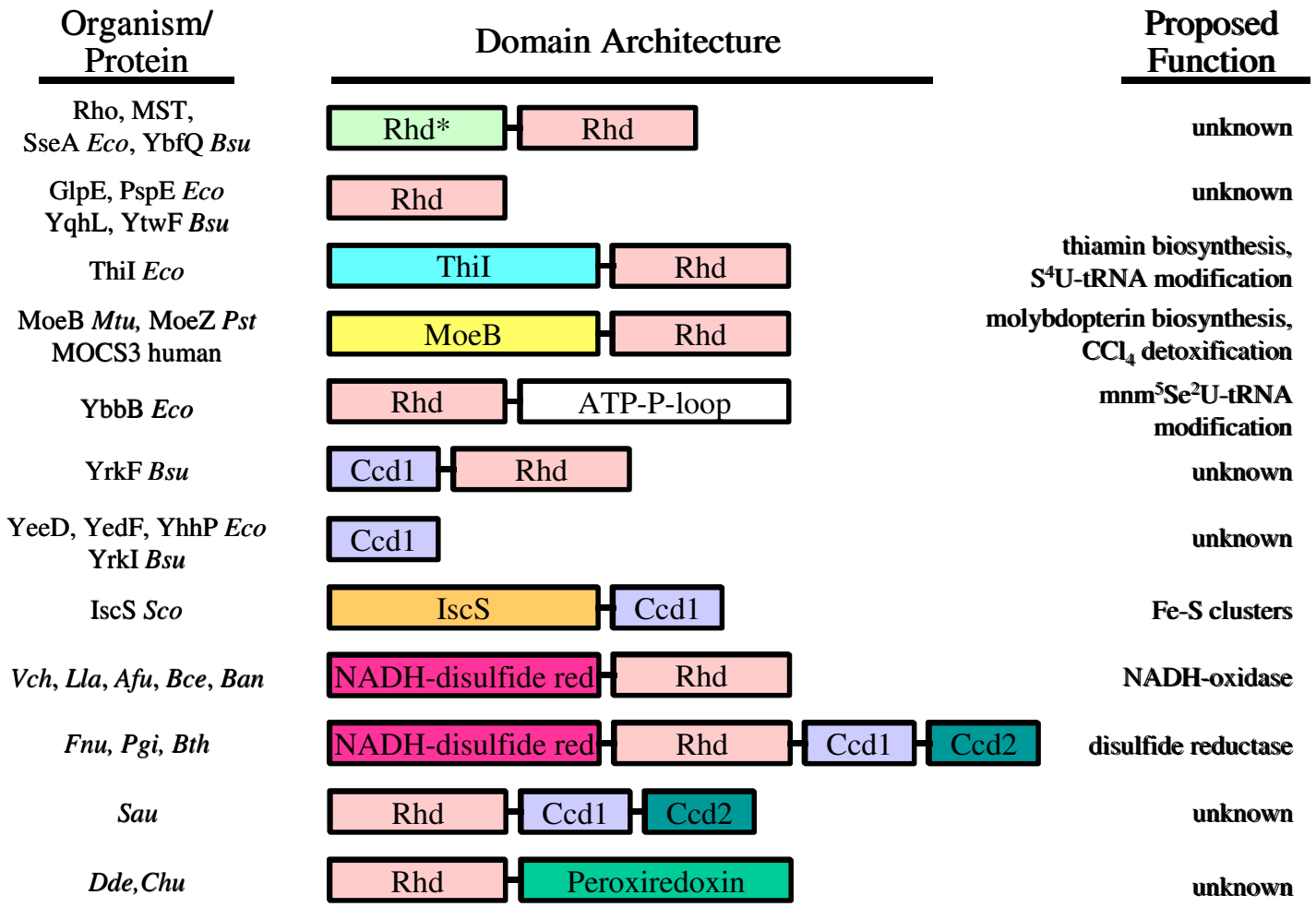

FIG. 1.2. Domain architecture of various rhodanese and Ccd1 proteins.

Rhd, catalytic rhodanese domain; Rhd*, pseudorhodanese domain; Ccd1, conserved cysteine domain 1; Ccd2, similar to predicted peroxiredoxins. *Eco*, *E. coli; Bsu*, *B. subtilis; Mtu*, *Mycobacterium tuberculosis*; *Pst*, *Pseudomonas stutzeri*; *Sco*, *Streptomyces coelicolor*; *Vch*, *Vibrio cholera*; *Lla*, *Lactococcus lactis*; *Afu*, *Archaeoglobis fulgidus*; *Ban, Bacillus anthracis*; *Fnu*, *Fusobacterium nucleatum*; *Pgi*, *Porphyromonas gingivalis*; *Bth*, *Bacteroides thetaiotaomicron*; *Sau*, *Staphylococcus aureus*; *Dde*, *Desulfovibrio desulfuricans*; *Chu*, *Cytophaga hutchinsonii*

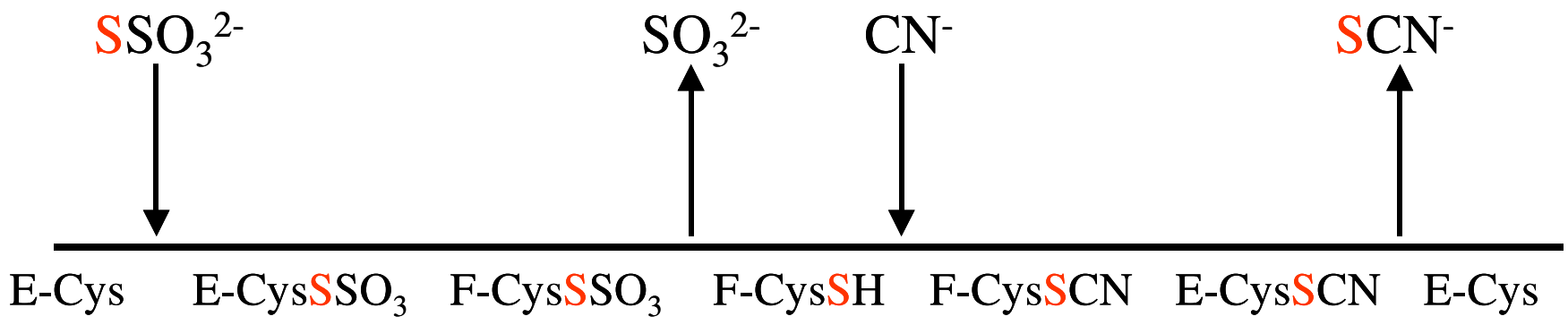

FIG. 1.3. Sulfane sulfur transfer from thiosulfate to cyanide catalyzed by rhodanese.

The Cleland diagram shows the double displacement mechanism characteristic of rhodaneses. Sulfane sulfur atom is shown in red. E-Cys, catalytic cysteine of the native rhodanese enzyme; F-Cys, rhodanese enzyme with bound substrate(s)

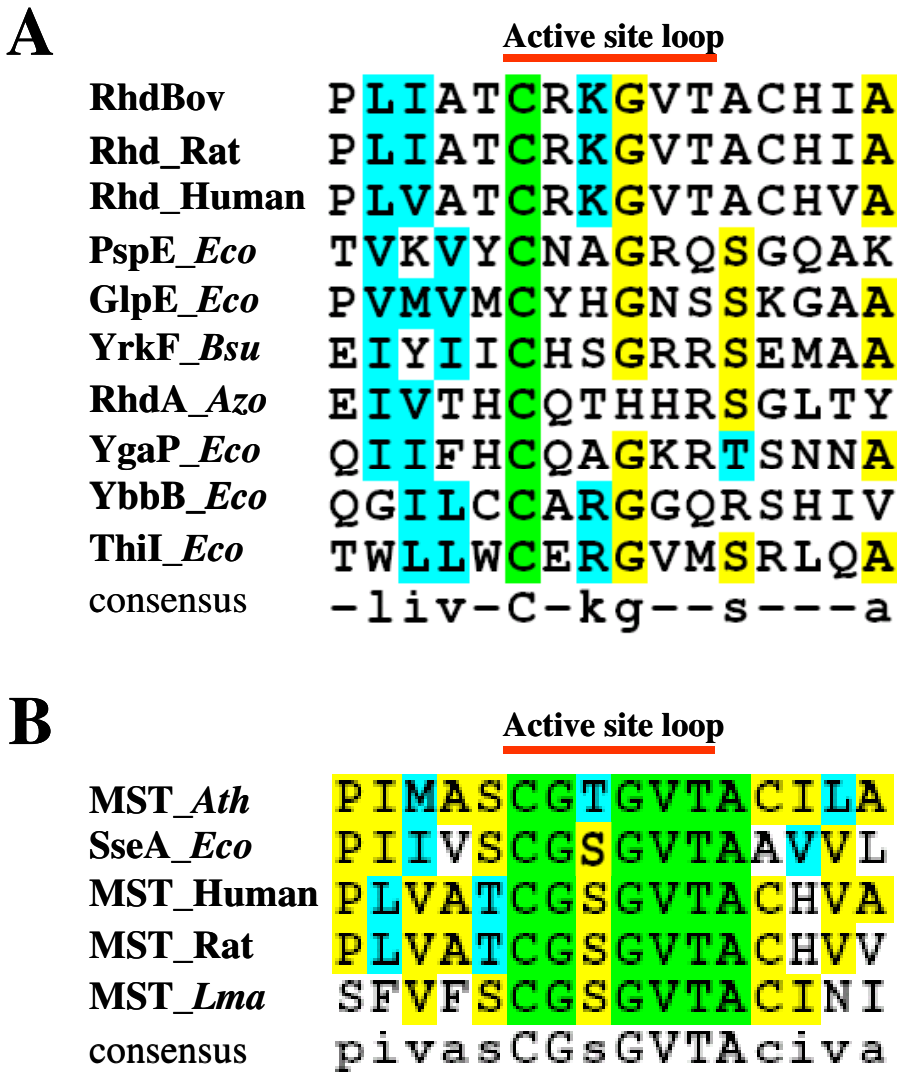

FIG. 1.4. Sequence alignment of rhodanese and MST active sites.

The active site residues of various rhodanese (A) and MSTs (B) were aligned using CLUSTALW and visualized using BOXSHADE. Green, completely conserved residues; Yellow, identical residues; Cyan, similar residues; White, different residues. (A) RhdBov (*B. taurus*, M58561), Rhd_Rat (*R. norvegicus*, P24329), Rhd_Human (*H. sapiens*, Q16762), PspE_*Eco* (*E. coli*, P23857), GlpE_*Eco* (*E. coli*, M96795), YrkF_*Bsu* (*B. subtilis*, CAB14594), RhdA_*Azo* (*A. vinelandii*, P52197), YgaP_*Eco* (*E. coli*, P55734), YbbB_*Eco* (*E. coli*, F64781), ThiI_*Eco* (*E. coli*, NP_414957). (B) MST_*Ath* (*A. thaliana*, CAB64716), SseA_*Eco* (*E. coli*, JX0320), MST_Human (*H. sapiens*, P25325), MST_Rat (*R. norvegicus*, P97532), MST_*Lma* (*L. major*, CAC85741).

1.3.2. Mercaptopyruvate sulfurtransferase (MST)

Mercaptopyruvate sulfurtransferase (MST) (EC 2.8.1.2) catalyzes the transfer of sulfur from mercaptopyruvate to a variety of thiophilic compounds that include cyanide, sulfite, and thiols (52). The physiological roles of MSTs are currently unknown and widely speculative (53). Though not as extensively characterized as the sulfurtransferase rhodanese, MSTs from rat liver (54), *Arabidopsis thaliana* (55), *E. coli* (53, 56), and *Leishmania major* (57, 58) have been studied. Kinetic studies of MSTs and rhodaneses show MSTs transfer sulfur through a sequential mechanism (59), whereas rhodaneses do so through a ping-pong mechanism (41).

The amino acid sequence of MSTs is related to rhodanese (up to 66% ID) and both MSTs and rhodaneses contain a six amino acid active site loop that begins with a catalytic cysteine residue (54). However, MSTs show little variability in the amino acid composition of the active site loops and are characterized by the consensus CG[S/T]GVT (53) (Figure 1.4 B). This is in contrast to rhodaneses, which tend to show substantial variability in the active site loop sequences (35) (Figure 1.4 A). Mutagenetic studies of the MST and rhodanese active sites reveal that changes in key residues can partially shift substrate specificities of the enzymes (i.e. an altered rhodanese displays MST activity, and *vice versa*) (54, 60). The substitution of the active site serine in rat liver (54) and *E. coli* (60) MSTs to lysine resulted in conversion to a more rhodanese-like activity. Recently, solved structures of *E. coli* (53) and *L. major* MSTs (57) revealed 3-dimensional folding similar to rhodaneses and allowed for comparison of structure-function relationships between rhodaneses and MSTs.

E. coli MST (SseA), solved to a resolution of 2 Å, consists of two identical rhodanese-like domains (53). Each domain is composed of a central β-sheet structure surrounded by α-helices. In the structure, the catalytic Cys^{237} appears to contain a bound persulfide sulfur. However, this is likely an artifact of the high concentration of $Na_2S_2O_3$ required for crystallization. Mass spectral and fluorescent studies indicate SseA does not maintain a stable persulfurated form, and the amino acid composition of the active site would not stabilize a persulfide sulfur (53, 56). The active site loop of SseA does not form the "cradle-like" shape observed in rhodaneses (38) and the Cys^{237} is shielded from solvent in one of at least two different conformations. The two different forms of the enzyme observed varied in the conformation of loop 61-67 and were named "open" and "closed" based on the solvent accessibility of Cys^{237} (53). The different forms of SseA observed might give insight into the catalytic mechanism of MSTs and explain why a ping-pong mechanism is not observed. The open form of loop 61-67 may allow Cys^{237} access to 3-mercaptopyruvate, which then can form a covalent thiosulfoxide at the active site. The sulfur would then be transferred to a nucleophilic molecule in a sequential manner (53).

The structure of *L. major* MST shows that the enzyme contains three domains. The N-terminal and central domains have structures similar to rhodanese and *E. coli* MST, with the active site Cys^{253} located within the central domain. The C-terminal domain consists of about 80 amino acids and its function is unknown (57). However, proteins with a C-terminal truncation are not stable because of an inability to fold correctly (58). The solved structure contains a sulfite molecule bound in the active site and persulfides on Cys^{253} and Cys^{331}. These modifications most likely resulted from

crystallization in buffer containing thiosulfate, as was done for SseA. However, the active site loop of *L. major* MST could possibly stabilize an active site persulfide, unlike SseA (57). The structure also reveals that the amino acids Gly^{254} and Ser^{255} (corresponding to bovine rhodanese Arg^{248} and Lys^{249}, respectively) may be important residues in determining the activity of the enzyme. Conversion of rhodanese Arg^{248} and Lys^{249} to glycine and serine increases the MST activity of rhodanese (59), and, as previously mentioned, conversion of the MST active-site serine to lysine results in an increase in rhodanese activity (54, 60).

1.4. Biosynthesis of sulfur-containing compounds

1.4.1. [Fe-S] clusters

[Fe-S] clusters (Figure 1.5) are important prosthetic groups that function in a number of biological roles (17, 61). [Fe-S] clusters are associated with proteins that function in many different cellular activities including electron transfer, gene regulation, and environmental signaling, and even participate in maintaining the structural integrity of some proteins (17, 61). Several distinct systems of [Fe-S] cluster assembly have now been identified and include the NIF (**ni**trogen **f**ixation), ISC (**i**ron-**s**ulfur **c**luster), and SUF (mobilization of **su**l**f**ur) machinery (14, 19, 62).

The first [Fe-S] cluster assembly system described began with the characterization of two gene products of the *nif* gene cluster in *A. vinelandii* (14). NifS is a PLP-dependent cysteine desulfurase that catalyzes the removal of sulfur from cysteine and its subsequent transfer to a conserved cysteine residue of the protein (14). The reaction catalyzed by NifS generates an enzyme-bound persulfide, which serves as the ultimate

sulfur source for the formation of [Fe-S] clusters specific for nitrogenase (15-17). This persulfide sulfur is transferred to NifU, a proposed scaffold protein involved in the formation of the [Fe-S] clusters of the nitrogenase complex (63).

NifU is a homodimer containing conserved cysteine residues in each of its three domains (63). The N-terminal domain includes three conserved cysteine residues responsible for the formation of "transient" [Fe-S] clusters, which can be transferred to other proteins (63). Substitutions of any of the conserved cysteines of the N-terminal domain will inhibit the maturation of the nitrogenase complex, but will not eliminate diazotrophic growth (63-65). The central domain of NifU contains four conserved cysteine residues that can coordinate one [2Fe-2S] cluster per NifU subunit. These [2Fe-2S] clusters are redox-active and are considered "permanent" clusters because they are not transferred to other proteins (63, 64). The function of the central domain [Fe-S] clusters is unknown, but it is believed that they may be involved in coordinating the formation or release of the transient [Fe-S] clusters. The C-terminal domain has two conserved cysteine residues and is similar in sequence to a class of proteins called Nfu proteins, which can assemble [2Fe-2S] and [4Fe-4S] clusters *in vitro* (63, 64, 66, 67). Mutagenesis of either of the cysteine residues in the C-terminus of NifU does not affect the diazotrophic growth of *A. vinelandii* unless accompanied with substitutions in the N-terminal cysteine residues (63, 65). Recently it was discovered that the C-terminal domain is also involved in nitrogenase-specific [Fe-S] cluster formation and may serve as part of a second scaffold system in NifU (65).

Genes encoding a second system involved in the assembly of [Fe-S] clusters, termed ISC, are found in many bacterial genomes (18, 62). Though the two [Fe-S]

cluster assembly systems (NIF and ISC) are similar, one apparently cannot substitute for the activity of the other (14). Whereas *nif* genes are responsible for the maturation of nitrogenase-specific [Fe-S] clusters, the ISC machinery is necessary for the formation of [Fe-S] clusters involved in general cellular processes (17, 18). Mutations in any of the genes in the *isc* operon (*iscSUAhscBAfdx*) result in a decrease in the activity of the [Fe-S] proteins involved in these processes (68-70). IscS and NifS are homologous and share a number of features including size and mechanism of cysteine desulfuration (18). IscU is the homolog to NifU. IscU is smaller than NifU, but displays similarities to the N-terminal domain of NifU (18). IscU serves as a scaffold for the assembly of [2Fe-2S] and [4Fe-4S] clusters. Studies with radiolabeled [^{35}S]-cysteine show the ability of IscS to transfer sulfur from cysteine to IscU (71). IscA, though not essential, is another protein that can serve as a scaffold for [Fe-S] cluster assembly (70, 72). However, recent studies have proposed that IscA functions in iron scavenging and donates iron to IscU for [Fe-S] cluster assembly during iron limiting conditions (73). *hscB* and *hscA* encode chaperone proteins and *fdx* encodes a ferredoxin (74-76).

Expression of the *isc* operon is regulated by the transcriptional repressor IscR by monitoring changes in a [2Fe-2S] cluster within the protein. IscR repressed expression of the *isc* operon when its [2Fe-2S] cluster is intact. However, if the [2Fe-2S] cluster within IscR is destroyed and not regenerated, then repression of the *isc* operon is suppressed (77).

The *E. coli* genome encodes two [Fe-S] cluster assembly systems, ISC and SUF (62). *E. coli* mutants containing deletions of the *isc* operon (*iscRSUA*) grow poorly, but display some level of residual activity of [Fe-S] proteins (70). Suf homologs are found in

many bacteria and Archaea (70) and were recently discovered in the chloroplasts of *A. thaliana* (78-80). The *suf* operon of *E. coli* (*sufABCDSE*) encodes six proteins. Transcription of the *suf* operon is induced during times of oxidative stress and iron starvation (81, 82). Expression of the *isc* cluster of *E. coli* was also induced under oxidative stress and iron limiting conditions. However, since the *isc* operon is regulated by changes in the [2Fe-2S] cluster within IscR and the *suf* operon has been shown to be regulated by OxyR (81) and Fur (82), *suf* is considered to be specifically induced under these stress conditions (83). *suf* mutants of *E. coli* are more sensitive to iron starvation than *isc* mutants and suggests that Isc proteins cannot efficiently synthesize [Fe-S] clusters in iron limiting conditions (83). This suggests Suf proteins are important during iron starvation.

SufA is homologous to IscA and serves as a scaffold protein for the assembly of [Fe-S] clusters (63). SufC is an atypical cytoplamic ABC-ATPase and forms a complex with SufBD (31, 32, 63). SufS displays cysteine desulfurase activity, though the specific activity of SufS is much lower than that of IscS (13, 32). Recent findings show SufS desulfurase activity is stimulated in the presence of SufE (31) and the activity is further increased in the presence of SufE and the SufBCD complex (32). SufE binds SufS and forms a SufSE complex (31). SufS can then transfer sulfur from the active site Cys^{364} to Cys^{51} of SufE (84).

The solved structures of SufS (28, 29) and SufE (32) (PDB code 1MGZ) reveal structural features that may explain the stimulated cysteine desulfurase activity displayed by the SufSE complex. As mentioned earlier, the structure of SufS displays an active site that is not conducive for cysteine desulfurase activity without a large conformational

change. The active site cysteine of SufS is buried within the hydrophobic region of the protein and is shielded from solvent accessibility (28, 32). Moreover, studies have shown that the transfer of sulfur from SufS to SufE is resistant to disruption by reductants (32). This suggests the active site persulfide formed on Cys^{364} of SufS during catalysis is not exposed to solvent and possibly transfers the sulfur atom only after a conformational change brought on by binding with SufE (32, 84).

SufE is thought to be a novel sulfurtransferase that is important in limiting sulfide release during conditions of oxidative stress and iron limitation (32, 83). SufE possibly serves as an intermediate sulfurtransferase in the formation of [Fe-S] clusters under these conditions. The mechanism of sulfur transfer proposed, in which a persulfide is formed on SufS and transferred to the intermediate enzyme SufE before ultimately being used in the formation [Fe-S], has been observed for IscS. The persulfide sulfur of IscS is transferred to IscU during [Fe-S] cluster assembly (84), and to ThiI in the formation of thiamin and 4-thiouridine in tRNA (71, 85) (see sections 1.4.2-3). It is interesting to note that the Suf machinery predicted by the genome sequence of *B. subtilis* lacks a SufE homolog. ThiI of *E. coli* (see sections 1.4.2-3) serves as a precedent for a rhodanese functioning as an intermediary sulfur-carrier. Thus, it is possible that a rhodanese could carry out the activity of the absent SufE in *B. subtilis*.

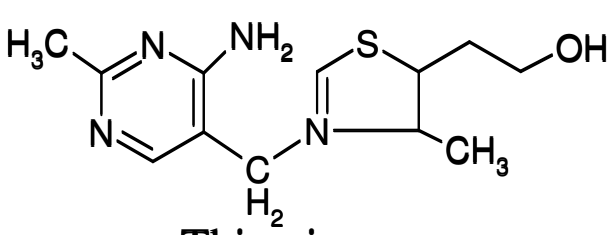

Thiamin

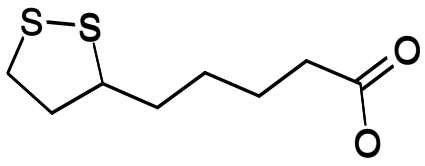

Lipoic Acid

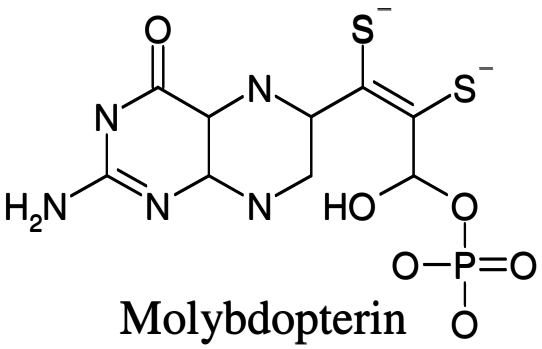

Molybdopterin

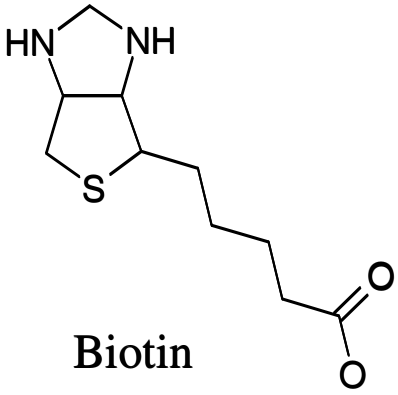

Biotin

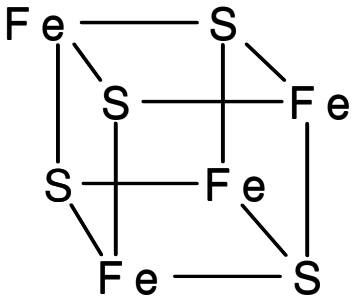

[4Fe-4S] cluster

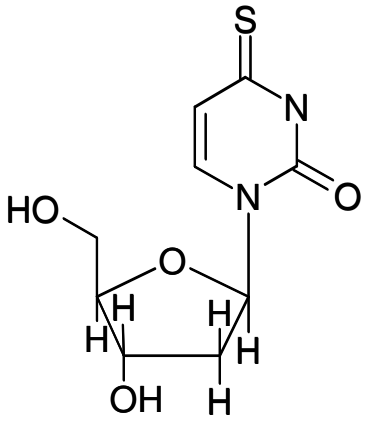

4-thiouridine

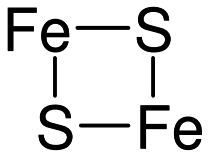

[2Fe-2S] cluster

FIG. 1.5. Sulfur containing cofactors, [Fe-S] clusters, and tRNA.

1.4.2. Thiamin

Thiamin (Vitamin B1) (Figure 1.5) is a water-soluble cofactor and, along with Vitamin C, is among the more unstable vitamins (86). Thiamin is an essential part of the human diet since it cannot be synthesized by humans (87). Thiamin can exist as a free coenzyme or in a phosphorylated form, such as thiamin pyrophosphate (TPP). TPP is a cofactor necessary for α-ketoacid decarboxylases, α-ketoacid dehydrogenases, and transketolases involved in carbohydrate metabolism (86, 87).

The biosynthesis of thiamin in prokaryotes involves the synthesis of the thiazole and pyrimidine rings in separate pathways (87, 88). The *thiC* gene is necessary for the synthesis of the pyrimidine ring (87, 88). The gene products ThiFGHIS and IscS, along with tyrosine, deoxy-D-xylulose, and cysteine, are necessary for the generation of the thiazole moiety in the Gram-negative bacteria *E. coli* and *Salmonella typhimurium* (87, 88). Loss in function of ThiI, ThiG, ThiF, ThiH, or IscS results in a thiazole auxotrophy (87). The ultimate sulfur source for thiazole ring formation is cysteine. The sulfur atom of cysteine is transferred to the active site cysteine of IscS forming an active site persulfide (16, 19, 89). IscS then transfers the sulfane sulfur atom to Cys^{456} of ThiI. Cys^{456} is located within a rhodanese-like domain of ThiI and is essential for sulfurtransferase activity *in vitro* (50, 89). ThiI transfers the sulfur atom to the C-terminus of ThiS after its adenylation by ThiF (23, 88). ThiS-COSH apparently serves as a stable intermediate sulfur source before it is incorporated into the thiazole ring (87). The two moieties of thiamin are then linked together by ThiE (thiamin phosphate synthase) to give thiamin phosphate and an additional phosphorylation reaction yields TPP. Previous attempts to reconstitute the formation of thiazole *in vitro* proved

unsuccessful because ThiH contains an oxygen-sensitive [Fe-S] cluster. However, recently the thiazole synthase activity was successfully reconstituted *in vitro* using cell-free extracts and proteins from adenosine-treated *E. coli* 83-1 cells (89). The addition of adenosine decreased cellular levels of thiamine, which in turn relieved repression of expression of thiazole biosynthetic enzymes. Under anaerobic conditions, the thiazole synthase activity was reconstituted with the addition of purified ThiGH-His (89).

The thiazole moiety was reconstituted *in vitro* using glycine, cysteine, and deoxy-D-xylulose, along with the *B. subtilis* proteins ThiF, ThiS, ThiO, ThiG, and a cysteine desulfurase (90). The synthesis of thiazole using *B. subtilis* proteins was slightly more straightforward than *E. coli* proteins because ThiO is oxygen-dependent and, as mentioned above, ThiH is oxygen sensitive. ThiF catalyzes the adenylation of ThiS and any one of four cysteine desulfurases from *B. subtilis* could transfer sulfur to the adenylated ThiS. ThiS-COSH serves as the source of sulfide for thiazole formation, but could be replaced by Na_2S. ThiO catalyzes the formation of an imine from glycine and ThiG catalyzes the formation of the thiazole ring (90). Four cysteine desulfurases are predicted by the genome sequence of *B. subtilis* (NifS, YrvO, NifZ, and CSD). NifZ transferred sulfur to ThiS most efficiently. It is interesting to note that NifZ is encoded adjacent to a ThiI homolog. ThiI of *B. subtilis* does not contain the C-terminal rhodanese extension observed in *E. coli* ThiI, and addition of ThiI to the reconstitution reaction did not stimulate thiazole production. Nevertheless, *E. coli* ThiI has been shown to enhance cysteine desulfurase activity of IscS (25), and ThiI of *B. subtilis* may interact with a rhodanese homolog during the *in vivo* formation of thiamin to stimulate activity. It is also possible that ThiI of *B. subtilis* is not part of the thiamin biosynthetic pathway.

Alternatively, ThiI might be used in the synthesis of 4-thiouridine in tRNA and could possibly interact with a rhodanese during the process.

1.4.3. Molybdopterin

Molybdopterin (MPT) (Figure 1.5) is a tricyclic pyranopterin with a *cis*-dithiolene moiety that functions in chelating molybdenum (91). The coordination of molybdenum with molybdopterin (catalyzed by MogA and MoeA in bacteria) results in the formation of active molybdenum cofactor (MoCo) (91, 92). MoCo is an essential cofactor for a variety of enzymes involved in two electron redox reactions (92). In fact, a fatal genetic disease is the result of MoCo deficiency in humans (91, 93). MoCo is present in all phyla, and the biosynthesis of MPT is part of a highly conserved pathway consisting of homologous proteins found in a variety of species (94).

The first stage of MPT synthesis involves the formation of precursor Z. In *E. coli* MoaA and MoaC catalyzes the conversion of a quinine nucleotide to precursor Z (91, 92). MPT synthase subsequently catalyzes the incorporation of sulfur atoms into precursor Z, generating the dithiolene moiety of MPT (91, 92).

MPT synthase in *E. coli* is a heterotetramer consisting of two subunits of MoaE (16.9 kDa) and two subunits of MoaD (8.8 kDa) (91, 92). MoeB activates MPT synthase through the adenylation of the C-terminal glycine residue of the conserved Gly-Gly motif of MoaD. The adenylation of MPT synthase by MoeB is similar to the mechanism of ThiS and ThiF in the thiamin biosynthetic pathway (91). Genetic characterization of MoeB reveals that it has an amino acid sequence similar to that of ThiF and structural examination of MoaD shows similarities to ThiS (91, 92). A subsequent sulfurtransferase

reaction generates a thiocarboxylate on the C-terminus of MoaD and serves as the direct sulfur donor for the formation of the dithiolene group of MPT (91). I*n vitro* studies reveal the thiocarboxylate group can be formed by three NifS-like proteins of *E. coli* (IscS, CsdA/CSD, and CsdB/SufS) (95). However, there is no conclusive evidence for the function of these proteins *in vivo* and crude extracts of *iscS* mutants in *E. coli* can convert exogenously added precursor Z to MPT at rates similar to parental strains, which suggests that IscS is not essential for thiolation of MoaD *in vivo* (95).

The human MPT synthase consists of MOCS2A and MOCS2B, which are homologous to MoaD and MoaE, respectively (96). The small subunit of the human MPT synthase (MOCS2A) was unable to complement *moaD E. coli* mutants *in vitro* without coexpressing MOCS3 along with MOCS2A and MOCS2B (96). MOCS3 is a MoeB homolog that contains a C-terminal rhodanese extension (51). MOCS3 displays rhodanese activity and was able to provide sulfur for the thiocarboxylation of MOCS2A in a defined *in vitro* system (51).

Since the MoCo biosynthetic pathway is highly conserved in many species and many of the essential proteins are homologs, the mechanism of sulfur transfer to precursor Z is believed to be similar in different organisms (94, 96). There is no direct evidence suggesting the participation of NifS-like proteins in the *in vivo* synthesis of MPT. However, data does suggest the requirement of a persulfide containing protein, which would act as the sulfur donor (95). Human MOCS3 (51) and CnxF of *Aspergillus nidulans* (97) are two examples of MoeB homologs that possess a C-terminal rhodanese domain. Due to the high conservation of the MoCo biosynthetic pathway, it is possible

that a stand-alone rhodanese participates in the transfer of sulfur for MPT synthesis in organisms where MoeB orthologs lack the fused C-terminal rhodanese domain.

1.4.4. Thionucleosides in tRNA

Modification of tRNA occurs in all organisms (26, 98). Various functions are associated with these modifications to tRNAs, which allow important interactions with proteins and other RNAs (26, 98). There are several modifications to the bases of tRNA that involve the addition of a sulfur atom. The thionucleosides of tRNA include 4-thiouridine (s^4U), 5-methylaminomethyl-2-thiouridine (mnm^5s^2U), 2-thiocytidine (s^2C), and 6-N-dimethyl-2-methylthioadenosine (ms^2i^6A), which are found in *E. coli* (26). The s^4U modification (Figure 1.5), found at position 8 of many bacterial tRNAs, serves as a photosensor for near-UV light (50, 99). When tRNA is exposed to near-UV light the s^4U undergoes a 2 + 2 cycloaddition with cytidine 13, which interferes with the tRNA's ability to serve as a substrate for aminoacylation. As a result, cells that contain this modification will accumulate uncharged tRNA molecules and enter a stage of growth arrest (50, 99).

Initial studies revealed two factors (A and C) that were necessary for s^4U synthesis (23). Loss of either factor caused cells to become deficient in s^4U in tRNA and to develop thiazole auxotrophy. Factor C was also found to be a PLP-dependent enzyme. It is now known that the initial studies led to the characterization of IscS and ThiI in *E. coli* (23). Both proteins are shared between the thiamin and s^4U biosynthetic pathways. It has also been shown that IscS is necessary for the biosynthesis of all thionucleosides in *E. coli* (26) and *S. typhimurium* (100). The mechanism of tRNA modification initially

involves the sulfur transfer from cysteine to IscS via a PLP-dependent cysteine desulfurase reaction and the formation of an enzyme persulfide intermediate. IscS can then transfer the S^0 to Cys^{456} in the rhodanese domain of ThiI. The mechanism for sulfur transfer from ThiI to uridine in tRNA has not yet been elucidated, but it has been discovered that a second cysteine residue of ThiI (Cys^{344}) plays a crucial role (99, 101). Mutants containing substitutions at Cys^{344} of ThiI are greatly impaired in their ability to synthesize s^4U. Moreover, in the absence of reductant, the wild-type ThiI can only turn over once. Therefore it is proposed that Cys^{344} forms a disulfide bond with Cys^{456}, resulting in sulfide transfer to uridine 8 during the formation of s^4U tRNA (99, 101) (Figure 1.6). Recently the minimal substrate required by ThiI for s^4U modification was found to be a mini-helix comprising the stacked acceptor and T stem containing an internal bulged region (102).

B. subtilis contains a variety of thionucleoside modifications of tRNA, including s^4U (103). However, the biosynthetic pathways yielding these thiolated tRNAs have yet to be elucidated. As mentioned above, the biosynthetic pathway of s^4U in *E. coli* involves the participation of ThiI, which also plays a role in thiamin biosynthesis. The genome sequence of *B. subtilis* predicts a ThiI ortholog adjacent to a cysteine desulfurase (NifZ). *B. subtilis* ThiI is not essential for the *in vitro* reconstitution of the thiazole ring of thiamin (90), but it could potentially be needed for s^4U synthesis. However, *B. subtilis* ThiI does not contain the C-terminal rhodanese domain that is essential for the function of *E. coli* ThiI. It is possible that a *B. subtilis* rhodanese participates in s^4U synthesis. The biosynthesis of other thionucleosides present in *B. subtilis* may also require a rhodanese.

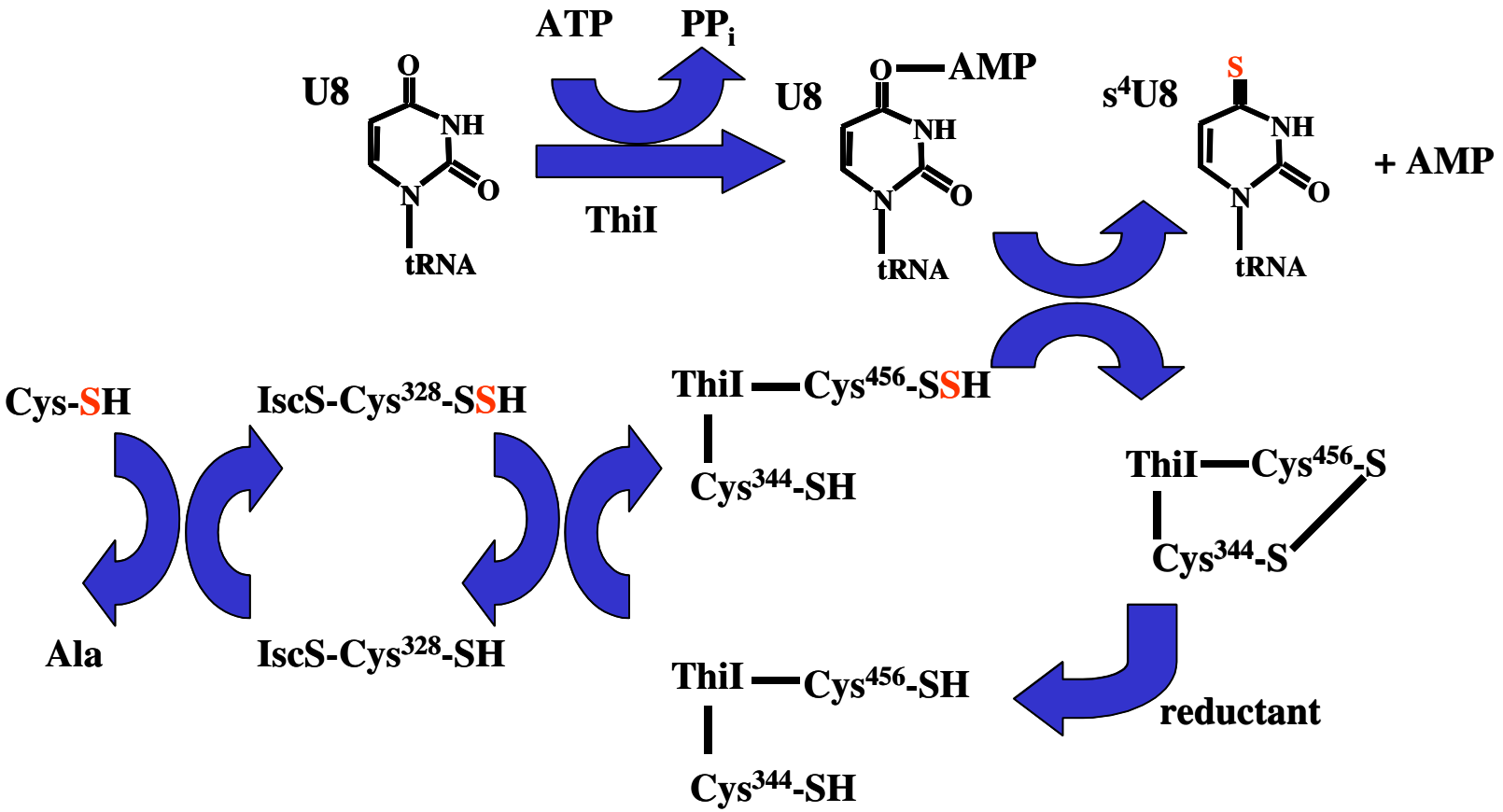

FIG. 1.6. Proposed scheme for sulfur mobilization and transfer during s^4U biosynthesis catalyzed by IscS and ThiI in *E. coli*. Red sulfur atom represents sulfur transferred during reaction. U8, uridine at position 8 of tRNA; superscripted numbers represent residue number in respective enzyme; Cys^{456}, active site cysteine in rhodanese domain of ThiI

1.4.5. Biotin

Biotin (Figure 1.5) is a water-soluble member of the vitamin B complex and is also known as vitamin H (104). Biotin functions as a cofactor for enzymes such as acetyl-CoA and pyruvate carboxylases involved in fatty acid and carbohydrate metabolism (104). Biotin deficiencies in animals cause abnormal developments in the skin and hair and reproductive problems (105). Severe biotin deficiency is not commonly seen in adult or infant humans because the vitamin is often supplemented in foods (106).

The final step of biotin synthesis involves the insertion of a sulfur atom into dethiobiotin (DTB) catalyzed by biotin synthase (BioB) (13, 107). Biotin synthase from *E. coli* is a 76 kDa homodimer that belongs to the family of "radical SAM (S-adenosylmethionine)"-dependent enzymes (107). The activity of BioB *in vitro* requires SAM, and a reduction system consisting of NADPH, flavodoxin, and flavodoxin reductase (108). It is generally accepted that the reduction system is involved in the cleavage of SAM into methionine and 5'-deoxyadenosyl radical (5'-dA•) (107, 108). One electron from flavodoxin is transferred to a [4Fe-4S] within BioB and then to SAM, generating 5'-dA• (107, 108). It is then believed that 5'-dA• abstracts a H• from DTB generating a DTB radical (DTB•) (107, 108).

However, a number of inconsistent reports about BioB have led to much confusion about the enzyme. Discrepancies have arisen as to the number and types of [Fe-S] clusters found within the BioB enzyme (109). The number of molecules of SAM and DTB associated with BioB is another area of considerable controversy. Some research groups report finding two molecules of SAM and one molecule of DTB associated with each BioB dimer (108, 110), whereas others report one molecule of SAM

and one molecule of DTB per subunit of BioB (107, 111). Moreover, evidence from different groups has led to two different proposed mechanisms for sulfur insertion into DTB catalyzed by BioB (108, 111-113). One proposal suggests that sulfur from a [2Fe-2S] cluster within BioB serves as the immediate sulfur source (108, 112). However, another research group proposes that BioB contains PLP-dependent cysteine desulfurase activity and catalyzes the sulfur insertion to DTB• via an enzyme-bound persulfide intermediate (111, 113).

Recently the crystal structure of BioB from *E. coli* has been solved (107). The structure has given new insight into the controversies surrounding BioB, including possible mechanisms involved in the incorporation of sulfur into DTB. The crystal structure of BioB, containing the substrates SAM and DTB, was solved to a resolution of 3.4 Å and displayed a triosephosphate isomerase (TIM) type $(\alpha/\beta)_8$ barrel for each subunit (107). The structure reveals one molecule of SAM and DTB bound per subunit of BioB along with one [2Fe-2S] cluster and one [4Fe-4S] cluster bound per subunit. The [4Fe-4S] cluster was located near the surface of the enzyme. This location is consistent with the ability of the [4Fe-4S] to accept an electron from flavodoxin in the generation of 5'-dA• (107).

The crystal structure did not support the hypothesis that BioB contains bound PLP. The structure did not show areas consistent with PLP-binding and the location of lysine residues in the crystal structure were not consistent with a PLP-dependent mechanism of sulfur insertion into DTB, which proposed sulfur insertion occurred via an enzyme-bound cysteine persulfide intermediate (107). Other groups have reported data

that support distinct binding sites for [4Fe-4S] and [2Fe-2S] clusters within the BioB monomer, and provides no support for a PLP-dependent reaction mechanism (109).

The position of SAM and DTB in the core of the enzyme is consistent with the proposed radical chemistry between SAM and DTB (107). DTB and the [2Fe-2S] cluster are located near each other in the enzyme, which suggests that the [2Fe-2S] cluster is the source of the sulfur for insertion (107). The [2Fe-2S] cluster was located within the TIM barrel fold and ligated to Cys^{97}, Cys^{128}, Cys^{188}, and Arg^{260} (107). The role of Arg^{260} as a ligand to a metal was of particular interest because it has never been seen before in biological systems and may serve an important function in the catalytic mechanism of the protein. Based on the location of this Arg residue a mechanism of sulfur insertion into DTB was proposed in which the Arg^{260} side chain could rearrange its position to bridge the two Fe atoms of the [2Fe-2S] cluster and facilitate the sulfur transfer (107).

Evidence shows that the most active form of BioB contains one [4Fe-4S] cluster and one [2Fe-2S] cluster (112, 114). This form of BioB can produce 0.7 – 0.9 equivalents of biotin per monomer of enzyme, though the enzyme can only turn over once *in vitro*. Jameson *et al.* report the [4Fe-4S] cluster is stable and a majority of the [2Fe-2S] cluster is destroyed under turnover conditions (114). However, the initial rate of degradation of the [2Fe-2S] cluster appeared to be faster than the formation of biotin (114). This observation could be explained if the rate limiting step occurs subsequent to the insertion of sulfur into DTB or if the immediate sulfur source is something other than [2Fe-2S] cluster, possibly a polysulfide or persulfide on the enzyme (114).

The biotin synthase reaction is conserved in many species, and biotin synthase has been characterized in organisms such as *B. subtilis* and *A. thaliana* (115, 116). In *A.*

thaliana biotin synthase is localized in mitochondria, and the reaction is stimulated by the addition of cysteine desulfurase (Nfs1) in *in vitro* reaction systems (116). *B. subtilis* contains a homodimeric BioB protein and evidence suggests it functions using a 5'-dA• derived from SAM in a manner similar to the *E. coli* mechanism. However, the *B. subtilis* BioB protein has been shown to be less active in *in vitro* systems (115). It was also observed that BioB from *B. subtilis* could not convert dethiobiotin to biotin in cell-free extracts from *E. coli* and *vise versa*. Thus, the enzymes are species specific. In *B. subtilis*, dethiobiotin can be converted to biotin without the addition of a sulfur source and suggests the presence of a [Fe-S] cluster within BioB that may serve as the sulfur donor. Therefore [Fe-S] clusters would need to be rebuilt in order for multiple turnovers of the BioB in *B. subtilis* (115).

Many questions still remain regarding the function of biotin synthase. One major question regards the number of turnovers observed with BioB. Researchers have been unable to produce more than one turnover in *in vitro* reaction systems (109). However, strong product inhibition by 5'-dA• may explain these results (111). The inability to turn over multiple times may also be due to an inability to regenerate the immediate sulfur source. Sulfur inserted into DTB has been suggested to directly come from the [2Fe-2S] cluster (107), or through an enzyme-bound persulfide or polysulfide subsequent to the [2Fe-2S] degradation (114). If either mechanism is correct, then it is likely a sulfurtransferase is present in the reaction for either regeneration of the [Fe-S] cluster or movement of the sulfur atom. The *E. coli isc* gene cluster can function in [Fe-S] cluster formation and repair and may serve in the regeneration of the sulfur source possibly coupled to other sulfurtransferases (114). It is important to note that *B. subtilis* does not

contain a gene cluster similar to *isc* and would need alternative enzyme or enzymes to facilitate the transfer of sulfur and regeneration of [Fe-S] clusters (115).

1.4.6. Lipoic acid

Lipoic acid (Figure 1.5) is an essential cofactor of enzyme complexes that catalyze oxidative decarboxylation reactions (117). Pyruvate dehydrogenase complex, α-ketoglutarate dehydrogenase complex, branched-chain 2-oxo acid dehydrogenase complex, and the glycine cleavage system are some examples of these enzyme complexes that require lipoic acid (118, 119). Lipoic acid functions as an active cofactor when it is attached to the lipoyl-accepting domains in subunits of these protein complexes. Most often the lipoic acid is bound to the ε-amino group of a conserved lysine residue (118, 119). Recent studies have shown lipoic acid may have important pharmacological and antioxidant properties (120).

In *E. coli*, the attachment of lipoic acid to target proteins has been shown to occur via two separate pathways (118). One pathway utilizes free lipoic acid from the medium and involves lipoate-protein ligase (LplA). This two-step process begins with the activation of lipoic acid by ATP, which is then transferred to the target subunit of the protein complex. Both steps are catalyzed by LplA (118). The second pathway of lipoyl group attachment utilizes lipoyl- or octanoyl-ACP (acyl carrier protein) from fatty acid synthesis. LipB catalyzes the transfer of the octanoyl group from ACP to the conserved lysine residue in the lipoyl-accepting domain. LipA (lipoyl synthase) then catalyzes the insertion of sulfur atoms into the bound octanoyl group to form the lipoyl derivative in a mechanism believed to be similar to that of biotin synthase (118).

Biochemical and genetic studies have shown that LipA is a member of the "radical SAM superfamily" (118, 119). LipA utilizes 5-adenosyl-L-methionine to generate 5'-deoxyadenosyl radical for the activation of C_6 and C_8 of octanoic acid. In a mechanism similar to biotin synthase, the reductive cleavage of SAM requires one electron from flavodoxin, which is then transferred to a [4Fe-4S] cluster bound to the enzyme (118, 119). Recent studies have shown that lipoyl synthase requires two equivalents of SAM for the generation of one equivalent of lipoic acid (119), suggesting that one equivalent of 5'-dA• is required for the removal of each of the two H• from octanoate. After the removal of the H• from the bound octanoyl substrate, LipA catalyzes the insertion of sulfur into the C_6 and C_8 positions (119).

The sulfur used in the insertion reaction most likely comes from a second bound [Fe-S] cluster (118). LipA contains two regions of conserved cysteine residues. The CxxxCxxC motif is common to all SAM radical proteins and binds the [4Fe-4S] cluster needed in 5'-dA• generation. The second motif, CxEAxCxNxxEC, is only found in LipA proteins and is thought to bind an additional [Fe-S] cluster used for sulfur insertion (118).

Recent work has shown that the physiological substrate for LipA for the pyruvate dehydrogenase complex is the octanoyl group bound to the lysine residue of the lipoyl-accepting domain (E2) as opposed to octanoyl-ACP (121). This finding suggested that LipA would have multiple substrates, each associated with the various lipoyl-accepting domains of different protein complexes, and was supported by evidence that an octanoyl moiety bound to the lipoyl-accepting subunit of the glycine cleavage system also served as a substrate for LipA (118, 121).

1.5. Physiological characterization of rhodaneses

Analysis of the domain architecture of an enzyme containing multiple domains can be a useful investigative tool in determining the physiological function of a protein if one of the domains is orthologous to a previously characterized protein. The known function of one domain can be used to predict the physiological function of the protein and may provide information regarding the function of the unknown domain. Since rhodaneses display a wide range of domain architectures, this investigative method is particularly useful for characterizing rhodanese-containing proteins.

One of the better-understood models for the participation of a rhodanese module of a protein in a biosynthetic pathway is *E. coli* ThiI and s^4U biosynthesis (Figure 1.6). The ThiI domain is typically involved in the biosynthesis of the thiazole ring (88, 122). However, the ThiI protein of *E. coli* has been shown to be involved in the biosynthesis of the thiazole ring of thiamin and in 4-thiouridine (s^4U) modification of tRNA (50, 50, 99, 101). Within the ThiI domain lies a region known as the THUMP region (named after **th**io**u**ridine synthases, **m**ethylases and **p**seudouridine synthases), which is predicted to be an RNA-binding domain (123). The ThiI protein also contains a functional carboxy-terminal rhodanese extension. Recent investigations have shown that the function of the rhodanese domain is critical to the activity of ThiI in s^4U biosynthesis (50).

The MoeB-rhodanese fusion proteins (Figure 1.2) are another group of rhodanese fusions that have been studied and serve as an important example of a rhodanese module of a multidomain protein participating in the activity of the enzyme. The molybdenum cofactor (MoCo) is an essential cofactor for several important enzymes including nitrate reductase. MoeB activates the MoaD/MoaE heterotetramer molybdopterin (MPT)

synthase by adenylation of a C-terminal glycine of MoaD, and a subsequent sulfurtransferase reaction thiolates the C-terminus. The thiolated MoaD can then serve as the direct sulfur donor for the biosynthesis of MPT, the main component of MoCo (91, 92). MOCS3 (human) and CnxF (*Aspergillus nidulans*) are MoeB homologs that contain a C-terminal rhodanese domain extension to the MoeB moiety (51, 124). The rhodanese-like domain of MOCS3 has been shown to be essential for the sulfur transfer in the *in vitro* thiocarboxylation of MOCS2A, the MoaD homolog in humans (51), and the C-terminal rhodanese domain of CnxF is essential for MPT synthesis *in vivo* (124). The *Pseudomonas stutzeri* protein MoeZ is another example of a protein containing an amino-terminal MoeB domain and a carboxy-terminal rhodanese domain (97, 125). Though MoeZ is not necessary for MPT synthesis, it is involved in the biosynthesis of the metal chelator [pyridine-2, 6-*bis* (thiocarboxylic acid)] (pdtc) that is essential for detoxification of carbon tetrachloride carried out by *P. stutzeri* (97). The C-terminal rhodanese extension of MoeZ is thought to be essential for the sulfurtransferase reaction involved in the formation of pdtc.

The use of fusion proteins as an investigative tool is limited to proteins containing at least one domain of known function. However, the analysis of the genomic context of a gene can be another useful tool for determining the physiological role of proteins without a domain of known function. YbbB of *E. coli*, another multiple domain protein, contains an N-terminal rhodanese domain fused to a C-terminal extension containing a domain with a P-loop (Walker A) motif (49). In some organisms, the *ybbB* gene is located adjacent to the gene *selD*, encoding selenophosphate synthetase (49). Thus the genomic context of *ybbB* suggested a role in selenium metabolism for the YbbB protein.

Indeed, YbbB was shown to be required for the conversion of 2-thiouridine to 2-selenouridine in tRNA. The rhodanese homology domain was found to be essential for selenium transfer from selenophosphate during the tRNA modification reaction (49).

B. subtilis contains four genes predicted to encode rhodaneses (YtwF, YqhL, YbfQ, and YrkF) (Figure 1.2). YrkF is a novel rhodanese in that it contains a C-terminal rhodanese domain and a N-terminal Ccd1 (conserved cysteine domain 1). YrkF is also encoded near another Ccd1 homolog (YrkI). Use of these genetic investigative tools described above may be useful in elucidating the physiological role of YrkF in *B. subtilis*.

1.6. YrkF: A unique two-domain rhodanese

Analysis of the *B. subtilis* genome reveals four genes predicted to encode proteins with the rhodanese homology domain, designated YtwF, YqhL, YbfQ, and YrkF. YrkF is a unique example of a rhodanese fusion protein in that it contains a carboxy-terminal rhodanese homology domain and an amino-terminal Ccd1 (conserved cysteine domain 1) consisting of about 75 amino acids. Only four other species of bacteria are known to contain a two-domain Ccd1-rhodanese protein (*Bacillus cereus*, *Bacillus anthracis*, *Oceanobacillus iheyensis*, and *Exiguobacterium*). Ccd1 homologs contain a characteristic C-P-x-P motif near the amino terminus. YrkF contains two conserved cysteine residues, one in each domain.

The Ccd1 domain is found as a single-domain protein in most Eubacteria and Archaea, but is also found as a module in multiple domain proteins (Figure 1.2). Though single domain homologs of the Ccd1 domain have been structurally characterized, the biochemical function of Ccd1 is still unknown. Two of the three single domain Ccd1

homologs of *E. coli*, YhhP (SirA) and YedF, have been characterized (126, 127). Deletion of *yhhP*, encoding the 81 amino acid SirA protein, leads to a filamentous morphology due to an apparent defect in FtsZ-ring formation (128). The solved structures of SirA (126) and YedF (127) reveal a two-layer αβ structure similar to domains in many RNA- and DNA-binding proteins, including the C-terminal domain of IF3 (129) and the predicted structure of the THUMP region of ThiI (123). Although SirA and YedF show structural similarities to DNA-binding proteins, it is important to note that there is no sequence homology shared with these nucleic acid-binding proteins. Two other examples of single domain Ccd1 homologs that have been sequenced are YrkI of *B. subtilis* and YeeD of *E. coli*. Analysis of the genomic context of *yrkF* reveals that *yrkI* is in close proximity to *yrkF* in the *B. subtilis* genome.

1.7. Present work

In the present study, bioinformatic, genetic, and biochemical approaches were used to characterize YrkF. A variant protein was created containing a cysteine to alanine substitution in the Ccd1 domain. The proteins were overexpressed and purified. Initial rhodanese assays confirmed that YrkF and YrkF^{C15A} are active rhodanese proteins. SDS-PAGE fractionation of purified YrkF and YrkF^{C15A} revealed banding patterns that suggested YrkF forms both intra- and intermolecular disulfide bonds. Subsequent analysis of the two proteins included cross-linking experiments to determine the proximity of the two cysteine residues in the 3-dimensional structure, and determination of the effect of the disulfide bond on rhodanese activity. The study also included kinetic analysis YrkF and YrkF^{C15A}, as well as the creation of a chromosomal deletion of *yrkF* in

B. subtilis. Mass spectral analysis of YrkF and YrkF^{C15A} was used to determine possible covalent modifications of the rhodanese active site upon treatment with DTT, sulfite, and thiosulfate. Inherent enzymatic and structural differences were observed when comparing YrkF and the C15A variant, suggesting that the cysteine residue in each domain of YrkF is important for its physiological function. Finally, molecular modeling approaches were used to create and analyze the structure of YrkF with and without an intramolecular disulfide bond under simulated conditions.

CHAPTER TWO

Materials and Methods

2.1. Materials

Reagents were purchased from Sigma or Fisher Scientific unless otherwise indicated. Oligonucleotides were synthesized by DNAgency (Malvern, PA). Restriction endonucleases and nucleotides were purchased from New England Biolabs. *Pfu* polymerase was from Stratagene, GenElute Bacterial Genomic DNA Kit (for use with *B. subtilis*) from Sigma, and dibromobimane (bBBr) from Molecular Probes (Eugene, OR). Glutamic acid endopeptidase (Glu-C) from *Staphylococcus aureus* V8 was purchased from Princeton Separations, Inc.

2.2. Bacterial strains and plasmids

The bacterial strains and plasmids used or constructed in this study are listed in Table 2.1 and Table 2.2, respectively. All *E. coli* strains are K-12 derivatives except for BL21(DE3), which is derived from *E. coli* B. *B. subtilis* strains are derivatives of strain 168.

Table 2.1. Bacterial strains

Bacterial Strains			
Organism	Strain	Genotype/Description	Reference
E. coli	DH5α F'	(F'Φ*80d lacZΔM15*) *endA1 recA1 hsdR17 supE44 thi-1 gyrA relA1*Δ(*lacZYA-argF*)U169	(130)
E. coli	DH5α Z1	DH5α *λatt lacI*^{q} *tetR* Sp^{r}	(131)
E. coli	BL21(DE3)	*hsdS gal* (*λcIts857 ind-1 Sam7 nin-5 lacUV5-T7* gene 1)	(132)
B. subtilis	PS832	Wild-type, trp^{+} revertant of 168	(133)
B. subtilis	JH1006	PS832 *yrkF::Er*^{r}	This work

Table 2.2. Plasmids

Plasmids		
Plasmid	Description	Reference
pT7-7	ColE1 origin Ap^r T7 promoter	(134)
pDG646	plasmid carrying Er^r cassette for *B. subtilis*, Am^r	(135)
pVK2B	pT7-7 carrying *yrkF* cloned into *Bam*HI of MCS	This work
pVK3	pVK2B deletion of *Hin*dIII site in MCS from *Cla*I to *Sal*I	This work
pFerm1	pVK3 carrying *yrkF::Er*^{r}	This work
pFMut3	pVK2B mutagenic plasmid	This work

2.3. Media and growth conditions

E. coli cells were grown in Luria Bertani (LB) media (136) at 37^{o} or 30 ^{o}C under aerobic conditions. *B. subtilis* strains were grown aerobically at 37 ^{o}C in LB, or 2xSG medium (137) or glucose minimal Spizizen medium supplemented with 0.005% tryptophan (138). Spizizen medium was modified to analyze the ability of the *yrkF* mutant (JH1006) to grow on nitrate as the sole nitrogen source. Potassium nitrate (4.9 mM) was substituted for ammonium sulfate (3.8 mM) in these experiments. Mutants were tested for thiamine auxotrophy by observing growth with and without 0.00004% thiamine. Strains transformed with plasmids were selected on media containing antibiotics at 100 μg per ml ampicillin (*E. coli*), and 0.5 μg per ml erythromycin plus 5 μg per ml lincomycin (macrolide-lincosamide-streptogramin B resistance). Erythromycin/lincomycin resistance was used to select *B. subtilis* mutants carrying the *yrkF* disruption and could not be used for selection in *E. coli*.

For the determination of rhodanese specific activity in the wild type (PS832) and *yrkF* mutant (JH1006), cells were grown overnight in LB (wt) or LB with 5 μg/ml erythromycin/lincomycin (JH1006). Cultures were centrifuged and supernatant was discarded to remove erythromycin/lincomycin. The cell pellet was then diluted in 35 ml LB and grown until they reached an OD600 ~ 0.6 – 0.8. Cultures were harvested by centrifugation at 3600 x g for 10 min and washed in 50 mM Tris-HCl (pH 7.2), 3 mM EDTA. Pellets were frozen at –70 °C until use. Frozen pellets were resuspended in 525 μL 50 mM Tris-HCl (pH 8.3), 1 mM EDTA, 1 mM DTT and sonicated on ice at 50% of full power for 3 times 30 s to lyse cells. Sonicated cells were microcentrifuged in the

cold for 5 min. The cell-free extract was assayed for rhodanese activity and protein to determine specific activity.

2.4. General Methods

2.4.1. Polymerase Chain Reaction, DNA electrophoresis, and ligation reactions

Polymerase Chain Reaction (PCR) was carried out using approximately 0.5 μg of chromosomal DNA from *B. subtilis* PS832 as a template, *Pfu* DNA polymerase, primers generated from DNAgency, and a GeneAmp PCR 9600 thermocycler. Agarose gel electrophoresis was used to analyze the relative size of DNA fragments based on known molecular weight markers. DNA was fractionated by electrophoresis in 0.75% agarose in 0.05 M Tris, 0.05 M boric acid, and 0.01 M EDTA (TBE) buffer containing 0.5 μg/ml ethidium bromide (136). DNA was extracted from the agarose gel using GFX™ PCR DNA and Gel Band Purification Kit (Amersham Pharmacia Biotech, Piscataway, NJ) following the provided instructions. Ligations were carried out using a 4:1 ratio of insert:vector. T4 DNA ligase was used as suggested by New England Biolabs. Ligation reactions were incubated at 16 °C overnight.

2.4.2. Preparation of competent *E. coli* cells and transformation

Competent *E. coli* cells were prepared following the methods described by Sambrook *et. al* using cold $MgCl_2$ and $CaCl_2$ (136). Approximately 100 μL of competent cells were incubated with about 1 pmol of DNA for 30 min on ice. The cells were then heat-shocked at 42 °C for 2 min and 1 ml of LB was added to the transformation mix. The cells were allowed to incubate at 37 °C for 60 min. A 200 μL aliquot of the cell

culture was spread onto LB plates with the appropriate antibiotic selection and incubated overnight at 37 °C.

2.4.3. Transformation of *B. subtilis*

To prepare *B. subtilis* for transformation, a modified method derived from the one proposed by Spizizen was followed (139, 140). *B. subtilis* PS832 was grown on 2xSG plates overnight at room temperature until the plate was covered with fine hazy growth. MS-I medium (14.6 mM NH_4SO_4, 77.9 mM K_2HPO_4, 42.8 mM KH_2PO_4, 3.3 mM sodium citrate, 0.5% glucose, 0.02% casamino acids, 0.10% yeast extract) was inoculated with cells from the overnight culture and incubated for 4.5 h at 37 °C with vigorous shaking. After incubation, 0.5 ml of the cell culture was then added to MS-II medium (4.5 ml MS-I plus 2.8 mM $MgCl_2$ and 0.55 mM $CaCl_2$) and incubated at 37 °C for 1.5 h with vigorous shaking. An aliquot of 0.3 ml of cell culture was added to 2 μg of DNA for 30 min and incubated with vigorous shaking at 37 °C. A 200 μL aliquot of the transformed cells were spread onto selective medium using sterile beads. Plates were incubated overnight at 30 – 37 °C.

2.4.4. Determining protein concentration

The concentration of protein was determined by the method described by Bradford (141). Known concentrations of bovine serum albumin (BSA) were incubated in Coomassie Protein Assay Reagent (PIERCE) and absorbance at 595 nm was used to generate a standard curve. Experimental protein solutions were treated with Coomassie

reagent and the absorbance at 595 nm was determined. The protein concentration was calculated based on the standard curve.

2.5. Construction of overexpression vectors pVK2B and pVK3

YrkF expression vector, pVK2B, was constructed by amplifying *yrkF* by PCR from template DNA of *B. subtilis* PS832 using the primers 0854000 (5'-GGAGGAACATATGATGAAAGCAAC-3') and 0854018 (5'-GCAAGGATCCCTACTCTTGTAC-3') containing restriction sites *Nde*I and *Bam*HI, respectively (underlined; *Nde*I contains the ATG translation start site). Ligation of the *Nde*I- and *Bam*HI-restricted *yrkF* PCR product (599 bp) to the similarly digested plasmid pT7-7 resulted in plasmid pVK2B. This plasmid was sequenced and used to transform expression strain BL21(DE3). To facilitate subsequent constructions, pVK3 was generated from pVK2B by cleaving with *Cla*I and *Sal*I (within the multiple cloning region) to remove the intervening *Hin*dIII restriction site. Following digestion, the ends were filled in using *Taq* polymerase, and the blunt ends were religated.

2.6. Oligonucleotide-directed mutagenesis

The cysteine (residue 15) of YrkF in the Ccd1 domain was changed to an alanine by PCR-mediated site directed mutagenesis consisting of three separate PCR reactions using pVK2B as the template and the following primers: overexpression primer a (previously described 0854000), mutagenic primer a (5'-AAGGTTTGGCGGcgcCAATGCCTA-3'), overexpression primer b (previously described 0854018), and mutagenic primer b (5'-TAGGCATTGgcgCCGCCAAACCTT-

3'). Lowercase letters indicate altered nucleotides resulting in a change in the codon and creation of a *Nar*I restriction site (underlined). PCR reactions one and two (Figure 2.1) utilized overexpression and mutagenic primers a and overexpression and mutagenic primers b, respectively, along with pVK2B template. The PCR products from these reactions were used as templates for overexpression primers a and b (Figure 2.1). The *Nar*I site created in the final PCR product was used to confirm the creation of correctly mutagenized DNA by endonuclease digestion and subsequent gel electrophoresis. The final PCR product generated was digested with *Nde*I and *Hin*dIII and ligated into the *Nde*I/*Hin*dIII sites of pVK3, resulting in pFMut3. pFMut3 was used to transform strain BL21(DE3) for overexpression of the variant protein YrkFC15A. The desired mutation was verified by sequencing the *Nde*I-*Bam*HI region of pFMut3.

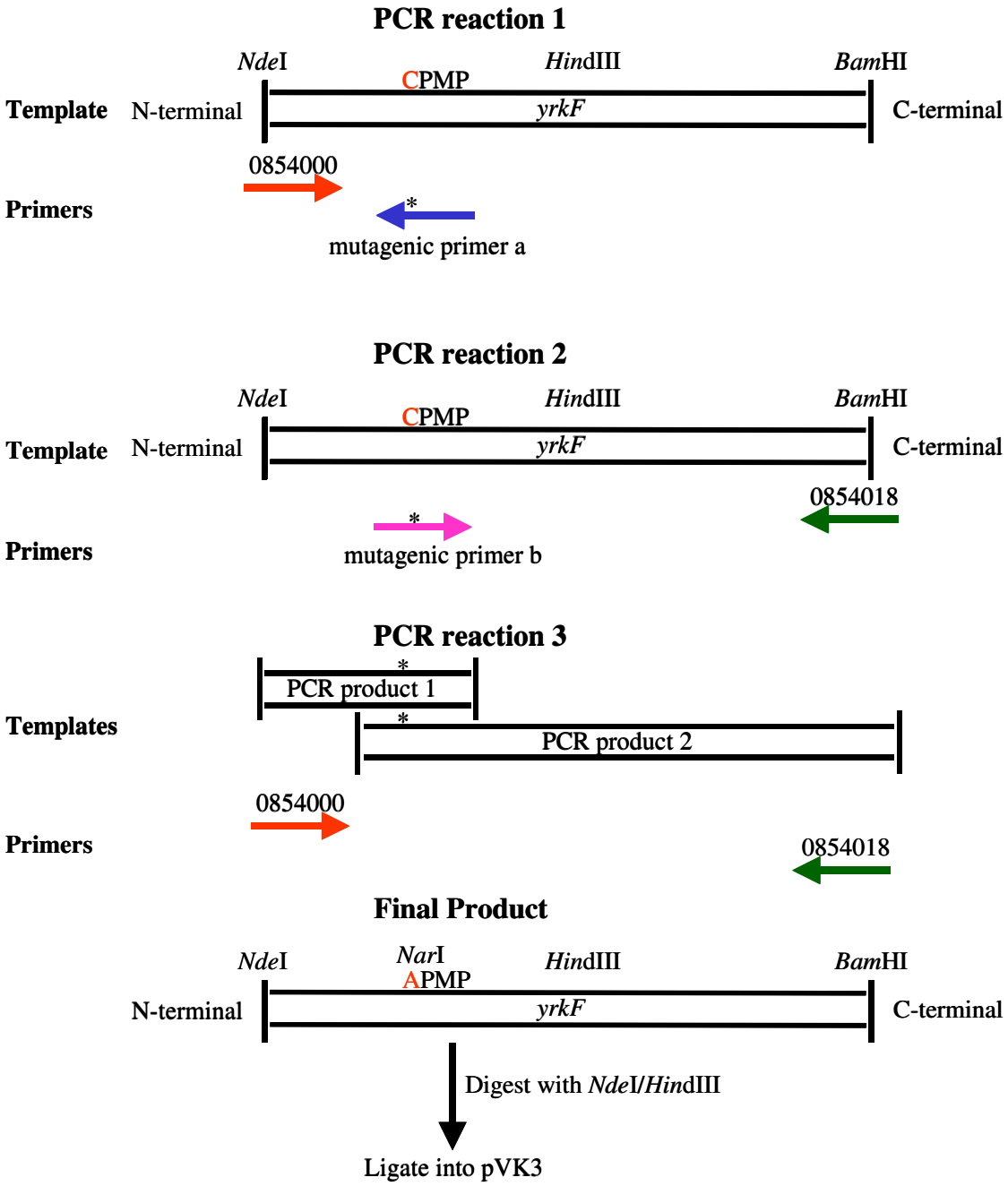

FIG. 2.1. Construction of YrkF^{C15A} variant via site directed mutagenesis

Schematic represents procedure followed to generate the pFMut3 overexpression vector (as described in Methods and Materials). Key restriction sites, *Nde*I, *Bam*HI, *Hin*dIII, and *Nar*I are highlighted. Primers, as described in text, as shown as arrows. *, site of codon mutation in primers and PCR products. CPMP, wild type CPxP motif. APMP, altered motif in YrkF^{C15A}.

2.7. Construction of plasmid pFerm1

In order to construct a *yrkF::Er*^{r} insertion, plasmid pFerm1 was constructed. The plasmid pVK3 (Table 2.2) was restricted with *Hin*dIII at a site within *yrkF* flanked by 316 bp upstream and 203 bp downstream. An erythromycin resistance cassette was extracted from plasmid pDG646 (Table 2.2) by digestion with *Hin*dIII and ligated into the digested pVK3 plasmid. The plasmid was used to transform DH5αF' and was recovered from colonies selected on an LB/Ap plates.

2.8. Deletion of the chromosomal *yrkF* gene

B. subtilis PS832 was transformed with pFerm1, which generated a *yrkF::Er*^{r} chromosomal disruption through a double-reciprocal crossover event. Competent *B. subtilis* PS832 cells were transformed with linearized pFerm1 and selected for erythromycin/lincomycin resistance. The genomic DNA of strain JH1006 was extracted with GenElute Genomic DNA kit. PCR amplification of the *yrkF* locus of JH1006 [using primers 0854000 and 0854018 (Figure 2.1)] confirmed the insertion of the approximately 2000 bp erythromycin resistance cassette.

2.9. Overexpression and purification of YrkF and YrkF^{C15A}

BL21(DE3) colonies (freshly transformed with *yrkF* overexpression plasmid pVK2B) were grown overnight at 30 ºC in 5 ml of LB media containing ampicillin. One liter of LB/Ap was inoculated with the overnight culture and grown at 30 ºC to log phase (OD 0.2 – 0.4) under shaking at 100 rpm. YrkF expression was induced by the addition of 0.4 mM isopropylthio-β-D-galactopyranoside (IPTG) for 2 to 3 h. Cells were

harvested and washed with 50 mM NaCl, 25 mM Tris-HCl (pH 8.3). The cell pellet was frozen at –70 ºC until used for purification.

The cell pellet was thawed in a 14 ml cold solution of 50 mM Tris-HCl (pH 8.7) and lysed by two passes through a French pressure cell at 12-16,000 psi at 4 ºC. All subsequent steps of the purification were performed at 4 ºC, with the exception of the chromatographic steps. The cleared lysate supernatant was collected after centrifugation at 15,500 x g for 20 min. Addition of 1% (w/v) streptomycin sulfate for 10 minutes and subsequent centrifugation at 14,000 x g for 30 min removed nucleic acids. The extract was loaded onto a prepacked Waters quaternary methylamine Q-polymethacrylate (10 by 100 mm; Protein-Pak Q15HR 1000Å) equilibrated at room temperature with a degassed solution of 25 mM Tris-HCl (pH 8.7). After thorough washing, the column was developed with a salt gradient from 0 to 0.3 M NaCl in the same buffer. Rhodanese activity eluted in a major peak and a minor peak at approximately 0.15 M NaCl.

For further purification of YrkF, active fractions from both eluted peaks were combined and treated with 1 mM DTT. The active fractions were then diluted 1:1 with 5 ml 25 mM Tris-HCl (pH 8.3), 1 mM DTT. The solution was applied to the anionic exchange column equilibrated with 25 mM Tris-HCl (pH 8.3), 1 mM DTT. All column solutions were degassed. A 0 to 0.3 M NaCl gradient in column buffer was used to develop the column. YrkF eluted in one major peak at about 0.15 M NaCl.

Purification of the YrkF^{C15A} variant protein followed the same procedure, but with pFMut3-transformed host cells, and without the second chromatography step under reducing conditions. The elution of protein from the anionic exchange column resulted in one major peak with rhodanese activity.

2.10. Polyacrylamide gel electrophoresis

Sodium dodecyl sulfate-polyacrylamide gel electrophoresis (SDS-PAGE) was performed as described (142). Samples of YrkF and YrkF^{C15A} were analyzed by electrophoresed after reduction with β-mercaptoethanol, or without reduction, in gels containing 12% or 15% polyacrylamide (w/v). The sample loading buffer contained 31.3 mM Tris-HCl (pH 6.8), 10% glycerol, 0.4% SDS and 0.0013% bromophenol blue with or without 5% β-mercaptoethanol. In some cases proteins were treated with 2.5 – 5 mM DTT to reduce disulfide bonds. The proteins were visualized with Fast Stain from Zoion Biotech, Inc. The molecular masses of the YrkF and YrkF^{C15A} subunits were estimated by comparison of their mobilities with those of MW standards.

2.11. Assay of rhodanese activity

Rhodanese activity was assayed in a 0.5 ml reaction containing 10 mM $(NH_4)_2SSO_3$, enzyme or cell-free lysate, and 100 mM Tris-acetate (pH 8.6). The reaction was started with the addition of 50 mM KCN, incubated at 25 ^oC for 3 min, and terminated with the addition of 0.25 ml of 15% (v/v) formaldehyde. Color was developed with 0.75 ml of ferric nitrate reagent [100 g of $Fe(NO_3)_3 \cdot 9\ H_2O$ and 200 ml of 65% HNO_3 per 1500 ml]. After centrifugation of the reaction mixture, the A_{460} of the sample was determined using a control reaction (no enzyme) as the blank (40). One unit of enzyme catalyzes the production of 1 μmole thiocyanate per minute and corresponds to an A_{460} change of 2.8 in this system.

Kinetic data of YrkF and the variant YrkF^{C15A} were generated by performing rhodanese assays at various concentrations of thiosulfate for a number of fixed

concentrations of cyanide. Rhodanese assays contained 0.167 and 0.194 μg of purified YrkF or YrkF^{C15A}, respectively. With KCN concentrations above 50 mM, an increase in pH was observed. To stabilize the pH of the reaction, a different buffer was used (200 mM Tris-glycine (pH 8.8)) and HCl was added to any reaction mix containing more than 50 mM KCN. The HCl concentration used at each concentration of KCN was determined empirically such that pH was maintained at 8.8 (Table 2.3).

The inhibitory effects of certain anions on YrkF and YrkF^{C15A} activity were also examined. The reactions contained 200 mM Tris-glycine pH 8.8, 5 mM $(NH_4)_2SSO_3$, 30 mM KCN, and 0.167 μg or 0.193 μg of YrkF or YrkF^{C15A}, respectively. Rhodanese activities were determined at various concentrations of potassium chloride, potassium sulfate, potassium phosphate, potassium acetate, and sodium sulfite.

Table 2.3. Maintenance of rhodanese assay pH by addition of HCl

Concentrations of solutions in rhodanese assay	
Concentration KCN (mM)	Concentration HCl (mM)[a]
200	125
175	110
125	70
100	50
75	35
65	30
50	25

[a] Values for the [HCl] were based on mock rhodanese assay solutions at which the pH stabilized at 8.8

2.12. Disulfide cross-linking

Disulfide cross-linking experiments were performed with both YrkF and the variant YrkF^{C15A} to determine the interactions between the sole cysteine of the rhodanese domain and the sole cysteine of the Ccd1 domain. The cross-linking experiments were used to determine if any intra- or intermolecular disulfide bonds could be formed in YrkF or the variant protein and were based on published protocols (143-146).

2.12.1. Cross-linking with dibromobimane (bBBr)

The fluorogenic dibromobimane (bBBr) is a thiol-specific bifunctional cross-linking reagent that can be used to determine approximate proximity of cysteine residues within a protein. The alkylating groups of bBBr can cross-link thiol groups of cysteine residues that are within 3-6 Å of each other. The reagent becomes highly fluorescent only when both alkylating groups have reacted and can be visualized using UV transillumination (143, 144).

Purified YrkF and YrkF^{C15A} were removed from –70 °C and thawed on ice. Before treatment with bBBr, each sample (500 µL) was dialyzed in 1 L of degassed buffer consisting of 50 mM Tris-HCl (pH 7.5) for 3 h using a Slide-A-Lyser® Dialysis Cassette (PIERCE) to remove any residual DTT that may have been present after the purification procedure. Approximately 45 µg of each of the dialyzed proteins was incubated with 1.1 mM bBBr at 4 ºC overnight. The samples were then analyzed on 15% SDS-PAGE gel under both reducing (with 5% β-mercaptoethanol) and non-reducing (no β-mercaptoethanol) conditions. The gel was visualized for fluorescence using a UV

transilluminator and photographed. The gel was then stained with Coomassie blue to visualize the protein bands.

2.12.2. Treatment with Cu(1,10-phenanthroline)$_2$SO$_4$ (CuPhen)

Disulfide cross-linking of cysteine residues in the purified proteins YrkF and the variant YrkF^{C15A} was induced by using the oxidizing agent Cu(1,10-phenanthroline)$_2$SO$_4$ (CuPhen). CuPhen is a oxidizing agent that induces the formation of disulfide bonds in proteins (145, 146). Before treatment with CuPhen, samples of YrkF and YrkF^{C15A} were treated with 10 mM DTT for 1 h at 4 ºC and dialyzed in 1L of 100 mM Tris-acetate (pH 8.6) overnight with 3 buffer changes to remove any residual DTT. After dialysis, samples were assayed for rhodanese activity. This activity was considered to be the activity of the fresh sample. Samples were then incubated at 4 ºC for 72 h. After the incubation at 4 ºC, samples were treated with oxidizing agent CuPhen, reducing agent DTT, or received no treatment in a final volume of 50 µL. Oxidizing reactions contained 100 mM Tris-acetate (pH 8.6), 20 µM enzyme, and 0.4 mM CuPhen (prepared by the addition of 4 µL of 10 mM 1,10-phenathroline (dissolved in ethanol) and 2 µL of 10 mM $CuSO_4$ to the reaction mix). Reducing reactions contained 100 mM Tris-acetate (pH 8.6), 20 µM enzyme, and 5 mM DTT. No treatment (control) samples contained only enzyme and buffer. All reactions were carried out at 37 ºC for 30 min. Samples were then assayed for rhodanese activity and compared that that of the fresh sample. Samples of YrkF and YrkF^{C15A} were analyzed in parallel for all steps.

The cross-linking of YrkF by CuPhen was also examined by SDS-PAGE. Approximately 22 µg of YrkF was treated with 2 mM DTT for 45 min on ice to reduce

all disulfide bonds. A portion of the sample was then treated with 0.4 mM CuPhen at 37 °C for 30 min. The remainder of the sample received no further treatment and was incubated at 37 °C for 30 min. The samples of YrkF treated with CuPhen and YrkF left untreated were then analyzed on 15% SDS polyacrylamide gels and visualized with Coomassie blue reagent.

2.13. Mass Spectrometry

Two separate mass spectral studies were performed on YrkF and YrkF^{C15A}. The first study used YrkF and YrkF^{C15A} fractions from the purification schemes mentioned in the Methods (section 2.9). Both samples were subject to treatment with 4 mM DTT on ice for 45 min then dialyzed overnight in 10 mM Tris-HCl (pH 8.0). These samples were then incubated on ice for an additional 45 min before being precipitated with methanol.

The second study utilized a fraction of YrkF that was purified with DTT present at all stages. This purification scheme differs slightly from that mentioned in section 2.9. The sample of YrkF^{C15A} analyzed in this study was purified in the absence of DTT, as described in section 2.9. The fractions of YrkF and YrkF^{C15A} were subjected to the treatments as described below in parallel for mass spectral analysis. Samples were first incubated with 4 mM DTT for 45 min on ice, and then dialyzed in 1 L 10 mM Tris-HCl (pH 8.0) for 2 h. After dialysis, the protein concentration was determined. About 2 nmol of each protein was removed from the samples and immediately prepared for mass spectrometry by methanol precipitation. The remaining DTT-treated samples were split into two equal fractions. One fraction was incubated with 4 mM $(NH_4)_2(SSO_3)$ and one fraction was incubated with Na_2SO_3. The samples were treated for 45 min on ice.

Samples were again dialyzed as before and the protein concentration was determined after dialysis. Approximately 2 nmol of protein sample was precipitated and washed, as described below, and saved for mass spectral analysis.

Protein samples were precipitated using the following procedure. Five volumes of cold methanol was added to the samples, which were then incubated on ice for 30 min. Proteins were pelleted by microcentrifugation at 4 °C for 20 min and were subjected to three 10-minute washes and microcentrifugation cycles with a 70% methanol mixture (performed at 4 °C). The dried pellet was stored at 4 °C and later used for mass spectral analysis.

After methanol precipitation, protein pellets were resuspended in 50% methanol, 10% formic acid at approximately 20 pmol/μL. The samples were analyzed using a Thermo Electron TSQ Quantum mass spectrometer equipped with an electrospray source. Samples were injected into the mass spectrometer at 3-5 μL per min using a 250 μL Hamilton gas-tight syringe. Spray voltage was 4000 volts, sheath gas pressure was 10 psi, capillary tube temperature was 270 °C, tube lens offset was 160 and the lens 0 offset was -1.3. The machine had previously been tuned and calibrated using caffeine as a standard. The m/z range from 550 to 1500 was scanned using Q1 with a 1.5 second scan time and a peak width of 0.7. Data were collected for approximately 5 to 10 min and the spectra were averaged using Xcalibur software. Deconvolution of the averaged spectra was performed manually. The mass spectral analysis was graciously performed by Keith Ray (Virginia Tech).

2.14. Homology modeling of YrkF

2.14.1. Sequence alignments of templates

A BLASTP search using YrkF as the query sequence gave alignments to both the rhodanese domain and the Ccd1 domain. *E. coli* GlpE (20% amino acid sequence identity) matched the YrkF sequence representative of the rhodanese homology domain. *E. coli* YhhP (37% amino acid sequence identity) served as the template for the C-terminal Ccd1 of YrkF. The PBD codes of the rhodanese homolog (GlpE) and the Ccd1 homolog (YhhP) are 1GN0 and 1DCJ, respectively. Two pair-wise sequence alignments (YrkF/GlpE and YrkF/YhhP) were obtained using the ClustalW (147) program at the Biology Workbench website and visualized using the BOXSHADE program (148).

2.14.2. Constructing a model for YrkF

Two independent models, one for each domain, were constructed using the program MODELLER (149, 150) under default parameters. 1GN0 served as the template for the rhodanese domain and 1DCJ served as the template for the Ccd1 domain. The program output 5 pdb files. The best-scoring (lowest energy) model for each of the two domains were chosen and combined into one pdb file, which was used for all subsequent procedures as the model for YrkF.

The LEaP module of AMBER 7.0 (151, 152) was used to slightly manipulate the YrkF model. A peptide bond was created to connect the two domains between Ser^{80} and Ser^{81} using the bond command. The bond command was also used to create a disulfide bond between Cys^{15} and Cys^{149}. The twist command was used to twist the two domains relative to one another until the cysteines were at a distance of about 6 Å. The YrkF

model was then solvated and Na^+ atoms were added to neutralize the system. AMBER parameter files were saved in LEaP and used for subsequent analyses.

2.14.3. Energy Minimization of the YrkF model

The resulting solvated model for YrkF was then subjected to energy minimization. Energy minimization was performed using Simulated Annealing with NMR-Derived Energy Restraints (Sander) in AMBER. The minimization of the entire system was performed for 300 steps using the steepest descent method. The procedure was run under distance restraints for the disulfide and peptide bonds that were created of 4.0 Å and 2.0 Å, respectively. The system was held at constant volume with no scaling pressure and at a constant temperature (300 K) after initial temperature scaling with a non-bonded cutoff of 9.0 Å.

After the initial minimization, the model was subjected to molecular dynamics simulations to equilibrate the water and sodium ions of the system. Sander was used to perform the MD simulations for 100 ps at a timestep of 2 fs with a non-bonded cutoff of 7.0 Å. The temperature was held constant at 300 K for the entire simulation. SHAKE was carried out to restrain bonds containing hydrogens. The resulting model was used to carry out two more energy minimizations. The first minimization was performed on the water and sodium ions under the parameters described above (without distance restraints). A final minimization was run on the whole system under the parameters described above. The subsequent model of YrkF was then subjected to final molecular dynamics simulations and analysis.

2.15. Molecular dynamics (MD) simulations of homology model

Molecular dynamics simulations were performed using the Sander program of AMBER over a period of 2 ns. The model was heated to 300 K over the first 30 ps. Over the next 50 ps, the system was equilibrated at constant volume. The rest of the MD simulation was run at constant pressure. An average model was generated over the last 200 ps of the simulation. This model was then minimized using the steepest descent method as described above to generate a final refined structure for YrkF.

A model of YrkF without a disulfide bond was constructed in the same manner. This model was subjected to the same energy minimization procedures and same MD simulations. Both models were analyzed visually using VMD (153) and the trajectories from the MD simulations were processed using the ptraj/rdparm program. The models were also subjected to analysis of the atomic fluctuation of amino acid residues. The root mean squared deviation (RMSD) of the models were analyzed to determine the stability of the model over the trajectory of the MD simulation.

2.16. Limited Proteolysis of YrkF

YrkF was subjected to limited proteolysis by endopeptidase Glu-C and then analyzed by SDS-PAGE. YrkF (30 μg) was treated with endopeptidase Glu-C at ratios of 1:100, 1:800, 1:2400, and 1:8000 (Glu-C:YrkF, by weight) in 50 mM Tris-HCl (pH 8.3) in a final volume of 90 μL. Reactions were incubated at 25 °C for various times. Proteolysis was stopped by addition of 5 μL of reaction mixture to SDS loading buffer containing β-mercaptoethanol and boiling for five min. For samples indicating 0 min proteolysis, 5 μL of the reaction mixture was added to SDS buffer and boiled

immediately after addition of protease. YrkF samples subjected to proteolysis were analyzed on 15% SDS-polyacrylamide gels and stained using Coomassie blue reagent to visualize protein bands.

CHAPTER THREE

Results

3.1. YrkF possesses rhodanese activity

The elucidation of the *B. subtilis* genome sequence (154) led to the discovery of four genes predicted to encode rhodanese homologs. One of these genes, *yrkF*, was predicted to encode a protein of 185 amino acids composed of a N-terminal Ccd1 and C-terminal rhodanese domain. Vicky Konnyu, an undergraduate researcher in our lab, initiated the work on YrkF by creating the expression vectors pVK2B and pVK3. These vectors overexpressed *yrkF* in *E. coli*. Crude extracts of overexpressed *E. coli* cells were assayed for rhodanese activity. It was found that rhodanese activity was elevated nearly 200 fold compared to induced cells containing the parent plasmid pT7-7. The results indicated that YrkF has rhodanese activity.

3.2. Purification and activity assays of YrkF and YrkF^{C15A}

To date, none of the four predicted rhodaneses encoded by the *B. subtilis* genome have been biochemically characterized. YrkF was overexpressed and purified in order to characterize the rhodanese. Janet Donahue established optimal conditions for the purification of YrkF and the following purification schemes were carried out in a combined effort. YrkF eluted as two peaks of activity during the first chromatographic step. Previous studies with the *E. coli* rhodanese PspE also revealed that the protein eluted as two separate peaks, which were determined to be a sulfur-free and persulfide form of the enzyme (155). Initial studies in determining the number of cyanolyzable sulfur atoms associated with YrkF appeared to indicate, though did not conclusively

prove, the presence of an extra sulfur associated with one of the peaks (data not shown). To optimize the purification of YrkF, the active peak fractions were pooled, the protein was reduced to one major form with DTT, and was rechromatographed. After this chromatographic step, one major peak was eluted at about 0.15 M NaCl. From 1 L of cell culture, the procedure recovered 10.9 mg protein, with 39% yield and 5.6 fold concentration in activity (Table 3.1). The protein was more than 98% pure based on visualization of protein by 12% SDS-PAGE.

The YrkF^{C15A} variant was purified in an attempt to determine the role of Ccd1 in the activity of the enzyme. YrkF^{C15A} was purified in the absence of DTT and required only one chromatographic step. The variant eluted as one major peak of activity at about 0.15 M NaCl. Determination of the number of cyanolyzable sulfur atoms associated with the enzyme indicated the possibility of an extra sulfur atom present, but again the data were inconclusive (data not shown). From 1 L of cell culture, the procedure recovered 14.6 mg protein, with 51% yield and 4.0 fold concentration in activity (Table 3.1). The variant was also more than 98% pure based on visualization of protein by 12% SDS-PAGE (data not shown).

Table 3.1. Purification of YrkF and YrkF^{C15A} from *B. subtilis*.

YrkF						
Step	Vol (ml)	Protein (mg)	Activity (U)	Sp Act (U/mg)	Yield (%)	Fold Purification
Cleared lysate	13.3	96	1802	18.8	100	1
SSS[a]	13.8	84.3	2208	26.2	123	1.4
Anionic Ex I	7.5	17.8	2026	114	112	6.1
Anionic Ex. II	4.5	10.9	708	106	39	5.6
YrkF^{C15A}						
Step	Vol (ml)	Protein (mg)	Activity (U)	Sp Act (U/mg)	Yield (%)	Fold Purification
Cleared lysate	13.8	101	2553	25.3	100	1
SSS[a]	14.2	84.5	2655	31.4	104	1.2
Anionic Ex I	4.5	14.6	1303	100	51	4.0

[a] Streptomycin sulfate supernatant

3.3. SDS-PAGE reveals multiple forms of YrkF and YrkF^{C15A}

During the purification of YrkF and YrkF^{C15A}, distinctive banding patterns were observed on non-reducing SDS gels. After the first chromatographic step, the two peaks of YrkF displayed separate banding patterns. One peak contained three bands (similar to that observed in Figure 3.1 with no DTT) and the other peak consisted mainly of band 3 seen in Figure 3.1. The single peak of purified YrkF^{C15A} revealed banding similar to that seen in Figure 3.1 with no DTT. When treated with DTT, YrkF and YrkF^{C15A} migrated as single bands displaying an apparent molecular mass of 28 kDa (band 2, Figure 3.1). Band 2 presumably contains the fully reduced, denatured form of each enzyme. Analysis of the purified fractions of YrkF or the variant, under non-reducing conditions, revealed the presence of a disulfide-linked dimer in both preparations (band 1, Figure 3.1). YrkF contained a third form (band 3, Figure 3.1) that migrated more rapidly. This form was not present in YrkF^{C15A}. Since YrkF^{C15A} has only one cysteine residue (therefore, cannot form intramolecular disulfide bonds) and treatment of YrkF with reductant eliminated this form, band 3 was hypothesized to contain YrkF with an intramolecular disulfide bond.

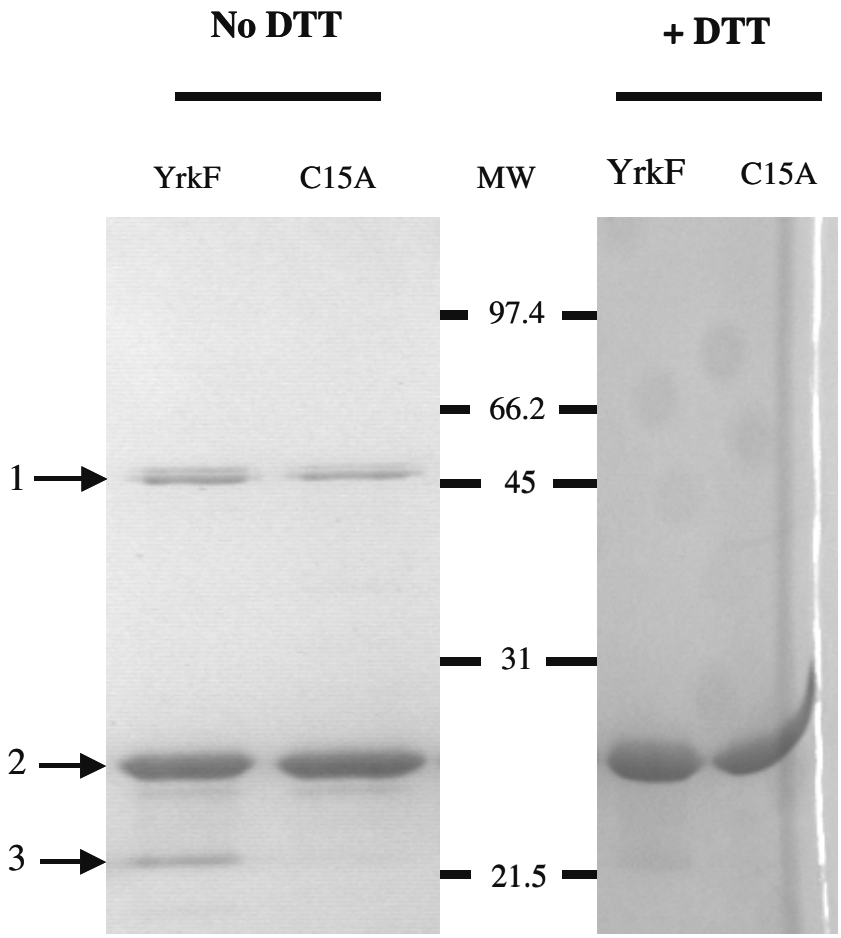

FIG. 3.1. Fractionation of YrkF and YrkF^{C15A} on 12% SDS polyacrylamide gel. YrkF and YrkF^{C15A} were analyzed on 12% SDS gels following treatment with 2.5 mM DTT or without treatment. Under non-reducing conditions the proteins migrated as 2 or 3 distinct bands. The disulfide cross-linked dimer, fully reduced sulfhydryl form, and compact intramolecular disulfide cross-linked form are indicated as bands 1, 2, and 3, respectively.

3.4. Chemical cross-linking of YrkF and YrkF^{C15A}

The rapidly moving form of YrkF observed on the non-reducing SDS gel (band 3, Figure 3.1) was predicted to be a compact form of YrkF resulting from the formation of an intramolecular disulfide bond. The hypothesis was supported by the fact that unreduced preparations of the C15A variant never contained this compact form. As a result, it was further hypothesized that Cys^{15} and Cys^{149} of YrkF were located in close proximity to each other in the 3-dimensional structure of the protein. The fluorogenic bifunctional alkylating agent, dibromobimane (bBBr), can be used to cross-link cysteine residues in proteins when the thiol groups are within 3 – 6 Å of each other (143, 144). The enzyme cross-linked with bBBr is expected to be resistant to reduction by DTT or β-mercaptoethanol, whereas that cross-linked by disulfide bonds would be sensitive. It was also hypothesized that cross-linking of the two cysteine residues would eliminate rhodanese activity. Therefore, the effect of auto- and chemical oxidation (by copper phenanthroline) on rhodanese activity of YrkF and YrkF^{C15A} was examined.

3.4.1. Chemical cross-linking with dibromobimane

After treatment with bBBr and visualization of the gel by UV transillumination, all three forms of YrkF (the compact form, the fully reduced sulfhydryl form, and the disulfide cross-linked dimer), as well as the two forms of YrkF^{C15A} were fluorescently labeled (Figure 3.2 A, lanes 1 and 2). Despite the non-specific fluorescence of the fully reduced forms, the most intense fluorescent band was that of the compact form of YrkF (Figure 3.2 A, lane 1). The intensity of fluorescence of the compact form of YrkF relative to the amount of protein present seems to imply that the dibromobimane reagent

cross-linked Cys^{15} and Cys^{149} successfully (Figure 3.2 A and B, lane 1). The inability to generate a fluorescent compact form of $YrkF^{C15A}$ is consistent with this conclusion.

Upon treatment with β-mercaptoethanol, the untreated samples of YrkF and the C15A variant migrated as the fully reduced sulfhydryl form (Figure 3.2 B, lanes 3 and 4). The Coomassie stained gel revealed that YrkF and $YrkF^{C15A}$ subjected to bBBr treatment were resistant to reduction by β-mercaptoethanol, which suggested that the compact (band 3) form and the dimer (band 1) are cross-linked with the bBBr reagent (Figure 3.2 B, lanes 1 and 2).

If the compact form observed in YrkF is due to an intramolecular cross-linkage, then it is anticipated that its formation would be independent of protein concentration. Therefore, a second experiment was performed to test the reactivity of bBBr forming intramolecular cross-links at various concentrations of YrkF. The molar ratio of YrkF:bBBr (1:40) in each reaction mixture was constant, but the volumes of the reactions ranged from 13 μL to more than 400 μL. Thus, the concentration of YrkF varied more than 30-fold. Following treatment, YrkF was precipitated with methanol using the same procedure for mass spectrometry sample preparation (see Methods). The precipitated protein was then dissolved in SDS-loading buffer and equal amounts of protein were loaded into each well of the SDS gel. The results showed a relatively constant amount of fluorescence for the compact form of YrkF, independent of YrkF concentration (Figure 3.3). Again, the Coomassie stained gel showed that YrkF incubated with bBBr was resistant to reduction by β-mercaptoethanol, indicating an intramolecular cross-link (Figure 3.3). Together, these results suggest that bBBr reacts optimally with the two cysteine residues of YrkF in forming an intramolecular cross-linked bridge with the

reagent. Since bBBr functions optimally with thiol residues approximately 3 – 6 Å apart, the data suggest that Cys^{15} and Cys^{149} are in close proximity to one another. However, the reagent was not 100% efficient in cross-linking YrkF, which suggests that the distance between the two cysteine residues of YrkF fluctuates to greater than 6 Å.

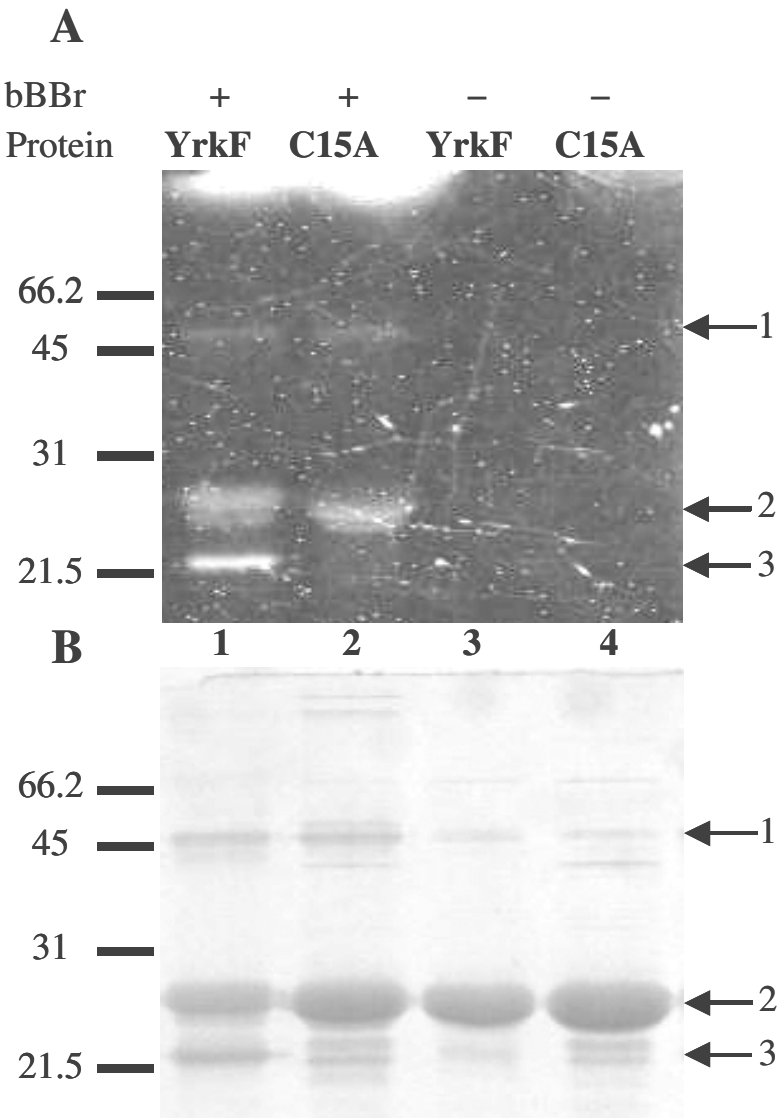

FIG. 3.2. Cross-linking of YrkF and YrkF^{C15A} with dibromobimane.
YrkF (lanes 1 and 3) and YrkF^{C15A} (lanes 2 and 4) were subjected to treatment with the bifunctional cross-linking reagent bBBr (as indicated) followed by treatment with β-mercaptoethanol as described in the Methods. The proteins were visualized for fluorescence on a UV transilluminator (A) and stained with Coomassie (B) following electrophoresis on a 15% SDS polyacrylamide gel. The disulfide cross-linked dimer, fully reduced sulfhydryl form, and compact intramolecular disulfide form are indicated with arrows as bands 1, 2, and 3, respectively. Several bands displayed in the C15A lanes are apparently due to slight impurities in the sample.

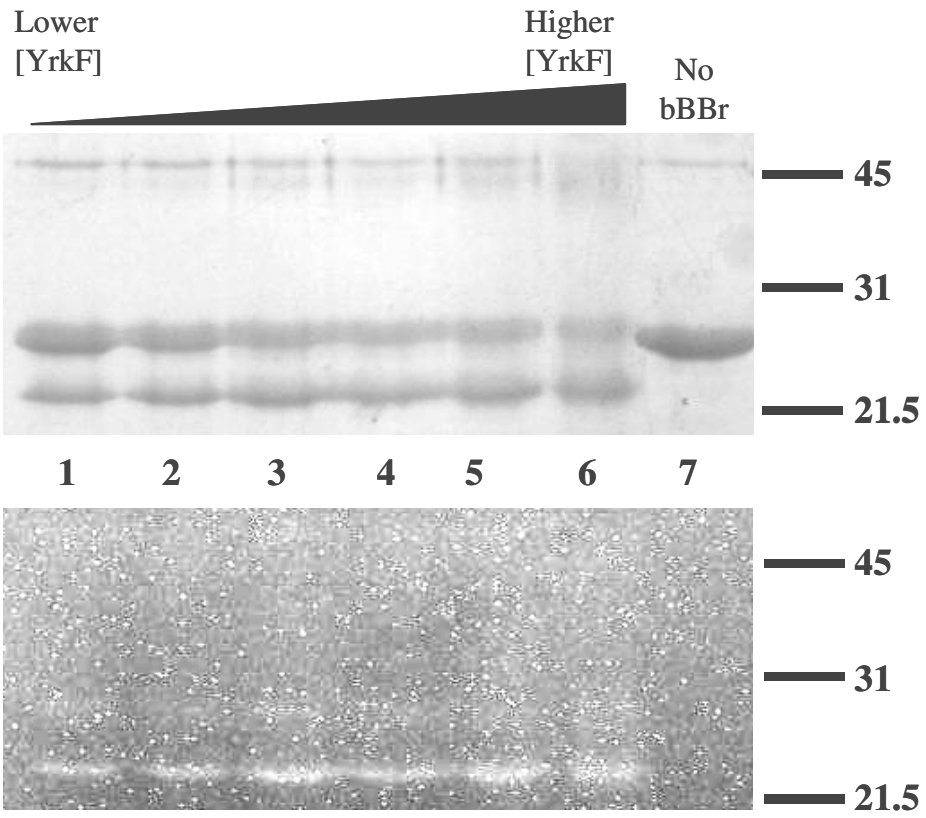

FIG. 3.3. Reactivity of YrkF to bBBr is independent of YrkF concentration. YrkF was treated with bBBr at a constant molar ratio, but in different volumes of reaction mix. Thus, the concentration of YrkF varied. After treatment with bBBr, YrkF was precipitated and then dissolved in SDS-loading buffer. Equal μg of YrkF was added to each well and electrophoresed on 15% SDS polyacrylamide gel in the presence of β-mercaptoethanol. YrkF was stained with Coomassie (top) and visualized for fluorescence on a UV transilluminator (bottom). Lanes 1-6 represent YrkF in the presence of bBBr at a constant molar ratio of 40:1 (bBBr:YrkF). The concentration of YrkF in reactions analyzed in lanes 1-6 was 3.6 μM, 7.1 μM, 13.3 μM, 23.9 μM, 45.6 μM, 115 μM, respectively. YrkF left untreated was analyzed in lane 7 at a concentration of 151 μM.

3.4.2. Chemical cross-linking with Cu (1,10-phenanthroline)

Functional rhodanese proteins contain an active site cysteine persulfide as a catalytic intermediate and, when isolated, often contain this persulfide. Oxidation of the cysteine residues of YrkF or the C15A variant via disulfide bond formation would cross-link the active site cysteine residues, essentially eliminating the active site persulfide and, presumably, rhodanese activity. The effect of autooxidation and induced oxidation on enzymatic activity was examined for YrkF and YrkF^{C15A}. CuPhen (Cu (1,10-phenanthroline)$_2$SO$_4$) is an oxidizing agent that induces the formation of disulfide bonds (145, 146).

To examine the effect of autooxidation, the rhodanese activity of YrkF was measured after incubation at 4 °C for 72 h. This sample was then treated with 0.4 mM CuPhen or 4 mM DTT for 30 min at 37 °C to examine the effects of chemically induced oxidizing and reducing conditions, respectively. The activity of YrkF decreased as an apparent result of autooxidation (Table 3.2). However, the autooxidation appeared to be reversible as treatment of YrkF with the reductant DTT resulted in the recovery of the original rhodanese activity and indicated that the enzyme was not in a denatured state (Table 3.2). The oxidizing reagent, CuPhen, appeared to further cross-link YrkF as indicated by a decrease in the rhodanese activity (Table 3.2). However, about 40 % of the rhodanese activity from CuPhen-treated samples was recovered over time in reducing conditions, suggesting CuPhen did not render YrkF inactive due to denaturation of the protein (data not shown).

The effect of CuPhen on the oxidation of YrkF was examined on SDS-PAGE. YrkF was treated with 2 mM DTT to reduce any disulfide bonds. The reduced YrkF was

then treated with 0.4 mM CuPhen at 37 °C for 30 min. YrkF treated with CuPhen and YrkF left untreated was analyzed on 15% SDS polyacrylamide gel (Figure 3.4). The gel shows that YrkF treated with DTT was reduced (Figure 3.4, band 2). However, YrkF samples treated with CuPhen were oxidized as indicated by the appearance of the dimer (Figure 3.4, band 1) and the intramolecular cross-linked form of YrkF (Figure 3.4, band 3). These results are consistent with the hypothesis that CuPhen oxidizes the two cysteine residues of YrkF, which then decreases rhodanese activity.

$YrkF^{C15A}$ behaved similarly when subjected to the same treatments. The variant enzyme was more prone to autooxidation, and treatment with the oxidizing agent CuPhen increased oxidation as indicated by the decreased rhodanese activity of the enzyme (Table 3.2). The activity of the variant was recovered upon treatment with reductant (Table 3.2). The data from treatment of both enzymes suggest that autooxidation and induced oxidation cause disulfide bond formation, which inhibits activity. Additionally, the oxidation and inhibition of activity is reversible as treatment with reductant results in the recovery of activity. Furthermore, SDS-PAGE analysis of $YrkF^{C15A}$ samples treated with CuPhen indicated the enzyme was cross-linked by the reagent (data not shown).

Table 3.2. Rhodanese activities of YrkF and YrkF^{C15A} under oxidizing and reducing conditions.

YrkF	
Incubation Condition	Specific Activity[a]
Fresh[b]	63.8
72 h 4 °C	27.2
30 min, 37 °C CuPhen[c]	5.3
30 min, 37 °C DTT[d]	63.3
YrkF^{C15A}	
Incubation Condition	Specific Activity[a]
Fresh[b]	31.1
72 h 4 °C	6.9
30 min, 37 °C CuPhen[c]	3.4
30 min, 37 °C DTT[d]	52.2

[a] Standard rhodanese (as described in Methods) activity given in U/mg

[b] After removal from –70 °C, samples treated with 10 mM DTT and dialyzed overnight (See Methods)

[c] 0.4 mM CuPhen was added to sample treated at 4 °C for 72 h

[d] 5 mM DTT was added to sample treated at 4 °C for 72 h

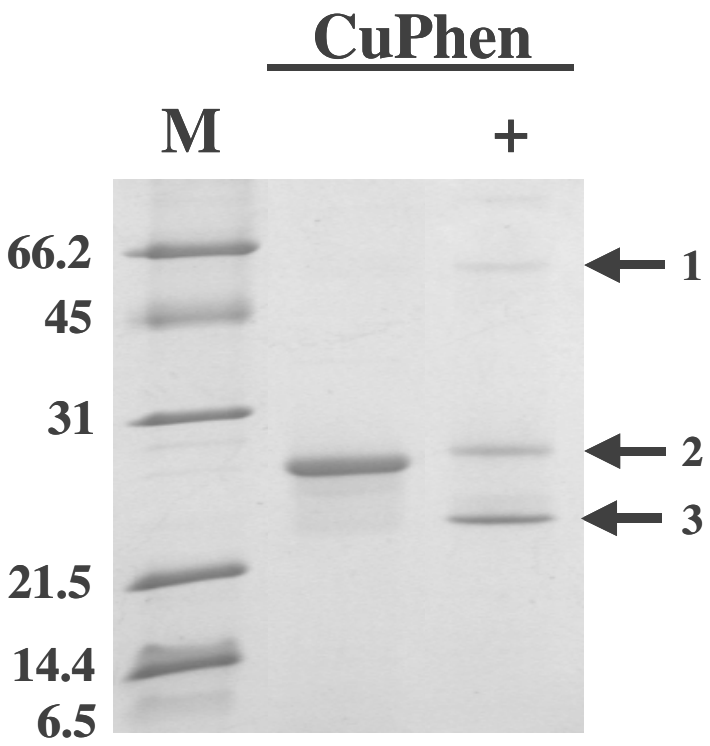

FIG. 3.4. Chemical cross-linking of YrkF by CuPhen.

YrkF was treated with 2 mM DTT to reduce the enzyme (band 2). YrkF was then treated with 0.4 mM CuPhen at 37 °C for 30 min. YrkF treated with CuPhen displays the oxidized dimer (band 1) and the intramolecular cross-linked form (band 3).

3.5. Covalent sulfur modifications of YrkF and YrkF^{C15A}

Mass spectral analysis performed on the rhodanese PspE of *E. coli* yielded mass-to-charge (*m/z*) ratios consistent with the hypothesis that the enzyme exists in both a sulfur-free form and a stable persulfide form (unpublished lab data). However, other apparent modifications to PspE included sulfite, thiosulfate, and polysulfide, presumably on the active site cysteine, which were increased by treatment with thiosulfate. Mass spectral analysis was performed on YrkF and YrkF^{C15A} to determine the nature of the active site cysteine in the "as isolated" YrkF and YrkF^{C15A}, and to determine if active-site cysteine could be readily modified in a stable state. Two separate mass spectral studies were performed (Table 3.3). The two studies will be referred to as study I and study II.

Table 3.3. Mass spectral studies of YrkF and YrkF^{C15A}

Study I			
Enzyme	Purification	Treatment	Precipitation
YrkF	DTT present in final step	4 mM DTT	45 min after dialysis[a]
YrkF^{C15A}	DTT absent	4 mM DTT	45 min after dialysis[a]

Study II			
Enzyme	Purification	Treatments	Precipitation
YrkF	DTT present throughout	4 mM DTT, SO_3^{2-}, or SSO_3^{2-}	Immediately after dialysis[b]
YrkF^{C15A}	DTT absent	4 mM DTT, SO_3^{2-}, or SSO_3^{2-}	Immediately after dialysis[b]

[a] Dialyzed in 10 mM Tris-HCl (pH 8.0) overnight

[b] Dialyzed in 10 mM Tris-HCl (pH 8.0) for 2 h

Results obtained from both studies indicate that YrkF with a cysteine persulfide is a stable form of the enzyme (Figure 3.5). Interestingly, the results from the two studies were slightly different. Study I revealed two charged species of YrkF, corresponding to the sulfur-free and persulfide (+32.6 Da) forms (Table 3.4). The predominant species was the persulfide form of the enzyme even after DTT treatment. However in study II, YrkF treated with DTT or sulfite exhibited only one charged species, equivalent to the sulfur-free form of YrkF in both cases (Table 3.4). YrkF from study II treated with thiosulfate displayed two charged species. One species corresponded to the sulfur-free form and one to the persulfide form (+31.5 Da), though the predominant species observed was the sulfur-free form. Results obtained from study II were consistent with similar studies involving RhdA (156). Surprisingly, complete removal of the persulfide sulfur from YrkF in study I was not seen when treated with 4 mM DTT. These results are noteworthy because treatment of RhdA with a low concentration of DTT (0.2 mM) removed its persulfide sulfur (156).

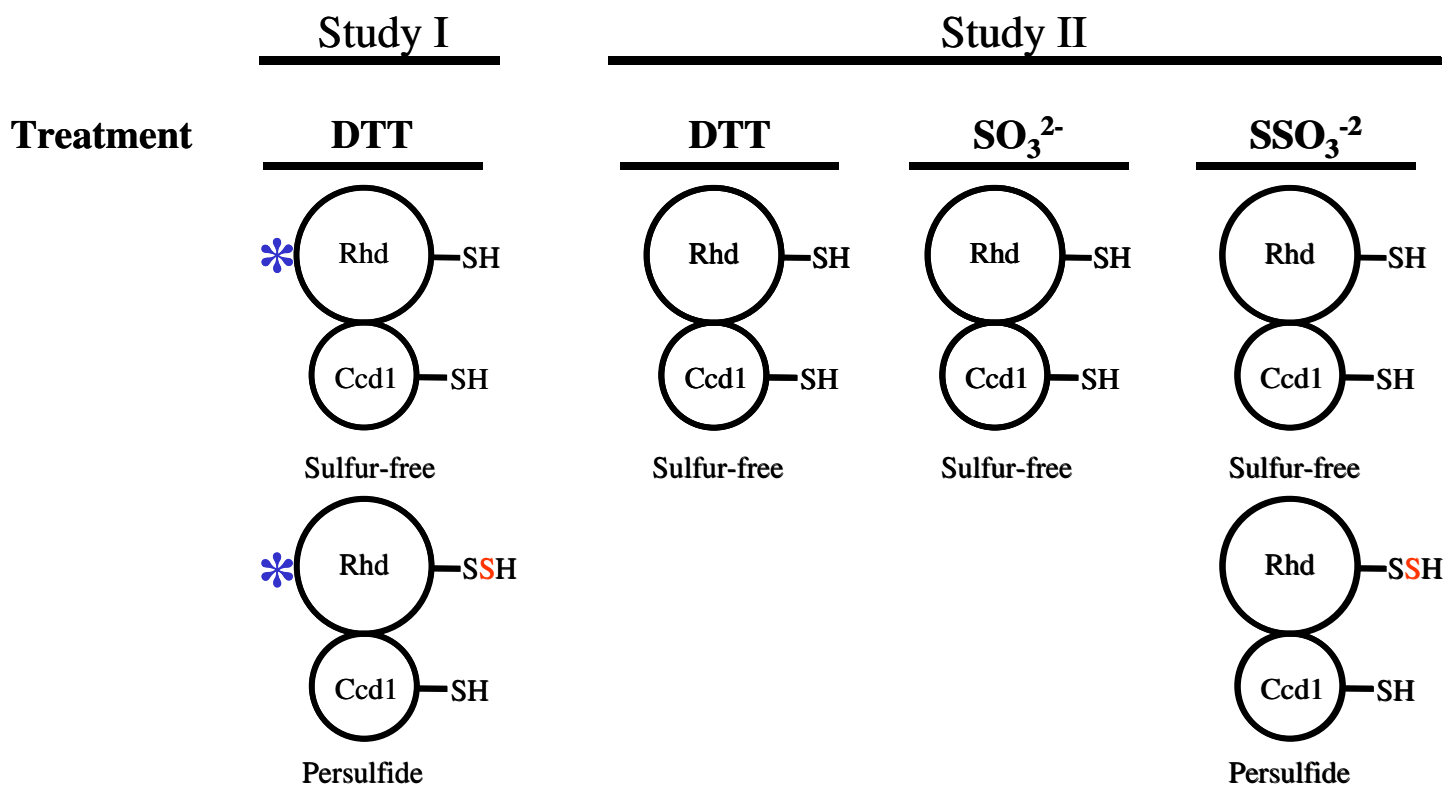

FIG. 3.5. Forms of YrkF consistent with data obtained by mass spectrometry.

Mass spectral studies I and II were performed following the indicated treatments (as described in the text). Rhd, catalytic rhodanese domain, SH, sulfhydryl group, S, persulfide atom, *, YrkF sample in which DTT was present only during final purification step.

Table 3.4. Mass spectral analysis of YrkF after various treatments.

Study I[a]			
Treatment[b]	# of charged species	Calculated Molecular Mass, Da[c]	Mass Difference (modified-unmodified), Da
DTT	2	20656.1 20688.7	32.6

Study II[d]			
Treatment[b]	# of charged species	Calculated Molecular Mass, Da[c]	Mass Difference (modified-unmodified), Da
DTT	1	20656.6	
Sulfite	1	20658.1	
Thiosulfate	2	20657.0 20688.1	31.5

[a] DTT (1 mM) was present only during final stage of purification. Sample was dialyzed overnight and was not immediately precipitated with methanol following dialysis.

[b] Samples were treated for 45 min on ice using 4 mM DTT, 4 mM sulfite, 4 mM thiosulfate.

[c] Average molecular mass was calculated based on the mass spectrum of each enzyme. Theoretical molecular mass of YrkF is 20654.6 Da.

[d] DTT (1 mM) present in all stages of purification. Samples were dialyzed for 2 h and were immediately precipitated with methanol following dialysis.

The mass spectral data for YrkF^{C15A} indicated that the variant was more readily modified than YrkF (Figure 3.6). Analysis of YrkF^{C15A} from study I displayed one charged species consistent with the formation of a disulfide-linked dimer (Table 3.5). The formation of dimers of YrkF^{C15A} in study I likely occurred as a result of not immediately precipitating the enzyme after initial DTT treatment due to a longer dialysis time. However, YrkF from study I displayed only monomer forms of the enzyme, which suggests that YrkF^{C15A} is more prone to oxidation than YrkF.

Other treatments of YrkF^{C15A} (study II) revealed a number of different modifications (Figure 3.6). Treatment of YrkF^{C15A} with DTT followed by immediate methanol precipitation and analysis revealed one charged species that was consistent with a sulfur-free form of the variant (Table 3.5). However, treatment with sulfite yielded charged species corresponding the sulfur-free form and a form containing an additional 79.6 Da (Table 3.5). These results are consistent with the addition of a sulfite molecule (80 Da) to the enzyme, presumably at the active site cysteine (Figure 3.6). Mass spectral analysis of YrkF^{C15A} after treatment with thiosulfate also revealed two charged species corresponding to the native enzyme and a +111.3 Da-species (Table 3.5). The results are consistent with the addition of a thiosulfate molecule (112 Da) to the enzyme. Furthermore, there was no indication that a stable persulfide formed on YrkF^{C15A} (Figure 3.6). These results suggest a persulfide sulfur form is more stable in YrkF and that YrkF^{C15A} is more susceptible to other modifications of the active site cysteine.

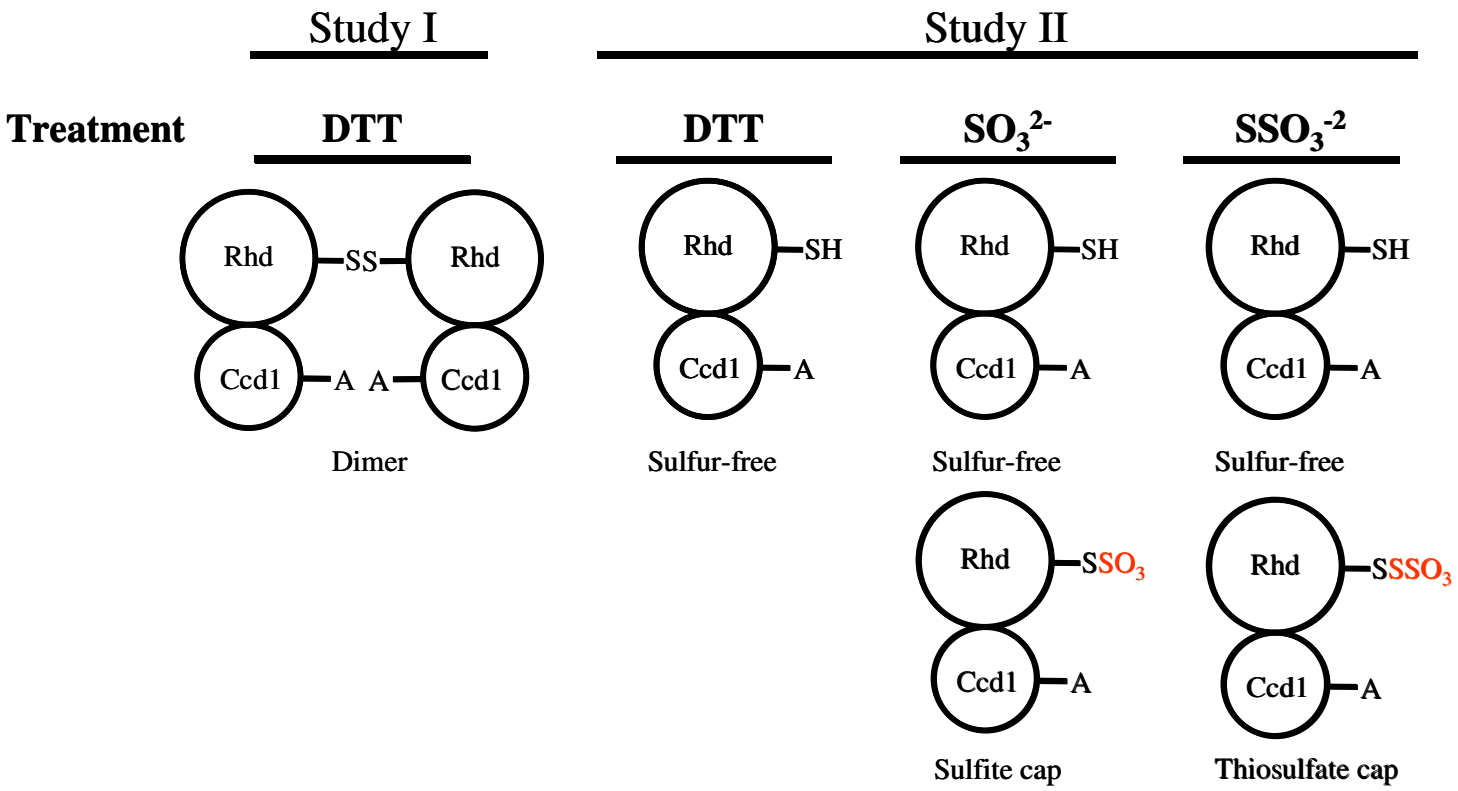

FIG. 3.6. Forms of YrkFC15A consistent with data obtained by mass spectrometry.

Mass spectral studies I and II were performed following the indicated treatments (as described in the text). Rhd, catalytic rhodanese domain, Ccd1, conserved cysteine domain 1, SH, sulfhydryl group, SSO_3, thiosulfate, SO_3, sulfite, "A", the Cys to Ala substitution in $YrkF^{C15A}$.

Table 3.5. Mass spectral analysis of $YrkF^{C15A}$ after various treatments.

Study I[a]			
Treatment[b]	# of charged species	Calculated Molecular Mass, Da[c]	Mass Difference (modified-unmodified), Da
DTT	1	41247.4[d]	

Study II[e]			
Treatment[b]	# of charged species	Calculated Molecular Mass, Da[c]	Mass Difference (modified-unmodified), Da
DTT	1	20625.3	
Sulfite	2	20625.4	
		20705.0	79.6
Thiosulfate	2	20626.0	
		20737.3	111.3

[a] DTT was absent during purification. Sample was dialyzed overnight and was not immediately precipitated with methanol following dialysis.

[b] Samples were treated for 45 min on ice using 4 mM DTT, 4 mM sulfite, 4 mM thiosulfate.

[c] Average molecular mass was calculated based on the mass spectrum of each enzyme. Theoretical molecular mass of $YrkF^{C15A}$ is 20,622.6 Da

[d] Theoretical molecular mass of disulfide-linked dimer is 41,243.2 Da

[e] DTT was absent during purification. Samples were dialyzed for 2 h. Samples were immediately precipitated with methanol following dialysis.

Results from the mass spectral analysis of YrkF and YrkF^{C15A} suggest that the Ccd1 Cys^{15} participates in stabilizing the enzyme. Cys^{15} apparently stabilizes the cysteine persulfide of YrkF such that it is not susceptible to removal by DTT unless subjected to prolonged treatment with the reductant (Figure 3.7). YrkF can regain the cysteine persulfide sulfur with thiosulfate treatment, which is consistent with previous reports on rhodaneses (Figure 3.7). Moreover, the variant, lacking Cys^{15}, is more prone to oxidation and has no indication of a possessing a stable cysteine persulfide at the active site after DTT treatment (Figure 3.6). The variant is also more prone to covalent modifications of the active site (Figure 3.8). These covalent modifications may be a result of reactions with the disulfide-linked dimer form of YrkF^{C15A} (Figure 3.8). Since YrkF^{C15A} readily oxidizes to a dimer and thiosulfate and sulfite can reduce disulfide bonds (3), the covalent modification of the active site by thiosulfate and sulfite could theoretically occur via reactions with the disulfide bond of a YrkF^{C15A} dimer (Figure 3.8).

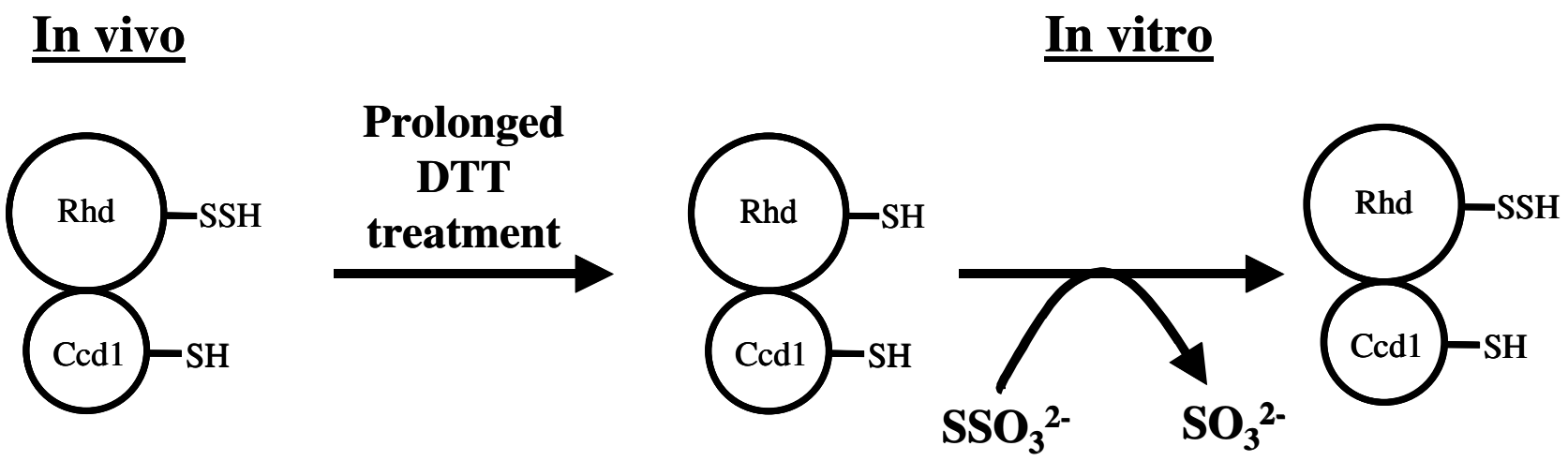

FIG. 3.7. Interpretation of mass spectral data for YrkF.

The above scheme is based on the results of mass spectral analysis of YrkF. Rhd, catalytic rhodanese domain, Ccd1, conserved cysteine domain 1

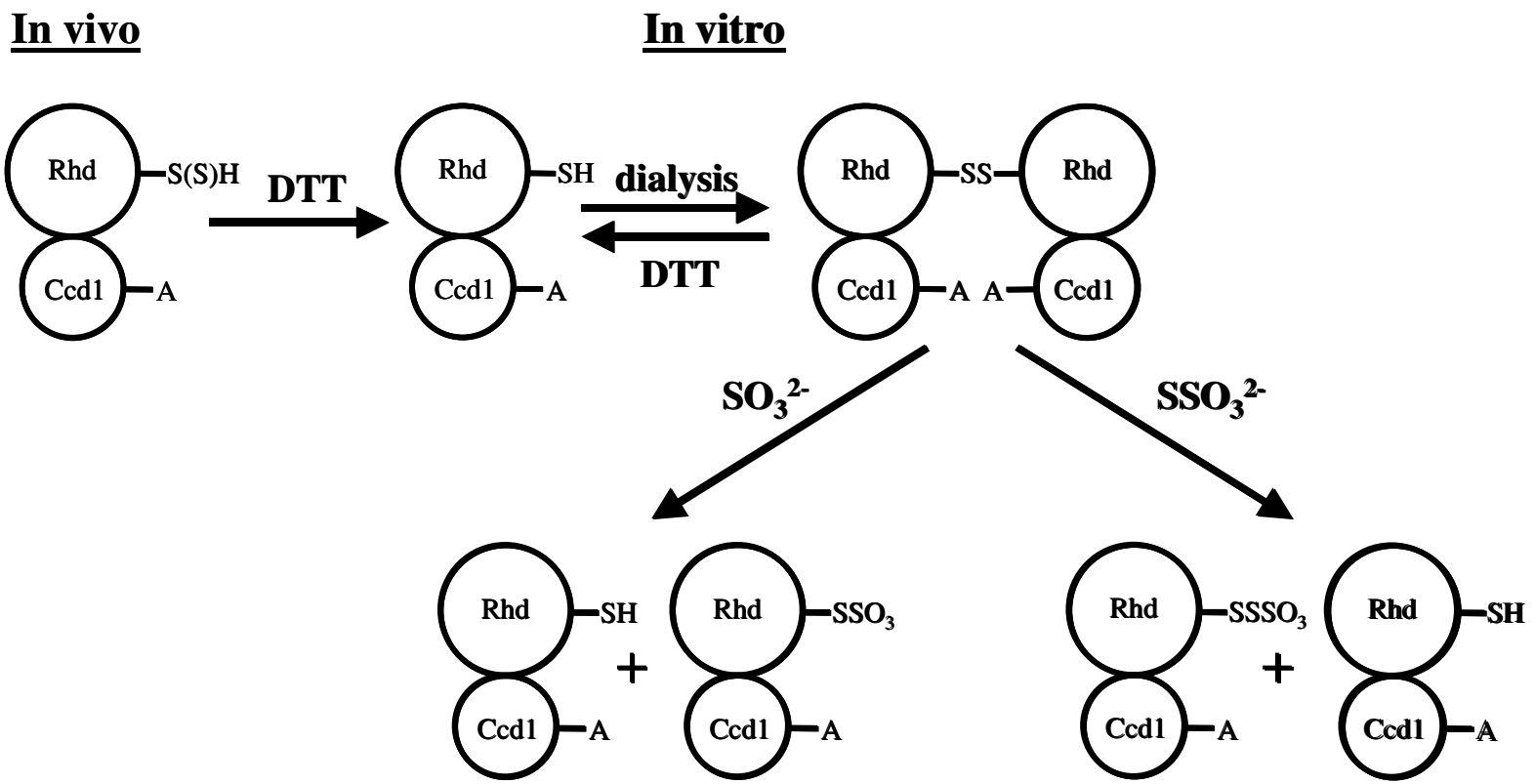

FIG. 3.8. Interpretation of mass spectral data for YrkF^{C15A}.

The above scheme is based on the results of mass spectral analysis of YrkF^{C15A}. Rhd, catalytic rhodanese domain, Ccd1, conserved cysteine domain 1, "A", the Cys to Ala substitution in YrkF^{C15A}

3.6. Kinetic analysis of the YrkF and YrkF^{C15A}

The catalytic properties of rhodaneses have been well characterized. Theses enzymes utilize a double-displacement (ping-pong) mechanism for the transfer of sulfane sulfur from thiosulfate to cyanide in which the transferred sulfur is covalently bound to the active site cysteine during the catalytic cycle (157). Rhodanese activities of YrkF were determined at various concentrations of SSO_3^{2-} at a series of fixed concentrations of CN^- and *vice versa*. The primary plots of velocity versus concentration of thiosulfate and cyanide displayed a normal hyperbolic response (Figure 3.9 A and B). The data from the analysis of YrkF were fit to a double reciprocal (Lineweaver-Burke) plot (Figure 3.10 A). The data from the activity measurements for YrkF fit an equation consistent with a ping-pong mechanism (Figure 3.10 A). A secondary replot (Figure 3.10 B) of the apparent V_{max} versus concentration of cyanide was used to calculate the apparent values for the K_m SSO_3^{2-}, K_m CN^-, V_{max}, and the k_{cat} of YrkF. The K_m for SSO_3^{2-} and CN^- of the wild type were 1 mM and 30 mM, respectively. The V_{max} was estimated to be 156 μmol SCN^- produced/min/mg and YrkF showed a k_{cat} of 81 s^{-1} (Table 3.6).

Based on initial kinetic data, the C15A variant did not display evidence of a double displacement mechanism. The primary plot of the velocity versus concentration of thiosulfate displayed a normal hyperbolic response (Figure 3.11 A), whereas the plot of the velocity versus cyanide concentration displayed a different response (Figure 3.11 B). The plot of velocity versus cyanide concentration indicates a sigmoidal response between measured rhodanese activity and the cyanide concentration (Figure 3.11 B). Since the kinetic data indicated that YrkF^{C15A} did not behave properly in response to the changing concentration of cyanide, the double-reciprocal replot was not consistent with a

ping-pong mechanism (Figure 3.12). Therefore, it was not possible to predict the catalytic mechanism of YrkF^{C15A} based on the kinetic data alone. However, the kinetic parameters of YrkF^{C15A} were estimated by reploting the apparent V_{max} values versus concentration of CN as was done for YrkF. The replots of the kinetic data for YrkF^{C15A} displayed apparent K_m values for CN^- and SSO_3^{2-} of 150 mM and 1 mM, respectively (Table 3.6). The estimated values of the V_{max} and k_{cat} of YrkF^{C15A} were calculated to be 98 μmol SCN^- produced/min/mg and 51 s^{-1}, respectively (Table 3.6).

Previous studies have shown rhodaneses to be susceptible to inhibition by sulfite and other anions (158, 159). The presence of the anions phosphate, sulfate, acetate, and chloride at an ionic strength of around 0.2 resulted in negligible decreases in rhodanese activity for both YrkF and YrkF^{C15A} (data not shown). The addition of 0.5 mM sulfite reduced the activity of both enzymes by about 65% (Figure 3.13). These data suggest that sulfite can compete with CN^- to accept sulfur from YrkF and YrkF^{C15A} and demonstrate that the enzymes are susceptible to product inhibition.

A

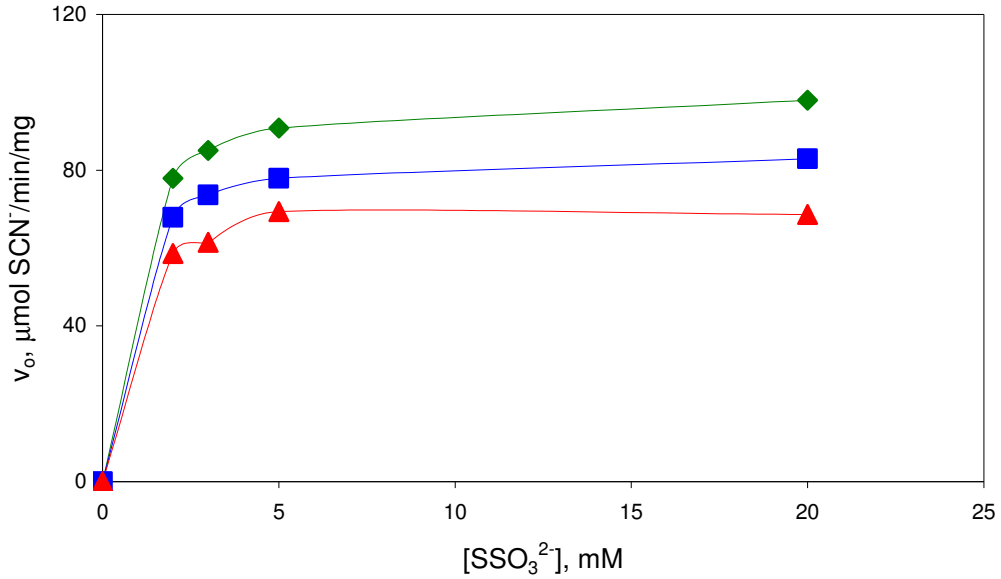

B

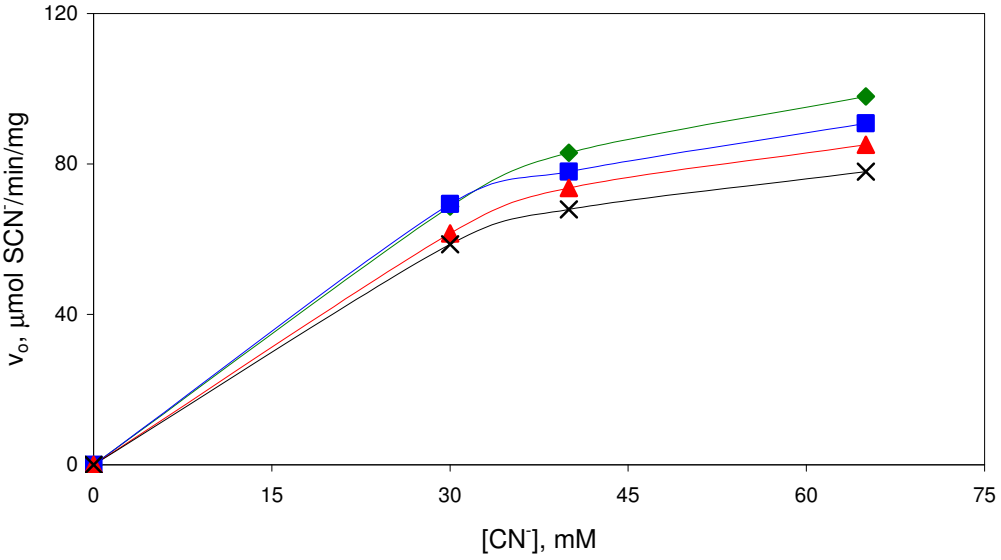

FIG. 3.9. YrkF kinetic characterization, velocity vs. substrate concentration.

The kinetic data for the thiosulfate:cyanide sulfurtransferase activity of YrkF was determined via rhodanese assays, as described in the text, containing 0.167 µg of protein. Plot of velocity versus the concentration of (A) SSO_3^{2-} at various fixed concentrations of CN^- or (B) CN^- at various fixed concentrations of SSO_3^{2-}. (A) Concentrations of cyanide 30 mM (▲), 40 mM (■), 65 mM (●). (B) Concentrations of thiosulfate 2 mM (x), 3 mM (▲), 5 mM (■), 20 mM (●).

A

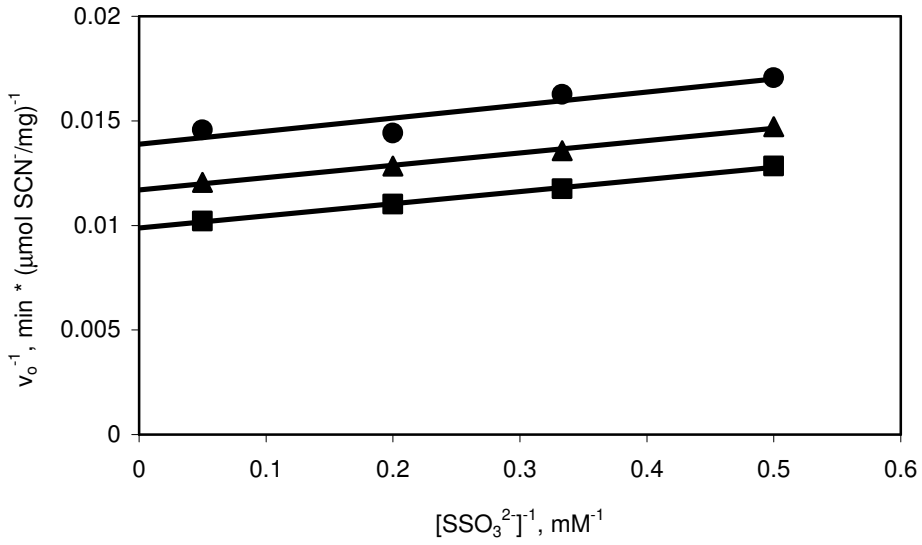

B

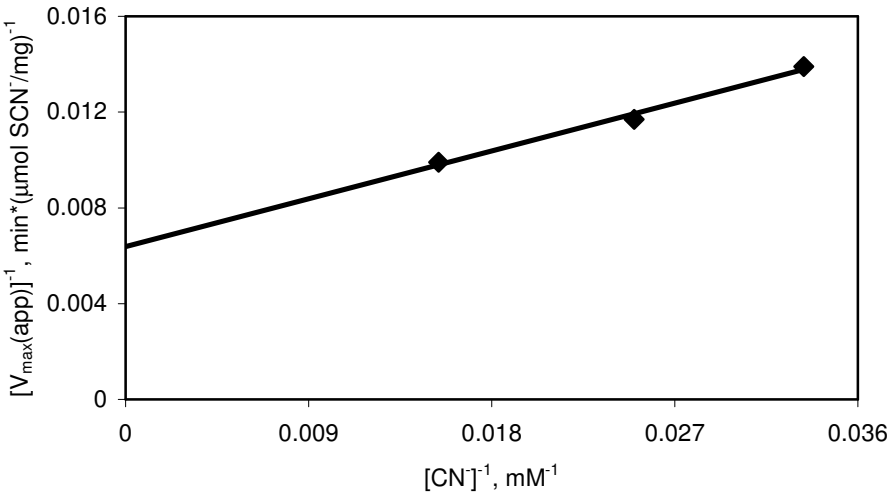

FIG. 3.10. Kinetic characterization of YrkF.

(A) The double-reciprocal replot of the rate of thiocyanate formed versus thiosulfate concentration for YrkF. The concentrations of cyanide used were 30 mM (●), 40 mM (▲), and 65 mM (■). (B) The secondary double-reciprocal replot of the apparent V*max* (y-intercept) from the data in panel A versus cyanide concentration.

Table 3.6. Estimated kinetic parameters of YrkF and YrkF^{C15A}.

Parameter	YrkF	YrkF^{C15A}
K_m SSO_3^{2-}	1 mM	1 mM
K_m CN^-	30 mM	150 mM
V_{max}	156 μmol SCN^-/min/mg	98 μmol SCN^-/min/mg
k_{cat}	81 s^{-1}	51 s^{-1}

A

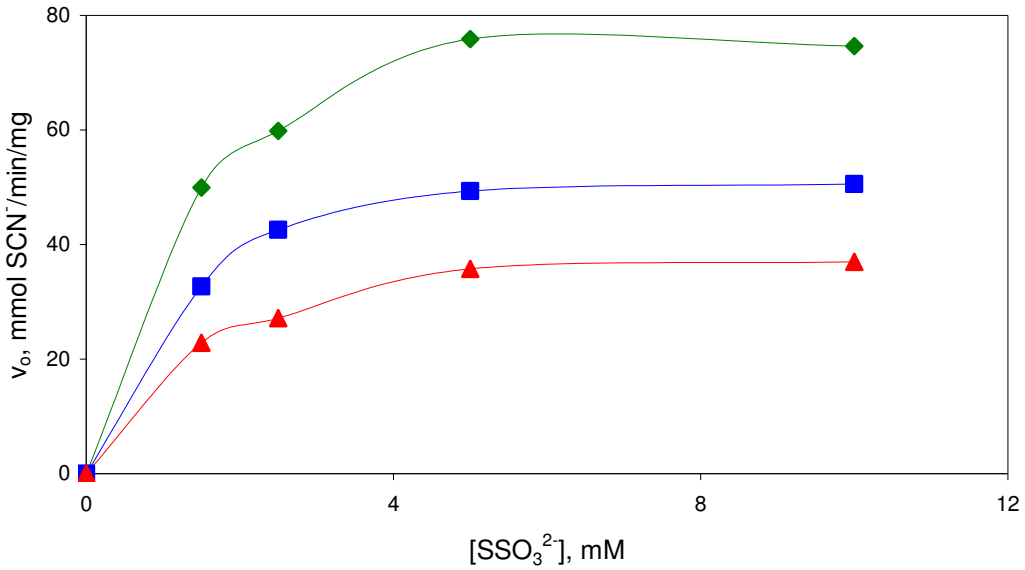

B

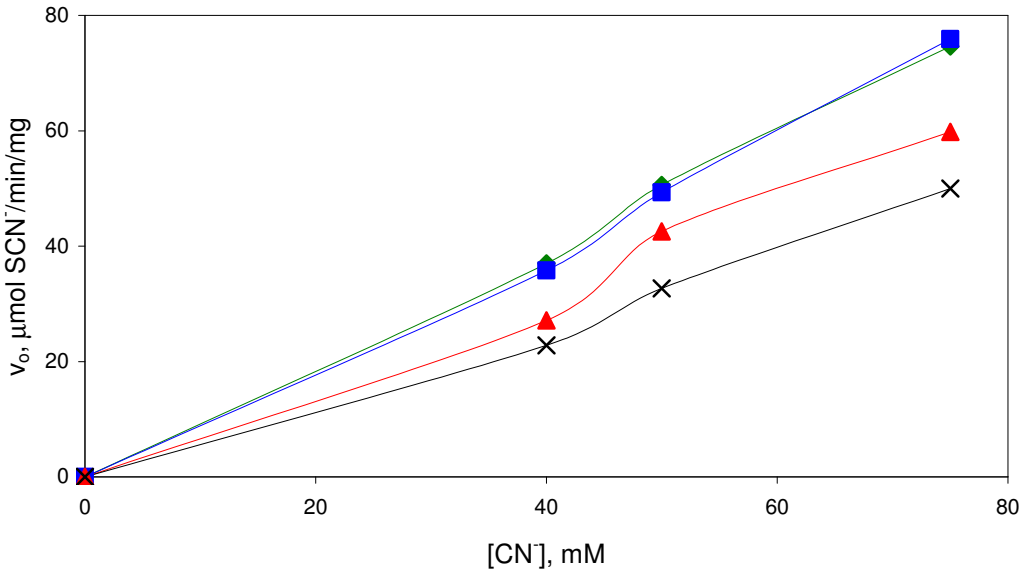

FIG. 3.11. YrkF^{C15A} kinetic characterization, velocity vs. substrate concentration.

The kinetic data for the thiosulfate:cyanide sulfurtransferase activity of YrkF^{C15A} was determined via rhodanese assays, as described in the text, containing 0.193 µg of protein. Plot of velocity versus the concentration of (A) SSO_3^{2-} at various fixed concentrations of CN^- or (B) CN^- at various fixed concentrations of SSO_3^{2-}. (A) Concentrations of cyanide 40 mM (▲), 50 mM (■), 75 mM (●). (B) Concentrations of thiosulfate 1.5 mM (x), 2.5 mM (▲), 5 mM (■), 10 mM (●).

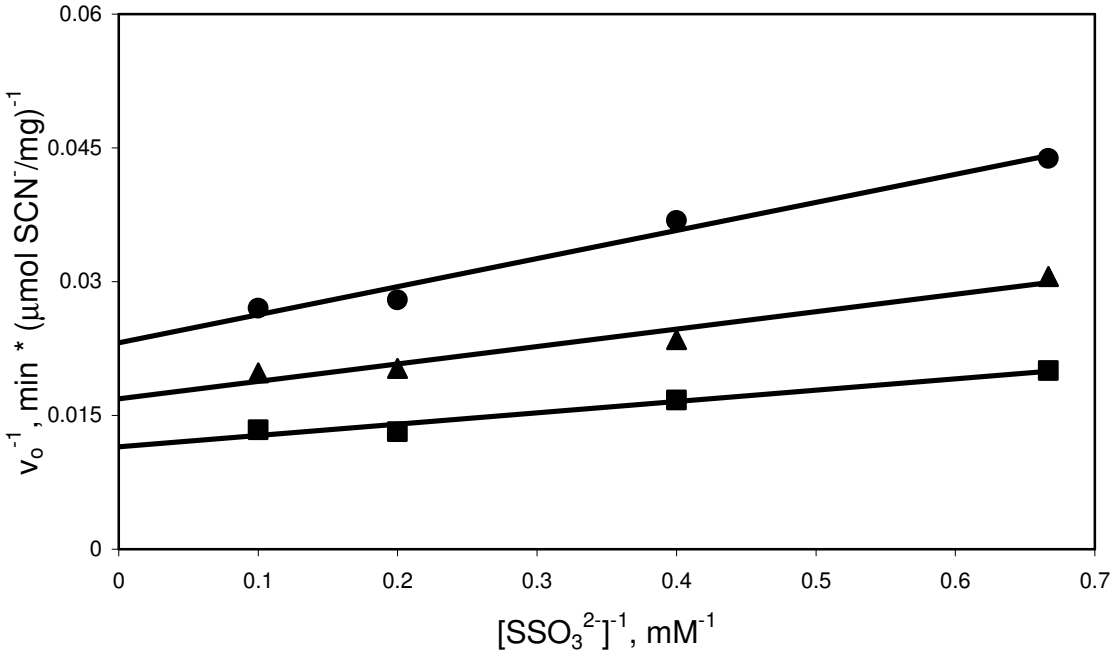

FIG. 3.12. Kinetic characterization of YrkF^{C15A}.

Panel shows graph of the double-reciprocal replot of the rate of thiocyanate formed versus thiosulfate concentration for YrkF. The concentrations of cyanide used were 40 mM (●), 50 mM (▲), and 75 mM (■).

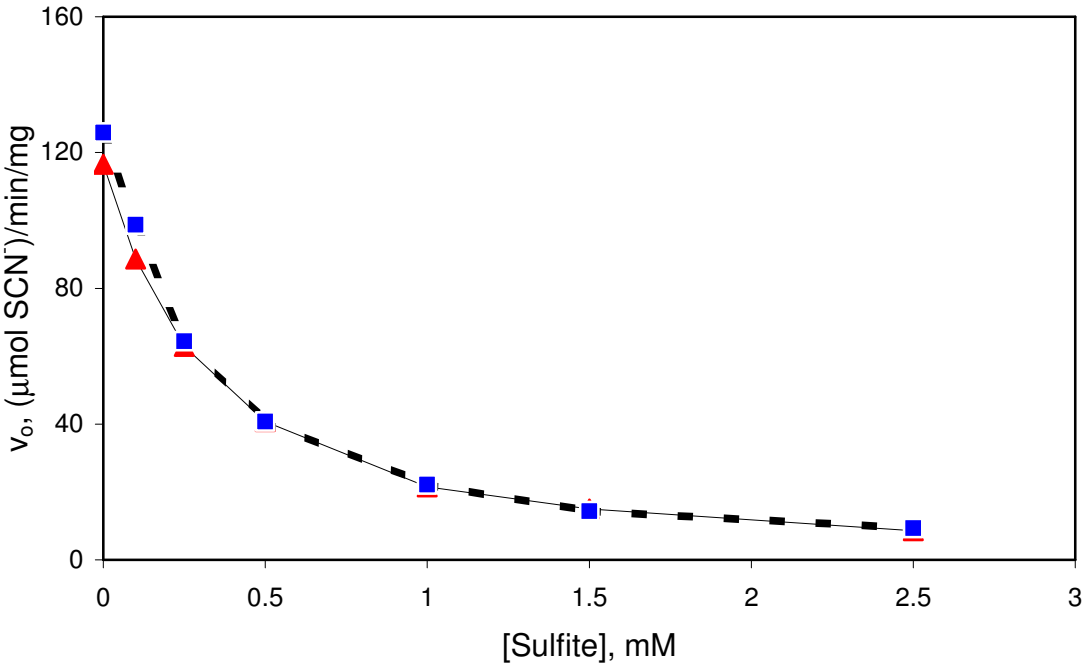

FIG. 3.13. Inhibition of YrkF and YrkF^{C15A} rhodanese activity by sulfite.
The activity of YrkF (▲) and YrkF^{C15A} (■) was determined in the presence of Na_2SO_3 as indicated. Reactions contained 200 mM Tris-glycine (pH 8.8), 5 mM $(NH_4)_2SSO_3$, 30 mM KCN, and 0.167 or 0.193 µg of YrkF or YrkF^{C15A}, respectively. Reactions mixtures were incubated at 25 °C for 3 min and rhodanese activity was determined as described in Methods.

3.7. Homology modeling of YrkF

Attempts to crystallize YrkF using the hanging drop method under conditions used to crystallize the rhodanese GlpE (160) were unsuccessful. However, a homology model was developed for the enzyme based on solved structures for proteins homologous to each of the two domains of YrkF. GlpE of *E. coli* (20% amino acid sequence identity) was used as the template for the rhodanese domain, and YhhP of *E. coli* (37% amino acid sequence identity) was used as the template for the Ccd1 domain. The two domains were independently modeled and then were connected by a six amino acid region of the protein that was not homologous to either domain. The connecting region was hypothesized to be a flexible tether region that connects the two domains. The two domains were positioned relative to one another based on results of the bBBr experiment, which indicated that the two cysteine residues are located in a close proximity to each other. These data from the bBBr studies drastically decreased the degrees of freedom for the position of the two domains relative to each other. Two separate models of YrkF were developed and subjected to Molecular Dynamics (MD) simulations. One model contained a disulfide bond connecting the two cysteine residues, and the other model did not contain a disulfide bond.

3.7.1. YrkF without an intramolecular disulfide bond

A model for YrkF was generated based on the average structure of the final 200 ps of the MD simulations (Figure 3.14). The model shows the N-terminal Ccd1 domain and the C-terminal rhodanese domain connected via a flexible tether. After MD

simulations, the distance between Cys^{15} and Cys^{149} increased from ~ 6 Å to ~ 11 Å. Each domain was then compared to the structure of its template.

The Ccd1 domain of YrkF was modeled on the basis of its alignment with the *E. coli* protein YhhP. YhhP contains a βαβαββ fold and forms a two-layered α/β sandwich (126). One layer is composed of the four β strands, and the other layer consists of the two a helices. Katoh *et al.* also highlight the fact that these α helices show a slightly bent conformation relative to one another (Figure 3.15). The Ccd1 domain modeled in YrkF shows many similarities to the structure of YhhP. The model indicates a βαβαββ topology like that of YhhP (Figure 3.15). Further examination reveals that the Ccd1 domain forms a hydrophobic core between the α helices, which are in the same bent conformation seen in YhhP.

The structure of a typical rhodanese domain displays an α/β topology, with α-helices surrounding a central β-sheet core (34, 39, 43). After MD simulations, the rhodanese domain of the YrkF model displayed a structure with similar α/β structures (Figure 3.16). The model of YrkF contained β-strands in the hydrophobic center of the enzyme flanked by α-helical structures and was comparable to the template GlpE (Figure 3.16).

The active site of YrkF is also comparable to GlpE, though the amino acid composition is quite different. Both active site loops are located following a β-strand and proceed into an α-helix. Further examination shows that the active site loop of YrkF displays a similar "cradle-like" fold characteristic of rhodaneses (34, 39). The active site cysteine sulfur lies at the bottom of the shallow pocket created by the active site loop (Figure 3.17). The structures of RhdA and GlpE reveal an active site cysteine persulfide

that is stabilized by a hydrogen-bonding network composed of the main chain amide groups, as well as by a strong positive electrostatic field produced by positively charged residues in the active site loop (35, 39). The distance between the main chain amide groups of the YrkF active site loop and Cys^{149} are similar to those observed in RhdA and GlpE (data not shown). The model also suggests that the active site residues of YrkF create a positive electrostatic field that could stabilize a persulfide sulfur (Figure 3.18).

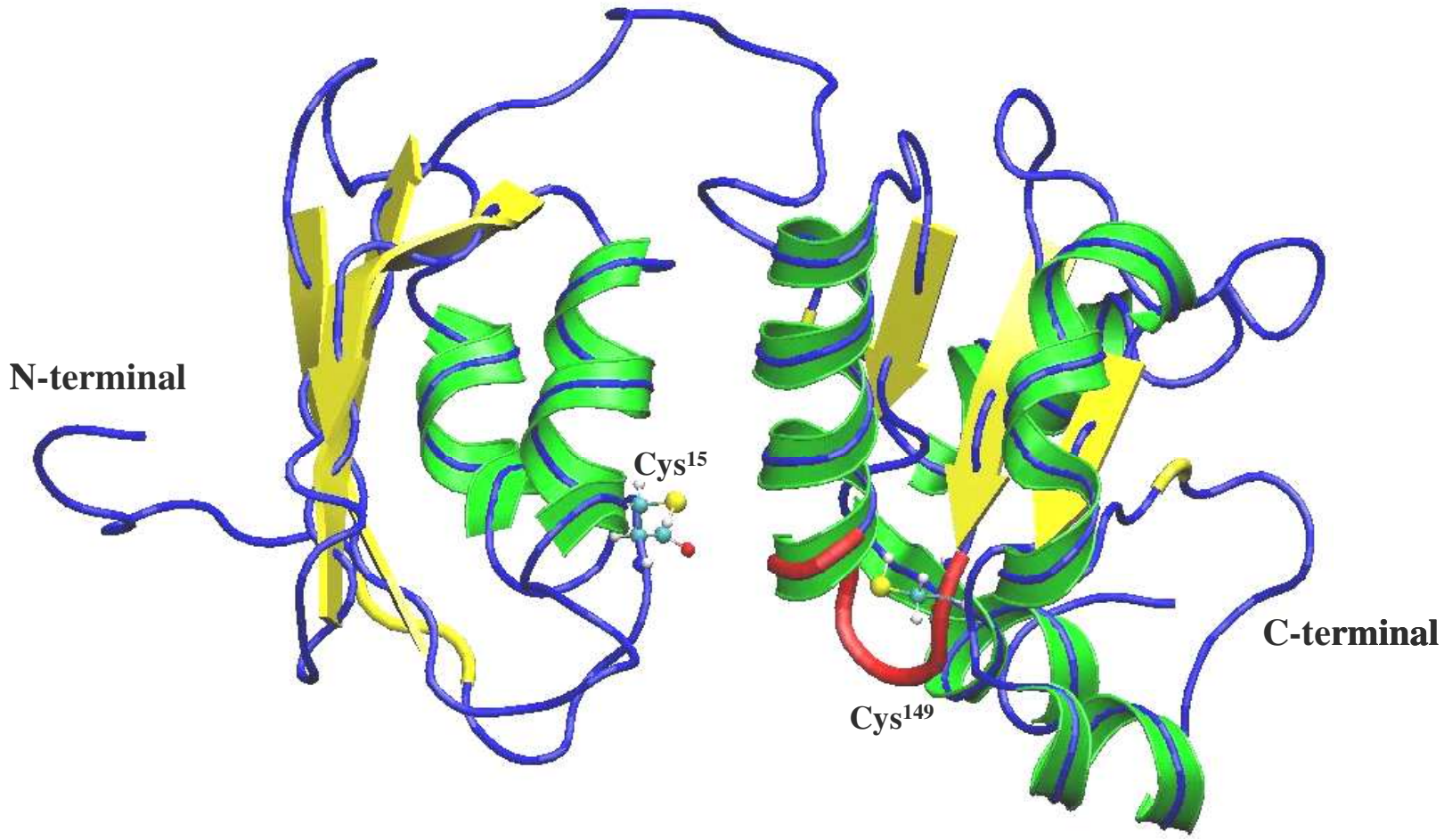

FIG. 3.14. Homology model of YrkF without a disulfide bond.

The active site loop of YrkF is shown in red. Cys^{15} and the catalytic Cys^{149} are labeled. Green, α-helices; Yellow, β-strands

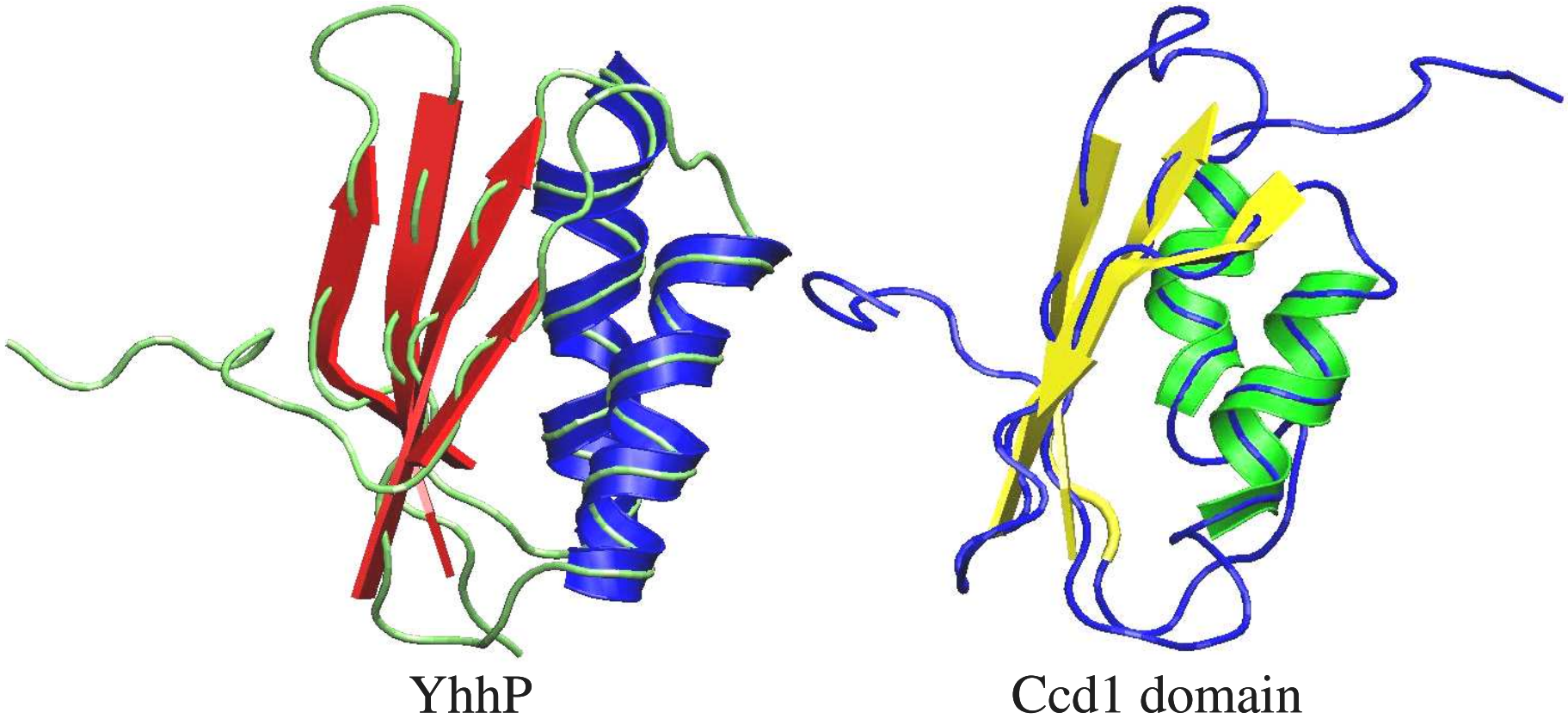

FIG. 3.15. Comparison of YhhP with the Ccd1 domain of YrkF model.

The template (YhhP) used to model the Ccd1 domain of YrkF is indicated. Blue, α-helices; Red, β-strands. The N-terminal domain of the YrkF model without a disulfide bond is also shown. Green, α-helices; Yellow, β-strands

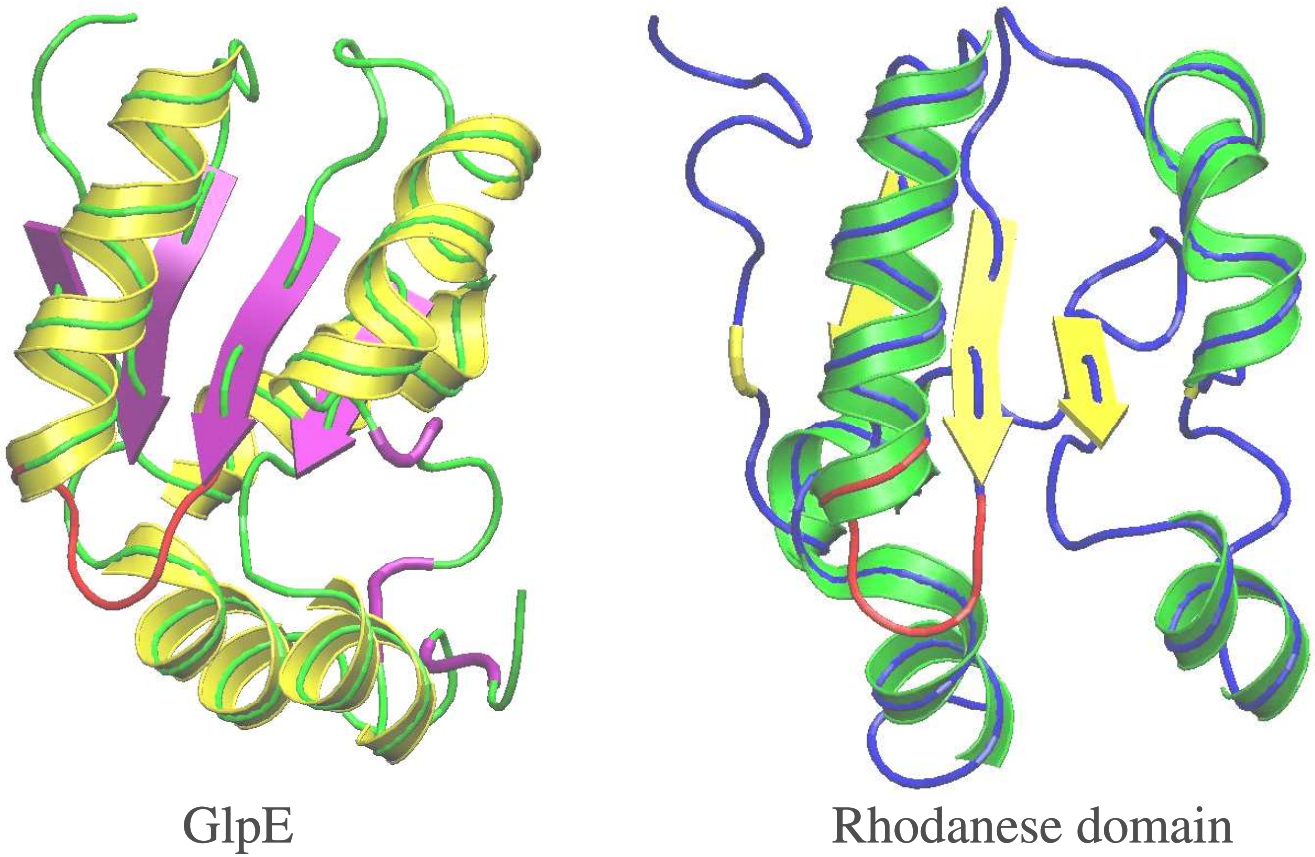

FIG. 3.16. Comparison of GlpE with the rhodanese domain of the YrkF model.

The template (GlpE) used to model the rhodanese domain of YrkF is indicated. Yellow, α-helices; Purple, β-strands. The rhodanese domain of the YrkF model not containing a disulfide bond is also labeled. Green, α-helices; Yellow, β-strands. The active site loop is highlighted in red.

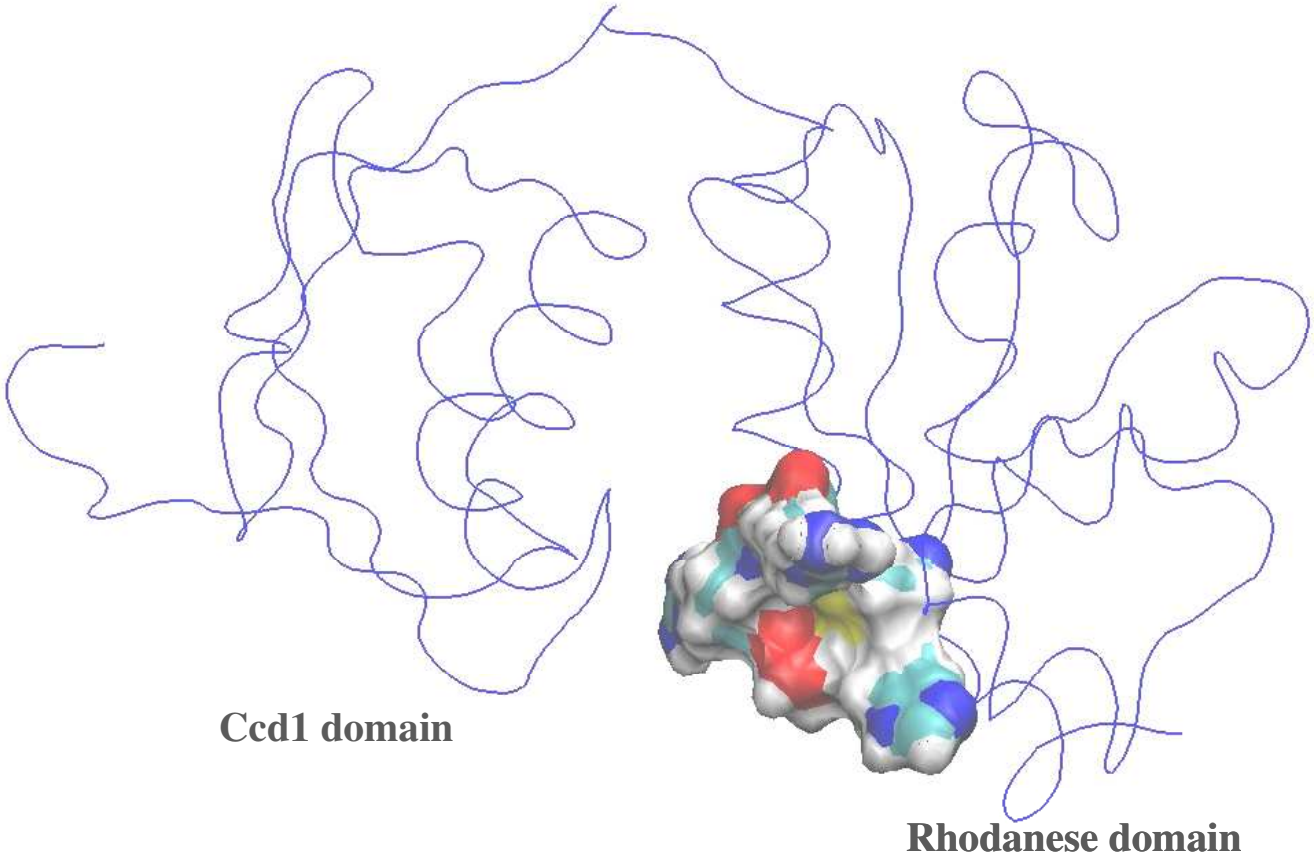

FIG. 3.17. Surface representation of the rhodanese active site loop.

The surface of the active site loop of the rhodanese domain from the first YrkF model is shown. Cyan, carbon; Blue, nitrogen; Red, oxygen; White, hydrogen; Yellow sulfur. A blue tube indicates the protein backbone and highlights the position of the active site relative to the two domains.

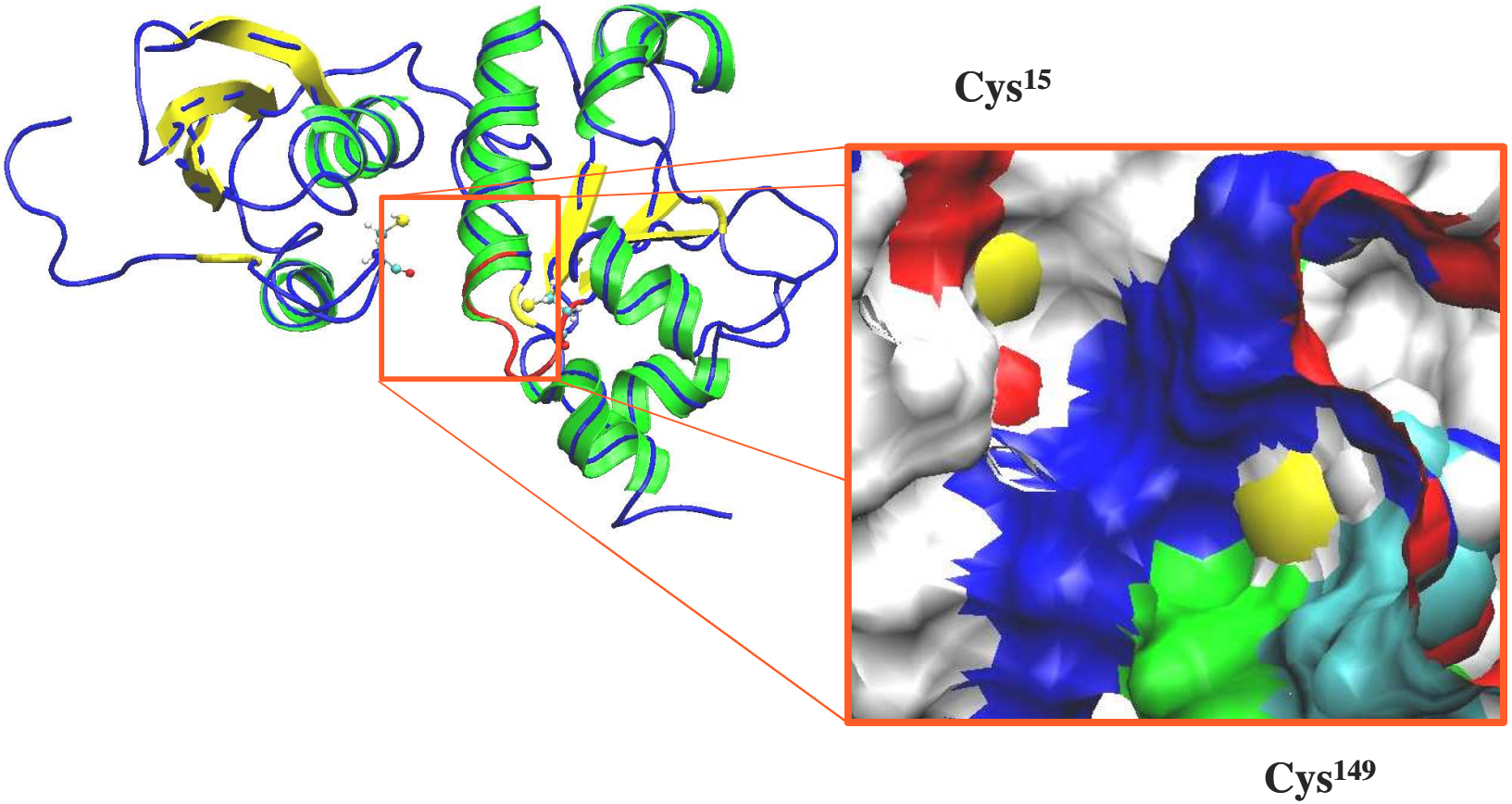

FIG. 3.18. Zoomed-in image of the rhodanese and Ccd1 interface including the active site loop.

The interface between the Ccd1 domain and the rhodanese domain of the first YrkF model is shown on the right. In the surface representation shown in the red box: Blue, positively charged residues; Red, negatively charged residues; White; polar residues; Green; non-polar residues. Cys^{15} and Cys^{149} are indicated.

3.7.2. YrkF with an intramolecular disulfide bond

A model of YrkF containing a disulfide bond was generated based on the final 200 ps of the MD simulations and evaluated (Figure 3.19). The overall structure of YrkF was conserved relative to the model without a disulfide bond. The N-terminal Ccd1 domain contained a α/β topology similar to that seen in the first model and the α-helices were in the same bent conformation as before (Figure 3.19). However, the C-terminal rhodanese domain of the disulfide cross-linked model became slightly more unraveled. Some of the α-helices and one β-strand are not as well defined in the cross-linked model as in the non-cross-linked model (Figure 3.19).

The cross-linked model also contained an active site fold similar to that of the first model. The distance between the main chain amide groups and the Cys^{149} were similar and the active site loop adopted a "cradle-like" shape. However, the disulfide bond caused a conformational change of the active site loop relative to the Ccd1 domain (Figure 3.20 A). The YrkF model without a disulfide bond present shows the active site pocket pointing down and away relative to the core of the Ccd1 and rhodanese domains (Figure 3.17). As a result of the disulfide bond, the active site pocket of the second YrkF model aligns directly with the Ccd1 domain and causes a greater interaction to occur at the domain interface (Figure 3.20 B). However, these results are to be expected by the introduction of a disulfide bond and may illustrate one reason for a decrease in activity observed in oxidized YrkF.

Crystal structures of tandem repeat rhodaneses (RhdA and bovine rhodanese) show that the two domains are orientated relative to one another on a 2-fold axis connected by a linker peptide (35, 43). Therefore, there is precedence for modeling YrkF

as two independently-folded domains, facing one another and connected via a peptide linker. Moreover, the structures of the models for YrkF are consistent the results observed from cross-linking experiments. Dibromobimane experiments suggest that Cys^{15} and Cys^{149} are within 3 – 6 Å of one another. Therefore, the position of the two domains relative to one another is likely correct for the YrkF model. Additionally, the position of the cysteine residues and the presence of a flexible loop would facilitate the formation of the cross-linked forms of YrkF observed in the bBBr and CuPhen experiments and the SDS gel analysis under non-reducing conditions. Finally, the position of the positively charged residues in the model of the active site is consistent with the hypothesis that a stable persulfide sulfur can form on YrkF.

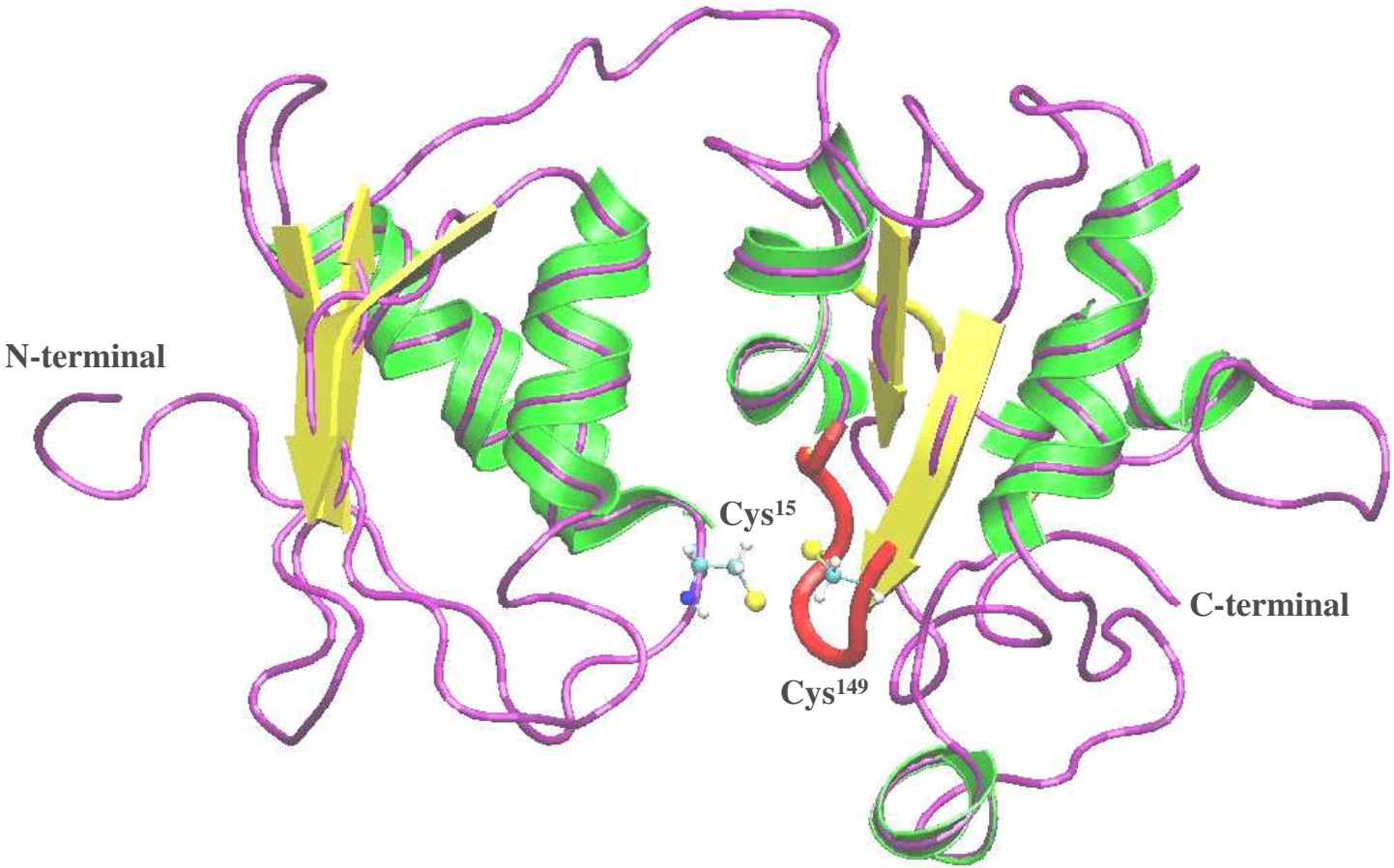

FIG. 3.19. Homology model of YrkF containing a disulfide bond.

The model of YrkF shown contains a disulfide bond, though not represented. The active site loop is highlighted in red and Cys^{15} and Cys^{149} are indicated. Green, α-helices; Yellow, β-strand

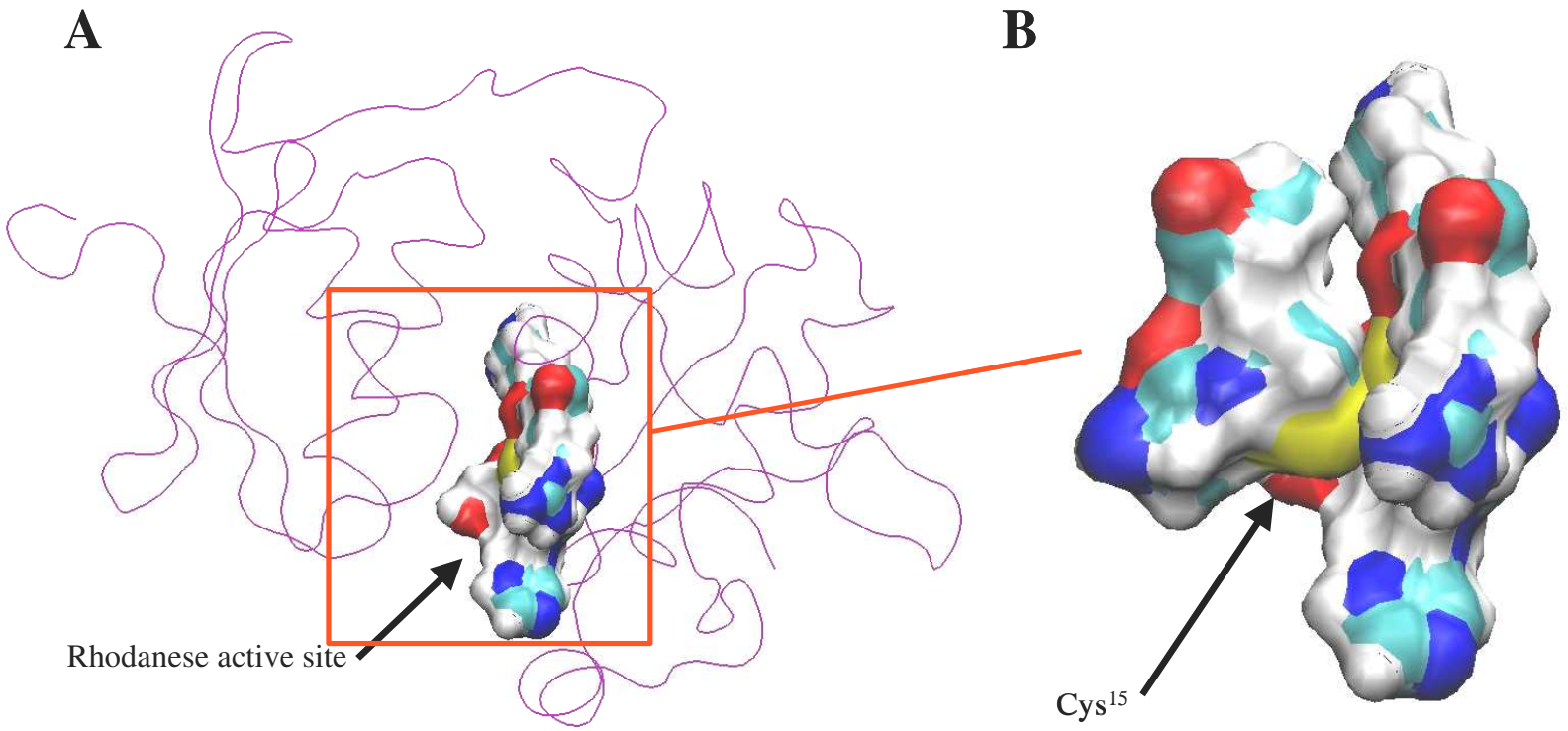

FIG. 3.20. Surface representation of the rhodanese active site loop in the second YrkF model.

The second YrkF homology model contained a disulfide bond between Cys^{15} and Cys^{149} (active site cysteine). (A) Rhodanese active site shown as surface representation. Cyan, carbon; Blue, nitrogen; Red, oxygen; White, hydrogen; Yellow, sulfur. The protein backbone is shown as a purple tube. (B) Close-up view of the active site loop and the Ccd1 domain interface. Both Cys^{15} and Cys^{149} are shown, but only Cys^{15} is labeled

3.8. Limited Proteolysis of YrkF

When developing the YrkF homology model, it was hypothesized that the two domains are connected via a flexible loop region of about six amino acid residues that do not align with either template (Figure 3.21). If the region encodes a flexible loop connecting the two domains, then the residues within the loop should be exposed to solvent and may be readily accessible to proteases. To test this possibility, limited proteolysis of YrkF was carried out using glutamic acid endopeptidase (Glu-C) from *Staphylococcus aureus* V8. There are two glutamic acid residues (Glu^{78} and Glu^{82}) that lie within the proposed flexible loop highlighted in Figure 3.21.

The homology model predicts that seven of the 23 Glu residues of YrkF are exposed to solvent, with the other residues located within the globular region of the protein. These seven residues are shown in Figure 3.22 A. The molecular masses of peptides resulting from Glu-C cleavage at each of these particular residues were calculated (Figure 3.22 B). Since undigested YrkF moves abnormally slowly on SDS-PAGE, it is impossible to assign exact masses to the peptide bands on the SDS gel (Figure 3.22 C). However, the observed banding pattern suggested YrkF was initially cleaved at three different sites at equal rates. Two of the cleavage sites create one large fragment (I and III) and one small fragment (II and IV). The third cleavage site generates peptides of near equal mass (V and VI) (Figure 3.22 C).

Analysis of the SDS-gel indicates cleavage at two separate sites that generate large peptide fragments (I and III) and their respective smaller fragments (II and IV). The size of the large peptide fragment that would be generated by cleavage at Glu^{33} would be relatively consistent with the migration band I and the small peptide would be

consistent with band II (Figure 3.22 B and C). Cleavage at Glu^{65}/Glu^{67} would generate two peptide fragments with sizes that would be consistent with bands III and IV (Figure 3.22 B and C). However, whether cleavage occurs at Glu^{65} or Glu^{67} cannot be distinguished based only on the SDS gel.

The migration of bands V and VI are consistent with cleavage at a residue that would generate two peptides of similar sizes. Proteolytic cleavage at Glu^{78}, Glu^{82}, Glu^{103}, or Glu^{114} could generate two peptides consistent with bands V and VI (Figure 3.22 B). Cleavage at Glu^{78} or Glu^{82} is considered most likely, since cleavage at Glu^{103} would generate peptides very similar in size (differing by only 1835 Da (Figure 3.22 B)) and cleavage at Glu^{114} would generate fragments quite different in size (4400 Da, Figure 3.22 B). The residue at which cleavage occurs cannot be determined unequivocally since the exact sizes of the peptide bands on the SDS gel are unknown. Nevertheless, cleavage at residue Glu^{78} or Glu^{82} (two residues within the proposed flexible loop) would generate bands consistent with those observed in Figure 3.22 C. Therefore, the results suggest the presence of a readily cleavable flexible loop even though there is no conclusive evidence that cleavage occurs at Glu^{78} or Glu^{82}. Mass determination or N-terminal sequencing of the peptide bands could resolve the issue.

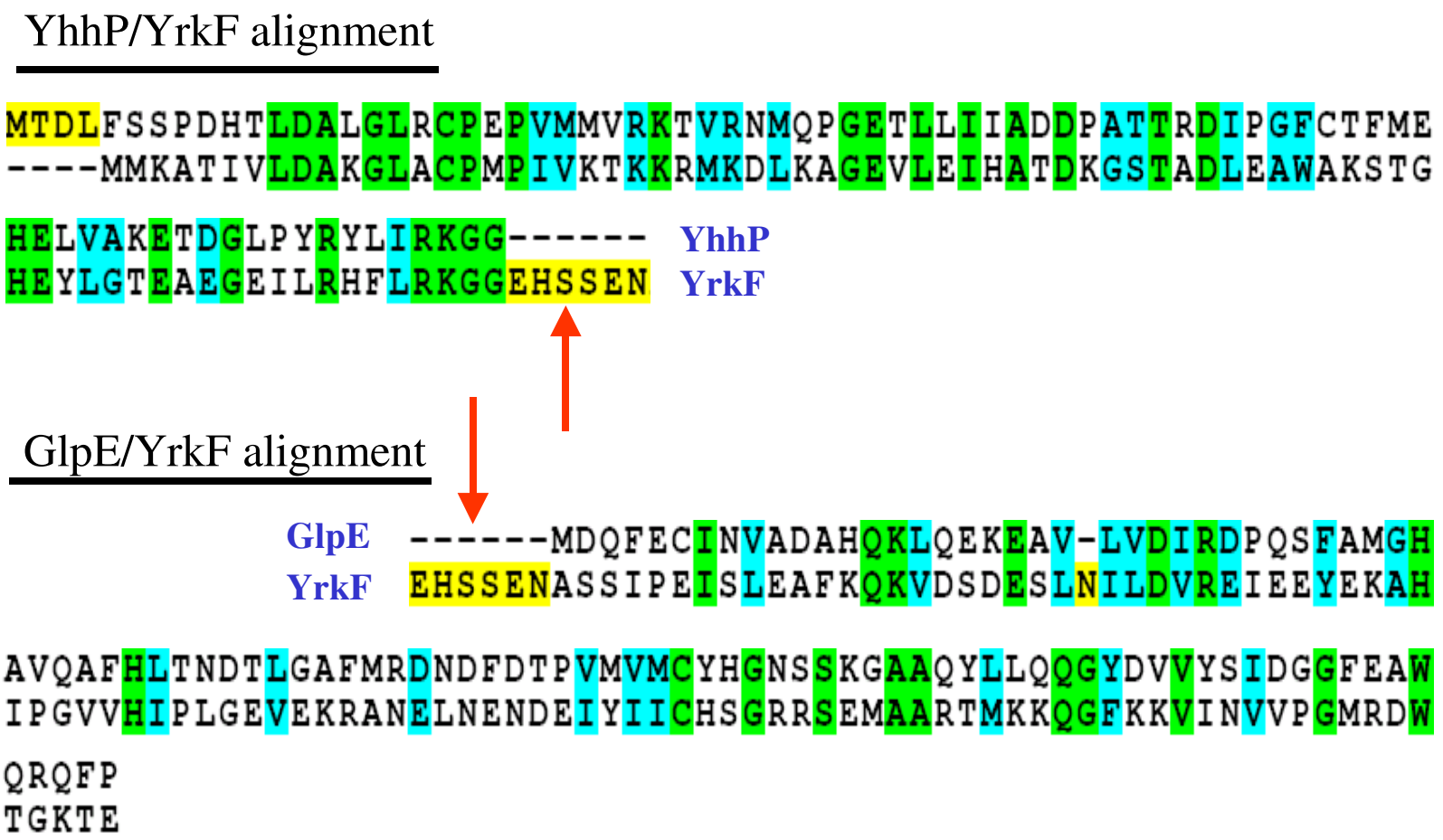

FIG. 3.21. YrkF sequence alignment with YhhP and GlpE reveals proposed flexible loop region.

The region hypothesized to be the flexible loop of YrkF is shown with red arrows. The sequences are colored as follows: Green, completely conserved residues, Cyan, similar amino acid residues, Yellow, no alignment with the template.

A

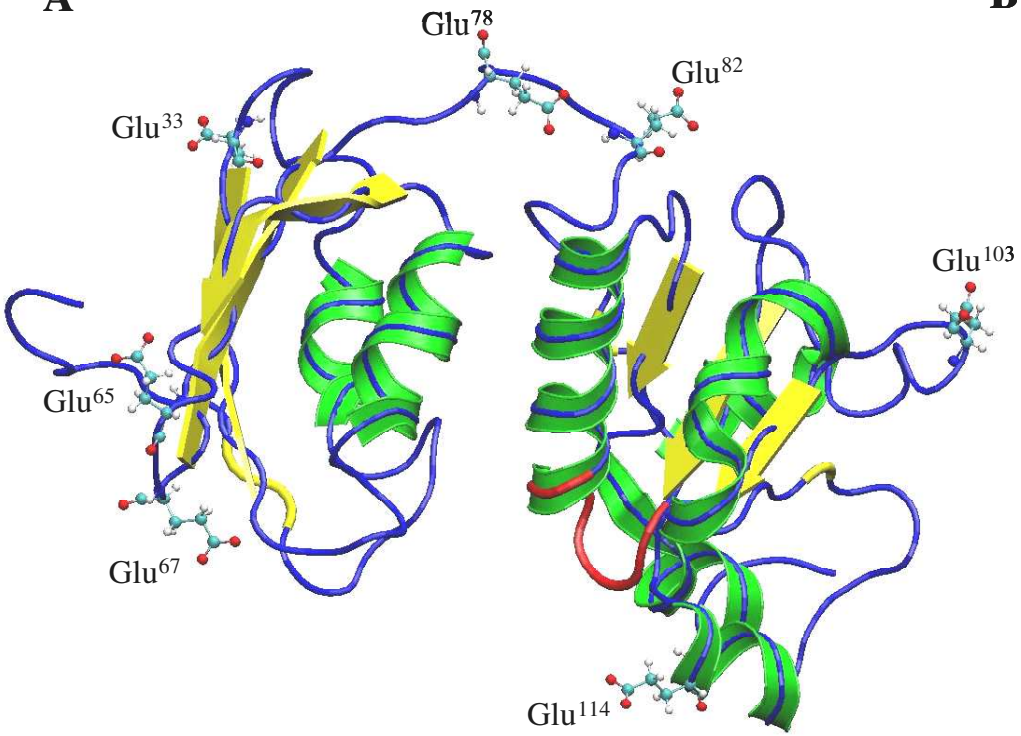

B

Cleavage site	Expected sizes (Da)	Difference in size of fragments (Da)	Sizes consistent with band #'s
Glu 33	17055 3618	13437	I II
Glu 65	13642 7030	6612	III IV
Glu 67	13456 7216	6240	III IV
Glu 78	12149 8523	3626	V VI
Glu 82	11708 8964	2744	V VI
Glu 103	11253 9418	1835	V VI
Glu 114	12536 8136	4400	V VI

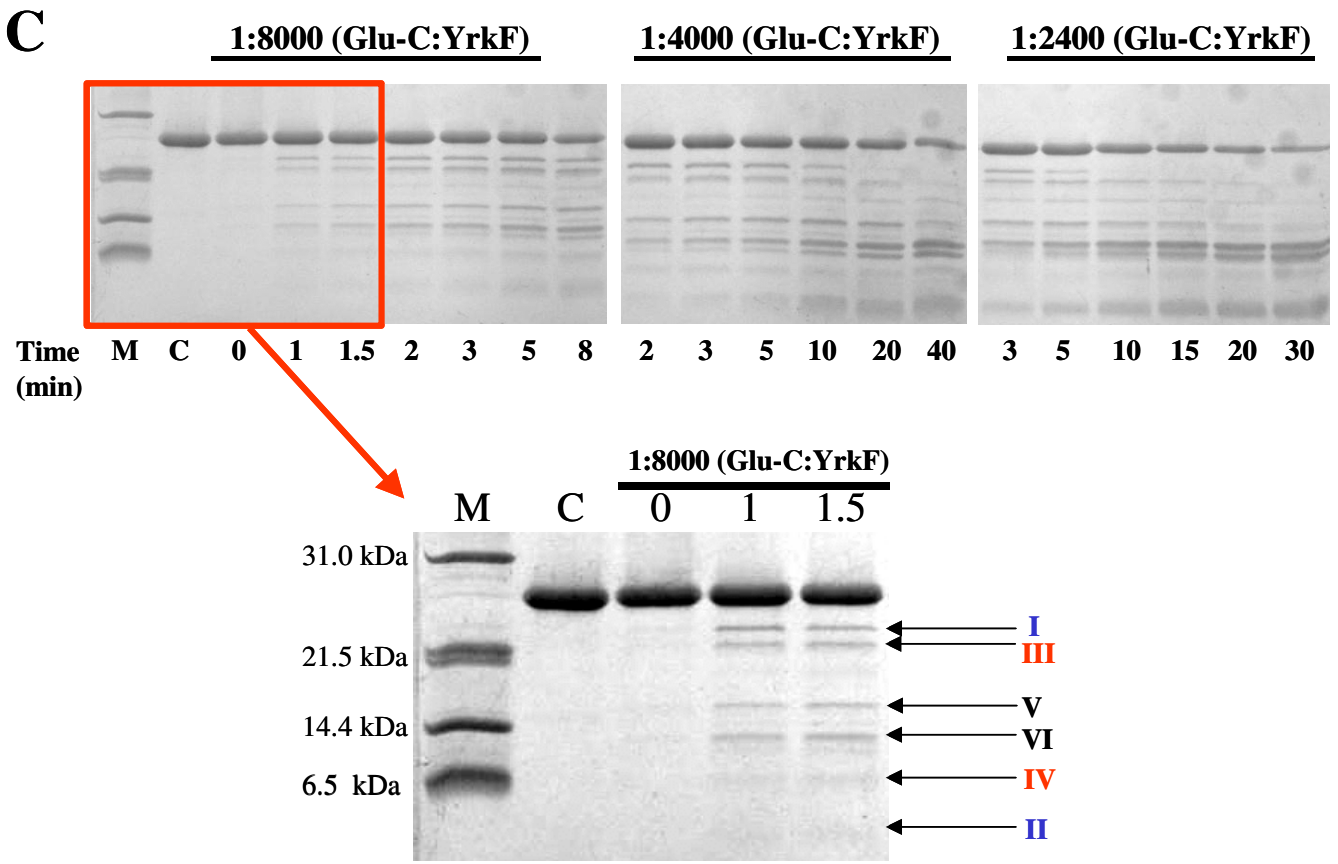

FIG. 3.22. Limited Proteolysis of YrkF with Glu-C.

YrkF was subjected to proteolysis with Glu-C at ratios of 1:8000, 1:4000, and 1:2400 (Glu-C:YrkF) as described in the Methods. (A) YrkF homology model highlighting glutamic acid residues 33, 65, 67, 78, 82, 103, and 114 that are predicted to be solvent exposed. (B) Sizes of expected peptides if Glu-C cleaved at one of the sites highlighted in panel (A). The fourth column matches the predicted fragment sizes with protein bands on gels in panel (C). (C) A 15% SDS-polyacrylamide gel. Roman numerals correspond to the peptide fragments indicated in panel (B). Time of exposure to protease is indicated at the bottom of each gel. M, molecular weight marker; C, control (no protease added).

3.9. Isolation and characterization of a *yrkF* mutant

The biosynthetic pathways of many sulfur-containing cofactors and tRNAs have yet to be completely elucidated. Since biosynthesis of sulfur-containing cofactors requires sulfurtransferase activity, rhodaneses have been hypothesized to participate in production of these compounds. In fact, the rhodanese-containing protein ThiI has been shown to be essential for thiamin biosynthesis in *E. coli* (50, 87). Additionally, rhodanese domains are often found fused to MoeB homologs. Studies have revealed that the rhodanese domain of these proteins is essential for their *in vitro* activity and suggest a possible role of rhodaneses in molybdopterin synthesis. To date, the complete biosynthetic pathways of these S-containing cofactors in *B. subtilis* have not been established. Therefore, it was hypothesized that YrkF may be needed for synthesis of sulfur-containing cofactors *in vivo*. To test the hypothesis, a *yrkF* mutant was created. The chromosomal *yrkF* gene was disrupted by the insertion of an erythromycin (Er^r) cassette in the middle of the gene as described in the Methods and Materials. PCR amplification of the *yrkF* locus of JH1006 confirmed the chromosomal insertion of the 2000 bp Er^r cassette (Figure 3.23).

B. subtilis has the ability to grow on nitrate or nitrite as its sole nitrogen source aerobically as well as anaerobically (161, 162). Under aerobic conditions, *B. subtilis* converts nitrate or nitrite to ammonium by way of assimilatory nitrate and nitrite reductases, which are distinct from the dissimilatory nitrate and nitrite reductases responsible for growth in anaerobic environments (161, 162). One of the cofactors required by nitrate reductase is the sulfur-containing molybdenum cofactor (161, 162). If YrkF is essential for molybdenum cofactor biosynthesis, then the *yrkF* mutant should not

be able to grow on nitrate as its sole nitrogen source. In order to establish whether YrkF is required for molybdenum cofactor biosynthesis, a *yrkF* mutant (JH1006) was plated on glucose minimal medium in the presence of ammonium or nitrate as the sole nitrogen source. The *yrkF* mutant and the wild type grew equally well on both nitrogen sources. Since *B. subtilis* mutants deficient in nitrate reductase are unable to grow on nitrate as the sole nitrogen source (161, 162), the results indicate that *yrkF* is not essential for the biosynthesis of molybdenum cofactor. The ability of the mutant to grow on unsupplemented minimal media also indicates that YrkF is not required for the biosynthesis of the other essential sulfur-containing cofactors (thiamin, biotin, and lipoic acid) or amino acids.

If YrkF contributes to the overall rhodanese activity of *B. subtilis*, then it is anticipated that cellular extracts of the *yrkF* mutant would have lower rhodanese activity than that of the wild type. Comparisons of rhodanese activity in the wild type (PS832) and JH1006 revealed an apparent decrease in activity. The mutant contained about 84% of the activity contained in the wild type strain (the specific activity of rhodanese extracts of PS832 and JH1006 was 0.84 ± 0.10 and 0.70 ± 0.03, respectively). The loss of *yrkF* and concomitant decrease in overall rhodanese activity suggests that YrkF is a functional rhodanese protein in actively growing cells. However, the results also indicate that there is another enzyme or enzymes in *B. subtilis* that contributes the majority of the rhodanese activity of the cell.

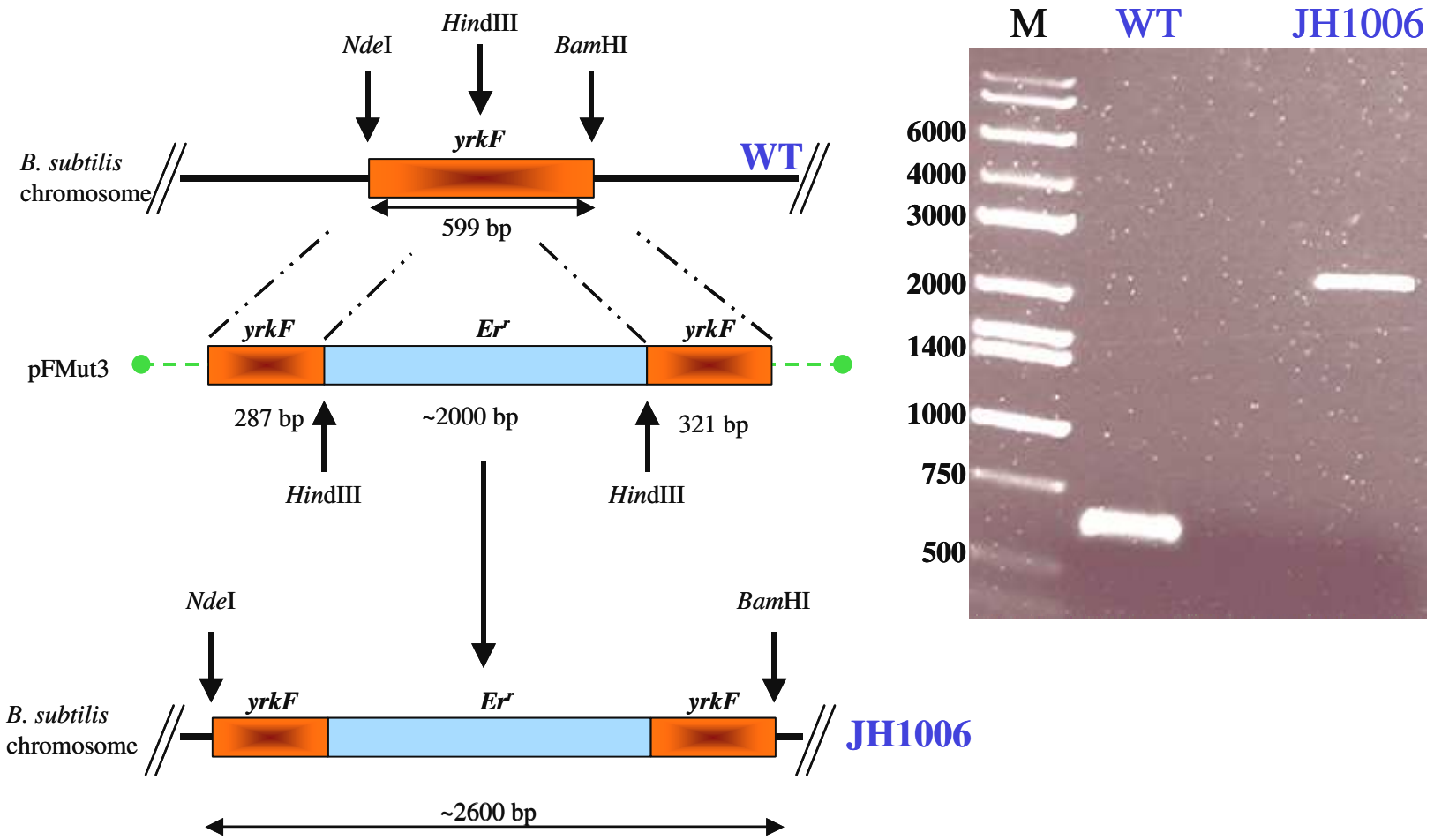

FIG. 3.23. PCR verification of *yrkF* chromosomal disruption.

The *B. subtilis* chromosomal disruption of *yrkF* was verified by PCR using chromosomal DNA from the wild type and the *yrkF* mutant (JH1006) as templates (see Methods). Homologous recombination used for construction of the mutant is shown on the left. Double arrows show the expected sizes of the PCR products. Analysis of PCR reactions by agarose gel electrophoresis is shown on the right. Lane M, molecular weight marker, lane WT, wild type, lane JH1006, *yrkF* mutant.

CHAPTER FOUR

Discussion

4.1. Physiological roles of rhodaneses

The physiological role of rhodaneses was originally believed to be the detoxification of cyanide (163). However, it is now evident that rhodaneses have a wide variety of functions and play significant roles in normal cellular metabolism. In addition to their possible role in detoxifying cyanide, evidence suggests rhodaneses may function in forming or repairing [Fe-S] centers in proteins (156, 164, 165) and modifying sulfur-containing enzymes, thereby regulating their activity (166, 167).

Two proteins from *E. coli* that contain the rhodanese domain, YbbB and ThiI, have been shown to be essential for modifications of nucleosides in tRNA (49, 50). YbbB is required for the conversion of 2-thiouridine to 2-selenouridine in tRNA. The active site cysteine of the rhodanese homology domain was found to be essential for selenium transfer from selenophosphate during the tRNA modification reaction (49). Additionally, rhodanese active site Cys^{456} of ThiI is critical for the biosynthesis of s^4U (50). Furthermore, the C-terminal rhodanese domains of MoeB homologs MOCS3 (human) and CnxF (*A. nidulans*) have been shown to be essential for sulfur incorporation during MPT synthesis *in vitro* and *in vivo* (51, 124). Recent findings also suggest that a single-domain rhodanese functions during MoCo biosynthesis in *Nicotiana tabacum* (168). This significant finding indicates that rhodaneses can have biologically-important functions as stand-alone proteins, as well as modules within multiple-domain proteins.

4.2. Characterization the rhodanese YrkF

4.2.1. General characteristics of YrkF

E. coli serves as an excellent bacterial model system for studying the physiological roles of enzymes, but its genome sequence predicts eight rhodanese paralogs. However, the *B. subtilis* genome predicts only four rhodaneses (YtwF, YqhL, YbfQ, and YrkF). Moreover, initial characterization of all four rhodaneses in *B. subtilis* indicates that only two (YtwF and YrkF) contain rhodanese activity *in vitro* (unpublished data). Therefore, using *B. subtilis* as a model system for studying the physiological functions of rhodaneses may be more straightforward due to a lower chance of genetic redundancy. The novel domain architecture of YrkF and the indication that cellular rhodanese activity decreases in *yrkF* mutants suggest that the protein may provide an important cellular function.

The first *B. subtilis* rhodanese to be characterized, YrkF offers an example of a novel protein that contains a single C-terminal rhodanese domain fused to an N-terminal Ccd1 domain. Interestingly, a gene encoding another Ccd1 homolog, *yrkI*, is located in the immediate vicinity of *yrkF*. Though Ccd1 has no known biochemical function, according to the COG database (169), a protein containing Ccd1 is a "predicted redox protein; regulator of disulfide bond formation". Like the rhodanese domain, Ccd1 (COG0425) is found by itself or as a module in a variety of proteins containing multiple functional domains. An example of a Ccd1 fusion includes a C-terminal extension to an IscS homolog in *Streptomyces coelicolor*. Ccd1 is also found sandwiched between a rhodanese domain and a Ccd2 (similar to peroxiredoxin) domain at the C-terminus of a protein containing a NADH-disulfide reductase domain in *Fusobacterium nucleatum*.

The rhodanese-Ccd1-Ccd2 architecture is also found in proteins in *Staphylococcus aureus* (Figure 1.2).

YhhP, one of three single-domain Ccd1 homolog in *E. coli*, displays structural similarity to many nucleic acid-binding proteins, including the C-terminal domain of IF3 (129), the R3H domain (170), and the predicted structure of the apparent RNA-binding domain (THUMP) of *E. coli* ThiI (123). ThiI is essential for the synthesis of 4-thiouridine in tRNA, and utilizes a rhodanese module within the protein to facilitate sulfur transfer to the uridine (50). Though Ccd1 homologs display structural homology to RNA- and DNA-binding proteins, there is no evidence to suggest YrkF binds nucleic acids. Preliminary data from gel-shift mobility assays indicate that YrkF does not bind tRNA. Additionally, the initial step in the purification of YrkF includes the precipitation of nucleic acids by the addition of streptomycin sulfate. If YrkF bound to nucleic acids, then it would likely precipitate with the addition of streptomycin sulfate.

4.2.2. Regulation of YrkF expression

Global analysis of expression of the bacterial transcriptome and proteome under stress conditions can be useful in understanding regulation of a particular gene. Discovery of altered gene expression in response to a particular growth condition or stress may provide clues regarding physiological function. The expression profile of the *B. subtilis* genome has been analyzed under various growth conditions including heat, salt, oxidative, and disulfide stress. Specifically, transcription of *yrkF* is significantly induced in response to heat in wild type (9 fold induction) and in σ^B (general stress factor

in gram-positive bacteria) mutants (6.1 fold induction), and under ethanol stress in σ^B mutants (5.7 fold induction) (171).

B. subtilis was also studied under oxidative stress conditions. When stressed with peroxide or superoxide, YrkF showed no apparent induction (172). However, when treated with diamide, a chemical that induces disulfide bond formation and thus creates disulfide stress in bacteria, the putative *yrkDEF* and *yrkHI* operons were strongly induced especially at later times of treatment (30 to 50 min) (173). It is interesting to note that after 50 min under disulfide stress conditions, both YrkF and YrkI were strongly induced (20 to 115 fold, respectively) (173). Disulfide stress is a form of oxidative stress that results in formation of non-native disulfide bonds on proteins. Disulfide bonds can cause misfolding of proteins and affect their overall function in the cell. Redox-active cysteine residues within proteins, such as thioredoxin, may play an important role in breaking these non-native disulfide bonds and in controlling damage during disulfide stress (173). Interestingly, thioredoxin, thioredoxin reductase, and other thioredoxin-like proteins were strongly induced by disulfide stress throughout the entire treatment (173).

4.2.3. Physical characteristics of YrkF

Typical rhodaneses cycle between a sulfur-free and a persulfide form during catalysis. Data from kinetic and mass spectral analyses suggest YrkF behaves similarly. Kinetic analysis indicated YrkF catalyzes the transfer of sulfur from thiosulfate to cyanide using a ping-pong mechanism. In this typical rhodanese-catalyzed mechanism (Figure 4.1 A) YrkF removes sulfur from thiosulfate to create an active site cysteine persulfide. The cysteine persulfide sulfur is then transferred to the sulfur-accepting

molecule cyanide. Dithiols such as DTT can also accept the sulfur from YrkF with subsequent formation of sulfide and oxidized DTT (data not shown).

Structural analysis of RhdA indicates that the enzyme purified in the absence of thiosulfate is expressed as a stable persulfide form (RhdA-S), which is thought to be stabilized by a strong positive electrostatic field generated by the active site residues and main-chain amide groups (35). Soaking RhdA-S in moderate concentrations of cyanide, DTT, or sulfite removes the persulfide and partially inactivates the enzyme, suggesting that RhdA-S is the native, active form of the enzyme. Thus, it has been proposed that RhdA-S accepts a second sulfur from thiosulfate during catalysis (38). Crystallization of bovine rhodanese (RhoBov) in the presence of high concentration thiosulfate revealed the presence of a thiosulfate molecule within 2 to 3 Å of the catalytic persulfide-containing Cys^{247} (47). The binding of thiosulfate in the active site appears to be facilitated by the location of Arg^{186} close to Cys^{247} (47). However, it was not determined if the thiosulfate molecule was covalently bound to Cys^{247} or bound only by electrostatic interactions. The location of the thiosulfate molecule does suggest the possibility of RhoBov proceeding through a catalytic mechanism where the active, sulfur-accepting form of the enzyme contains a cysteine persulfide (47).

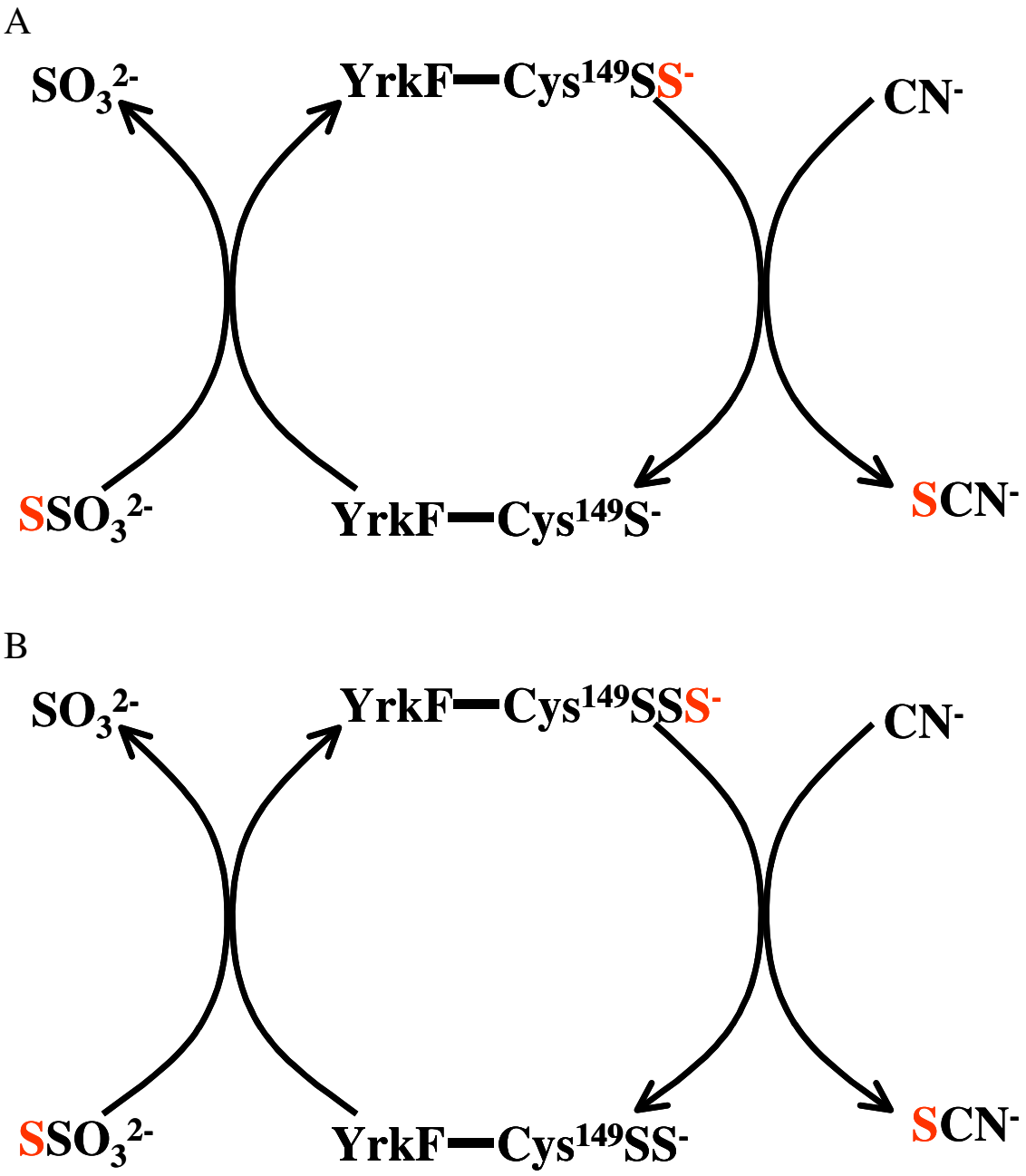

FIG. 4.1. Rhodanese catalytic mechanism for YrkF.

Mechanism for the thiosulfate:cyanide sulfurtransferase reaction catalyzed by YrkF in the sulfur-free form (A) and the persulfide form (B).

Mass spectral analysis of YrkF indicated the presence of a sulfur-free form (YrkF) and a stable persulfide form (YrkF-S). However, there was no indication of a covalently bound thiosulfate molecule in YrkF as proposed by the crystal structures of RhoBov (47) or as observed in $YrkF^{C15A}$ mass spectral analysis. Prolonged incubation of purified YrkF in DTT or sulfite removed the persulfide sulfur and incubation in thiosulfate regenerated modest amounts of the active site persulfide. Preliminary kinetic data also suggested that incubation of YrkF in KCN prior to assaying for activity slightly inhibited the enzyme (data not shown). These data agree with results that were observed for RhdA-S and raise the possibility that the persulfide form of YrkF is the active enzyme (Figure 4.1 B).

However, a more in depth analysis of the results would tend to favor a mechanism in which the sulfur-free form of YrkF is the native, active form of the enzyme. Prolonged treatments with cyanide can ultimately cause an enzyme to denature (Dr. Walter Niehaus, personal communication). Therefore, treatment of YrkF with cyanide may show apparent inhibition of the enzyme, not due to release of the active site persulfide, but due to denaturation of the enzyme. Furthermore, YrkF was often treated with DTT at high concentrations for prolonged periods of time before activity assays. There was no evidence that this treatment led to inhibition of the rhodanese activity and in fact DTT treatment often increased activity. Therefore, the mechanism for the sulfur transfer from thiosulfate to cyanide catalyzed by YrkF in the rhodanese assay likely proceeds as indicated in Figure 4.1 A.

One mass spectral study indicated the presence of both the sulfur-free YrkF and YrkF-S after DTT treatment. These results are different from those obtained after similar

treatments of RhdA and RhoBov. The presence of YrkF-S even after DTT treatment suggests the sulfane sulfur bound to Cys^{149} of YrkF is highly stable. The active site sequence of YrkF is similar to that of RhdA in that both contain multiple positively charged residues that would create a strong positive electrostatic field. The homology model of YrkF suggests that the active site of YrkF could form a network of strong positive electrostatic interactions to help stabilize a persulfide (Figure 4.2 A). The active site of RhdA also shows that the persulfide is stabilized by the surrounding positive charge (Figure 4.2 B). However, the predicted architecture of the active sites alone does not explain the possibility that Cys^{149} of YrkF forms a more stably bound persulfide than Cys^{230} of RhdA. One possibility is that the sulfur atom is bridged between Cys^{15} and Cys^{149} of YrkF.

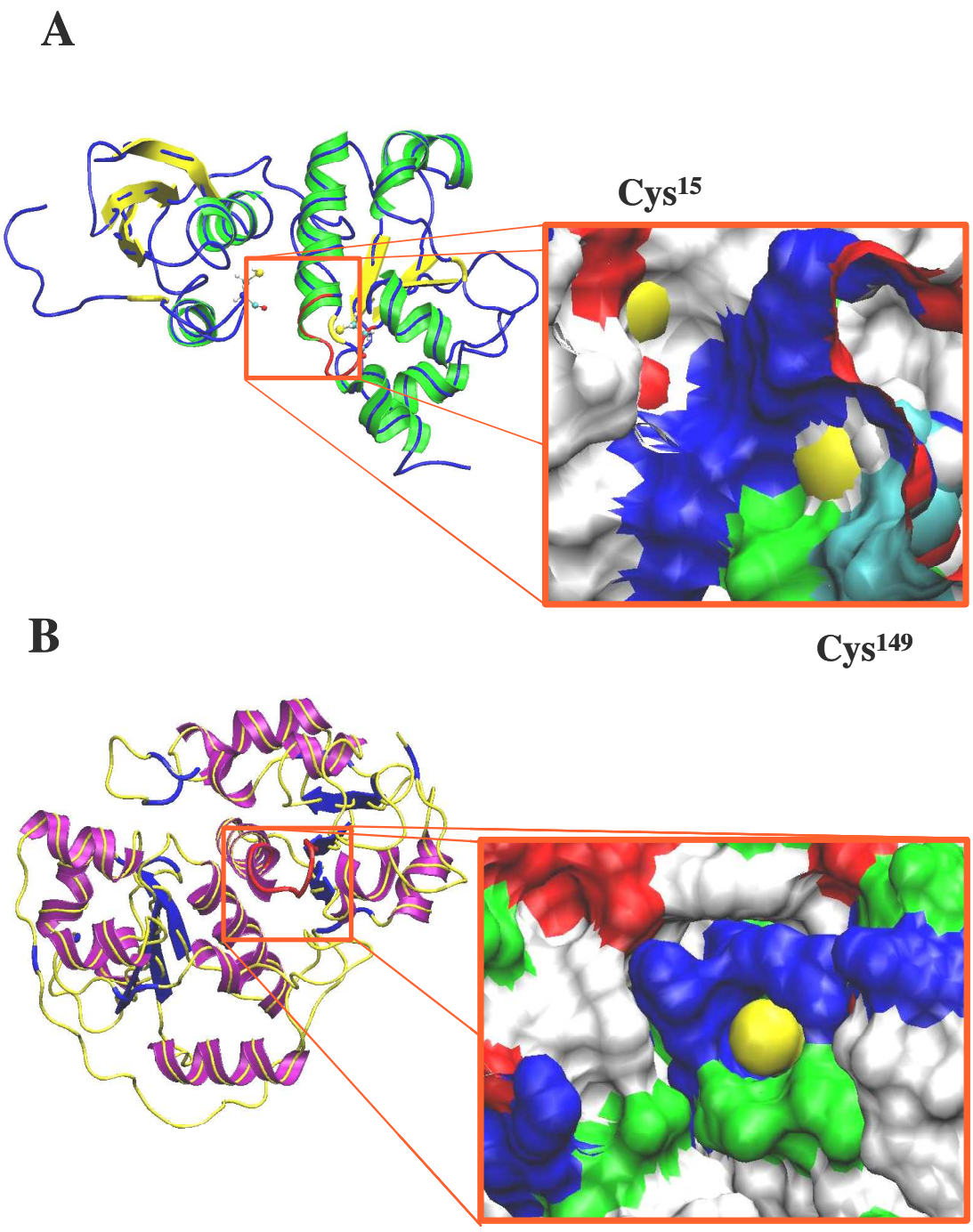

FIG. 4.2. Surface representations of the YrkF and RhdA active sites.

The YrkF (A) and RhdA (B) active sites are represented as surface models. Green, polar residues; Blue, positively charges residues; Red, negatively charged residues; white; polar residues; Yellow, sulfur atom of cysteine. The two cysteine residues of YrkF are indicated. The respective ribbon structure, highlighting α-helices and β-sheets, of each protein is also shown.

On the other hand, analysis of the YrkF^{C15A} variant revealed distinct differences that may reflect the importance of the Ccd1 cysteine residue for normal enzymatic function or structural stability. Mass spectrometry and cross-linking experiments show that the variant is more prone to oxidation via the formation of disulfide cross-linked dimers. Incubation of YrkF^{C15A} in thiosulfate or sulfite yielded covalent modifications, presumably of the active site cysteine, by the respective anion. Furthermore, the presence of a persulfide form of the variant (YrkF^{C15A}-S) was never detected by mass spectrometry after treatment with DTT, sulfite, or thiosulfate. These results suggest substitution of Cys^{15} with Ala causes YrkF^{C15A} to become more oxidation sensitive and possibly destabilizes the active site persulfide.

Though the variant displayed rhodanese activity, repeated kinetic analyses never yielded data that was consistent with a ping-pong mechanism typical of rhodaneses. However, there is no convincing evidence that would suggest YrkF^{C15A} utilizes a mechanism other than ping-pong, and it is unlikely that the mechanism of the enzyme completely changes by substitution of an amino acid residue not located directly within the active site loop. Therefore, it is more likely that the catalytic mechanisms of YrkF and YrkF^{C15A} both proceed as ping-pong. The Cys^{15} to Ala substitution changes some aspect of the protein that causes a difference in the cataylsis of YrkF^{C15A}. Since mass spectral data obtained for the variant indicated that the enzyme did not contain a stable persulfide, then the catalytic differences between the two enzymes may be a result of a change in the stability of the active site cysteine persulfide due to the effects of the Cys to Ala substitution.

Kinetic analysis of YrkF^{C15A} reveals substrate dependency curves that indicate the possibility of cooperativity between cyanide concentration and the activity of the enzyme (Figure 3.11 B). Further analysis of the kinetic data reveals that at lower concentrations of cyanide the activity of YrkF^{C15A} is much lower than that of YrkF (Table 4.1). Therefore, double reciprocal plots of the data were non-linear and typical ping-pong kinetics were not observed. However, when the concentration of cyanide was high, YrkF^{C15A} displayed activity comparable to YrkF (Table 4.1). These data can be explained if the sulfur transferred onto Cys^{149} of YrkF^{C15A} is highly unstable relative to the sulfur transferred onto Cys^{149} of YrkF. At high concentrations of cyanide, the enzyme is saturated with substrate and can readily donate its persulfide sulfur, even if the persulfide sulfur atom is unstable (Figure 4.3 A). However at lower concentrations of cyanide, the unstable persulfide sulfur easily leaves the enzyme active site (possibly forming elemental sulfur) causing the efficiency of sulfur transfer to cyanide to decrease (Figure 4.3 B). The competing process that occurs due to the destabilization of the persulfide sulfur causes YrkF^{C15A} rhodanese activity to be lower than expected, which gives the appearance that the mechanism deviates from ping-pong.

Table 4.1. Rhodanese activities of YrkF and YrkF^{C15A}

20 mM SSO_3^{2-}			
[CN^-] (mM)	Sp Act. YrkF (U/mg)	Sp Act. YrkF^{C15A} (U/mg)	Ratio[a]
65	98.0	101.2	1.03
40	82.9	59.8	0.72
30	68.6	38.2	0.56
5 mM SSO_3^{2-}			
[CN^-] (mM)	Sp Act. YrkF (U/mg)	Sp Act. YrkF^{C15A} (U/mg)	Ratio[a]
65	90.8	95.0	1.05
40	77.9	57.4	0.74
30	69.4	33.3	0.48

[a] (Specific activity YrkF^{C15A}/Specific activity of YrkF)

A

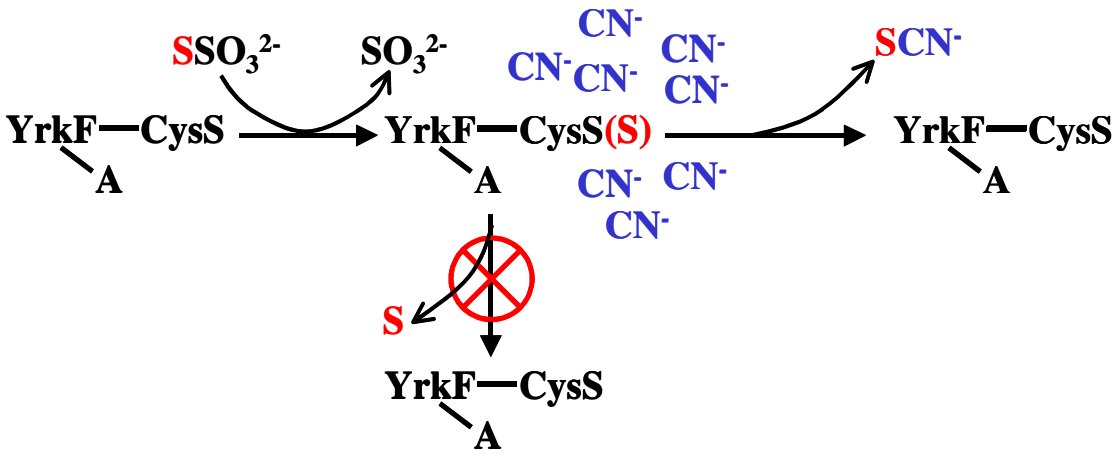

B

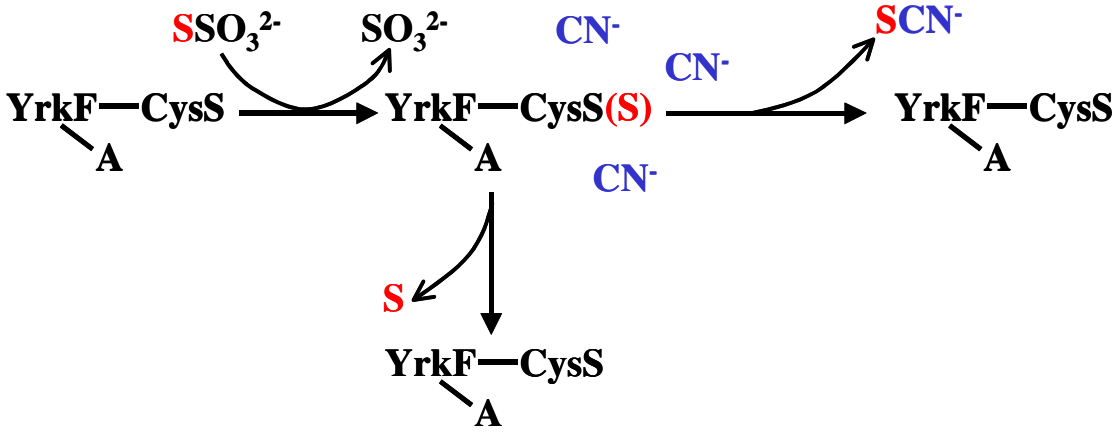

FIG. 4.3. Scheme for transfer of an unstable persulfide to cyanide in YrkF^{C15A}. The following scheme highlights the transfer of the sulfane sulfur (red) to cyanide (blue) at high (A) and low (B) concentrations of cyanide. (A) An unstable sulfur atom is transferred to cyanide at high concentrations. (B) At low concentrations of cyanide, the activity of YrkF^{C15A} appears to be lower due to a competing process in which the unstable persulfide sulfur atom leaves the enzyme and is not transferred to cyanide.

The differences observed between YrkF and the variant suggests that substitution of Cys^{15} affects the overall function of the enzyme by changing the stability of the active site persulfide, the stability of the enzyme, or both. One possible explanation for the apparent effects of the Cys to Ala substitution is that introduction of a hydrophobic residue in a location near the active site changes the fold of the protein or the ability of the enzyme to bind solvent molecules. These changes may affect the stability of the active site persulfide and change the ability of $YrkF^{C15A}$ to catalyze sulfur transfer. However, the homology model of YrkF predicts that the amino acids surrounding Cys^{15} create a hydrophobic pocket around the residue (Figure 4.2 A). Therefore, a substitution of the hydrophobic residue Ala may not drastically affect this region of the protein.

A second possible explanation is that Cys^{15} functions in stabilizing the persulfide in YrkF. Cys^{15} may function by forming a stable trisulfide intermediate as proposed for cystathionase (7, 174), or, more simply, form a hydrogen bond with the persulfide sulfur. The model of the active site of YrkF shows that the active site pocket is lined with positively charged residues between Cys^{15} and Cys^{149} (Figure 4.2 A). This network of amino acid residues is similar to that RhdA (Figure 4.2 B). However, RhdA does not contain a second cysteine residue comparable to Cys^{15} of YrkF. Therefore, if Cys^{15} can form a bond with the persulfide sulfur or if the presence of a hydrogen bond stabilizes the persulfide, then this may help explain the differences in persulfide stability observed between YrkF and RhdA.

4.2.4. Possible interactions between Cys^{15} and Cys^{149} of YrkF

Data from circular dichroism (CD), fluorescence quenching, and molecular dynamics simulations indicate that the two domains of RhdA are rigid structures. Therefore the tether connecting the N-terminal rhodanese domain to the C-terminal rhodanese domain does not permit bending or large conformational changes during catalysis (175). However, since the N-terminal domain of YrkF is a Ccd1, then the enzyme may behave differently than rhodaneses that contain a tandem-repeat domain architecture.

Studies with the cross-linking reagent bBBr indicate that Cys^{15} and Cys^{149} of YrkF are readily cross-linked but not with 100% efficiency. This observation suggests that the distance between the two residues fluctuates. A flexible tether connecting the two domains of YrkF would facilitate this movement. The region of YrkF linking the two domains appears to be solvent-exposed, as shown by its apparent susceptibility to cleavage by protease. The presence of a solvent-exposed loop is consistent with the hypothesis of a flexible tether. Therefore, YrkF was modeled based on the possibility of a flexible tether that would facilitate movement of the two domains relative to one another. Upon analysis of the trajectory of the MD simulations using the visualization program VMD, there was a slight indication that the two domains of YrkF can bend relative to one another. However, visualization of the trajectory of the YrkF models was difficult due to the inability of the software to recognize some parameter and coordinate files. Therefore, at this point the conclusion that the tether connecting the Ccd1 domain and the rhodanese domain bends on a hinge is speculative at best.

4.3. Possible physiological roles of YrkF

Analysis of a *yrkF* mutant strain indicates that YrkF is not essential for *B. subtilis* viability and is not essential for the biosynthesis of thiamin, biotin, lipoic acid, and molybdopterin. Though the *yrkF* mutant had no apparent phenotype, it is interesting to speculate on possible roles of the enzyme *in vivo*. My research may provide significant findings that lead to the discovery of the physiological function of YrkF.

Evidence suggests Cys^{15} may play a role in stabilizing the enzyme and the active site persulfide, and there is a possibility that YrkF can bend on a flexible tether. Additionally, it has been shown that Cys^{15} can form a disulfide bond with Cys^{149}. Therefore, one possible mechanism of reaction for YrkF is that Cys^{15} displaces the sulfane sulfur from the active site, similar to a mechanism proposed for ThiI (99) (Figure 4.4). One way to test this hypothesis would be to treat YrkF and $YrkF^{C15A}$ with 5,5'-dithiobis (2-nitrobenzoic acid) (DTNB) similar to an experiment performed with bovine rhodanese (176). The sulfur-free form of RhoBov is inactivated by covalent modification of the active site Cys^{247} by DTNB. Treatment with cyanide displaces the thionitrobenzoate from the active site cysteine and full activity is recovered. However, enzymatic activity cannot be recovered if Cys^{254} is mutated to Ser, which suggests that thiocyano-modified Cys^{247} transfers cyanide to Cys^{254} to recover activity (176). Furthermore, the active site persulfide form of the enzyme is not inactivated by DTNB, which suggests that the persulfide form of the enzyme is more resistant to oxidation and not reactive to DTNB (176). If YrkF and $YrkF^{C15A}$ are subjected to similar treatments as bovine rhodanese and $YrkF^{C15A}$ cannot recover activity, then the role of Cys^{15} may be to displace various components (possibly S^0 or S^{2-}) from the active site Cys^{149}.

Furthermore, if Cys^{15} functions in stabilizing a persulfide sulfur, then it would be expected that $YrkF^{C15A}$ would be more susceptible to DTNB inactivation.

Since YrkF appears to contain a highly stable persulfide sulfur, the enzyme could be involved in sulfur mobilization. Therefore, YrkF would function as a protein that transfers a reactive sulfur species, such as sulfide or sulfane sulfur, to its physiological acceptor molecule (Figure 4.4). Thus, the persulfide sulfur could serve as a sulfur source for nonessential sulfur-containing molecules. Recently, it was discovered that *thiI* mutants of *B. subtilis* do not produce s^4U but do produce thiamin (unpublished data, Dr. Charles Lauhon, Univ. of Wisconsin). Since ThiI proteins are often associated with a rhodanese domain and *B. subtilis* ThiI lacks a C-terminal rhodanese domain found in *E. coli* ThiI, YrkF or another rhodanese may participate in s^4U synthesis *in vivo*. Therefore, the *yrkF* mutant could be tested to see if it lacks any of the thionucleosides, including s^4U.

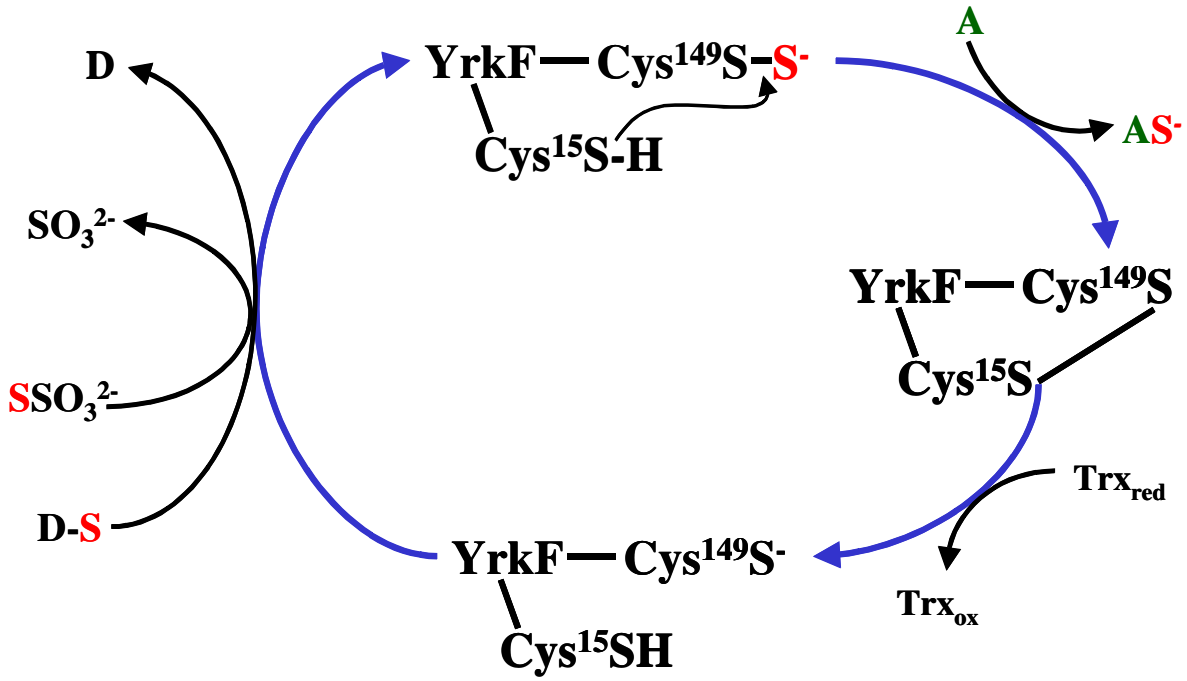

FIG. 4.4. Proposed mechanism for displacement of sulfur from active site of YrkF. The persulfide sulfur (red) is released as sulfide or transferred to an acceptor (A) when a disulfide bond forms between Cys^{15} and Cys^{149}. Trx, thioredoxin; D, physiological sulfur donor; A, physiological sulfur acceptor.

The formation of non-native disulfide bonds in proteins and sulfur-containing molecules, such as coenzyme A, has potentially devastating consequences. Recent studies revealed that transcription of *yrkF* is induced during heat and disulfide stress conditions (171, 173), and may indicate that YrkF is important in maintaining normal cellular activity during times of stress. Furthermore, YrkF has several characteristics that would suggest that the enzyme could fulfill a role during disulfide stress.

One of the likely functions of proteins induced during disulfide stress conditions is to reduce abnormal disulfides to thiols. An example of a protein system that functions in reducing disulfides in *B. subtilis* is thioredoxin and thioredoxin reductase (177). In fact, transcription of genes encoding these proteins is induced 10 – 26 fold during disulfide stress (173). Cys^{15} and Cys^{149} of YrkF can form a disulfide bond and could theoretically function in a role in reducing non-native disulfides. YrkF could cycle between a form with and without a disulfide bond while breaking non-native disulfides in proteins and other sulfur-containing molecules (Figure 4.5).

A second possible function of proteins induced during disulfide stress is to protect proteins and sulfur-containing molecules from further or repeated oxidation, possibly by "capping" the sulfhydryl groups. Since persulfide sulfur has been shown to protect bovine rhodanese from covalent modifications, S^0 provided by a rhodanese such as YrkF is a possible candidate to serve as a "capping" molecule. Evidence suggests that YrkF forms a highly stable persulfide intermediate and kinetic studies of YrkF using DTT as a sulfur-acceptor demonstrate YrkF has the ability to donate sulfur to thiols and dithiols. Therefore, YrkF could "cap" the thiol groups of proteins and sulfur-containing molecules susceptible to disulfide oxidation with a sulfur atom to reverse and to prevent further

disulfide bond formation (Figure 4.5). If a physiological role of YrkF is to regulate disulfide bond formation during stress conditions, then *yrkF* mutants may be sensitive to disulfide stress.

YrkF is a unique two-domain protein that contains the rhodanese and Ccd1 modules prevalently found throughout life. Further progress in this area of research has the potential to unveil novel, specific roles for both rhodaneses and Ccd1 proteins. One cannot help but think that this initial research with YrkF may pioneer new discoveries with rhodaneses and sulfur metabolism.

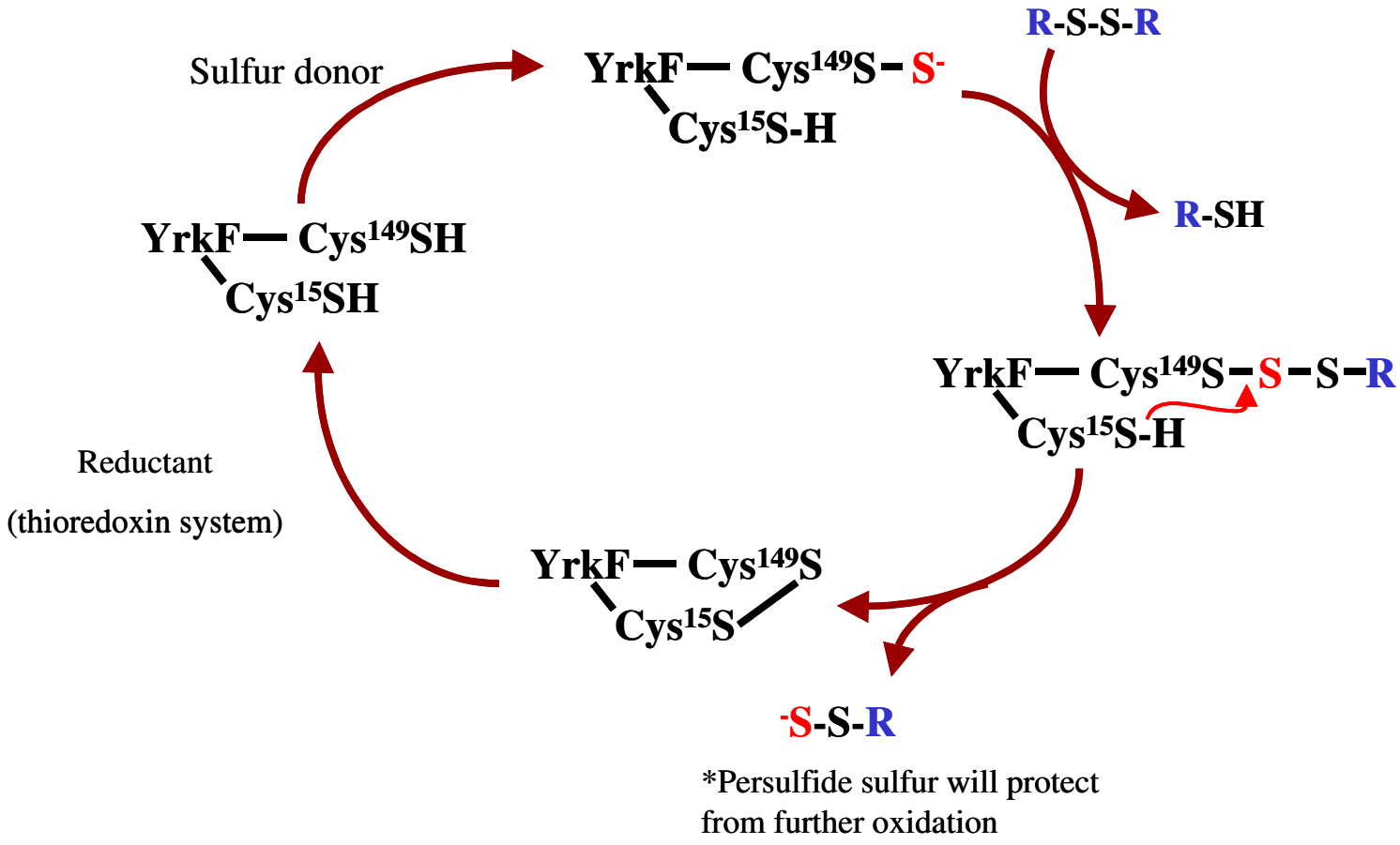

FIG. 4.5. Proposed mechanism for the disulfide bond regulation by YrkF.

R, represents protein or thiol-containing molecules with non-native disulfide bonds; S, represents sulfur mobilized by YrkF.

CHAPTER 5

Reference List

1. **Woollins, J. D.** 1996. Chemistry of sulfur, p. 1-19. *In* S. Mitchell (ed.), Biological Interactions of Sulfur Compounds. Taylor and Francis, London.

2. **Beinert, H.** 2000. A tribute to sulfur. Eur.J.Biochem **267**:5657-5664.

3. **Roy, A. B. and P. A. Trudinger**. 1970. The chemistry of some sulfur compounds, p. 7-42. *In* The Biochemistry of Inorganic Compounds of Sulfur. Cambridge University Press.

4. **Torchinskii, Y. M.** 1974. Sulfhydryl and Disulfide Groups of Proteins. Consultants Bureau, New York.

5. 1984. Sulfur: Its Significance for Chemistry, for the Geo-, Bio-, and Cosmosphere and Technology. Elsevier Science Publishers, Amsterdam, New York.

6. **Iciek, M. and L. Wlodek**. 2001. Biosynthesis and biological properties of compounds containing highly reactive, reduced sulfane sulfur. Pol.J.Pharmacol. **53**:215-225.

7. **Toohey, J. I.** 1989. Sulphane sulphur in biological systems: a possible regulatory role. Biochem J. **264**:625-632.

8. **Sundaram, S. G. and J. A. Milner**. 1996. Diallyl disulfide inhibits the proliferation of human tumor cells in culture. Biochim.Biophys.Acta **1315**:15-20.

9. **Wlodek, L., M. Wrobel, and J. Czubak**. 1993. Transamination and transsulphuration of L-cysteine in Ehrlich ascites tumor cells and mouse liver. The nonenzymatic reaction of L-cysteine with pyruvate. Int.J.Biochem. **25**:107-112.

10. **Ray, W. K., M. B. Potters, A. M. Mansuri, and T. J. Larson**. 2000. Characterization of a 12-kilodalton rhodanese encoded by *glpE* of *Escherichia coli* and its interaction with thioredoxin. J.Bacteriol. **181**:2277-2284.

11. **Szczepkowski, T. W. and J. L. Wood**. 1967. The cystathionase-rhodanese system. Biochim.Biophys.Acta **139**:469-478.

12. **Abdolrasulnia, R. and J. L. Wood**. 1979. Transfer of persulfide sulfur from thiocystine to rhodanese. Biochim.Biophys.Acta **567**:135-143.

13. **Mihara, H. and N. Esaki**. 2002. Bacterial cysteine desulfurases: their function and mechanisms. Appl.Microbiol.Biotechnol. **60**:12-23.

14. **Jacobson, M. R., V. L. Cash, M. C. Weiss, N. F. Laird, W. E. Newton, and D. R. Dean**. 1989. Biochemical and genetic analysis of the *nifUSVWZM* cluster from *Azotobacter vinelandii.* Mol.Gen.Genet. **219**:49-57.

15. **Zheng, L., R. H. White, V. L. Cash, R. F. Jack, and D. R. Dean**. 1993. Cysteine desulfurase activity indicates a role for NIFS in metallocluster biosynthesis. Proc.Natl.Acad.Sci.U.S.A. **90**:2754-2758.

16. **Zheng, L. and D. R. Dean**. 1994. Catalytic formation of a nitrogenase iron-sulfur cluster. J.Biol.Chem. **269**:18723-18726.

17. **Frazzon, J., J. R. Fick, and D. R. Dean**. 2002. Biosynthesis of iron-sulphur clusters is a complex and highly conserved process. Biochem.Soc.Trans. **30**:680-685.

18. **Zheng, L., V. L. Cash, D. H. Flint, and D. R. Dean**. 1998. Assembly of iron-sulfur clusters. Identification of an *iscSUA-hscBA-fdx* gene cluster from *Azotobacter vinelandii*. J.Biol.Chem. **273**:13264-13272.

19. **Flint, D. H.** 1996. *Escherichia coli* contains a protein that is homologous in function and N-terminal sequence to the protein encoded by the *nif*S gene of *Azotobacter vinelandii* and that can participate in the synthesis of the Fe-S cluster of dihydroxy-acid dehydratase. J.Biol.Chem. **271**:16068-16074.

20. **Mihara, H., T. Kurihara, T. Yoshimura, K. Soda, and N. Esaki**. 1997. Cysteine sulfinate desulfinase, a NIFS-like protein of *Escherichia coli* with selenocysteine lyase and cysteine desulfurase activities. Gene cloning, purification, and characterization of a novel pyridoxal enzyme. J.Biol.Chem. **272**:22417-22424.

21. **Mihara, H., M. Maeda, T. Fujii, T. Kurihara, Y. Hata, and N. Esaki**. 1999. A *nifS*-like gene, *csdB*, encodes an *Escherichia coli* counterpart of mammalian selenocysteine lyase. Gene cloning, purification, characterization and preliminary X-ray crystallographic studies. J.Biol.Chem. **274**:14768-14772.

22. **Zheng, L., R. H. White, V. L. Cash, and D. R. Dean**. 1994. Mechanism for the desulfurization of L-cysteine catalyzed by the *nifS* gene product. Biochemistry **33**:4714-4720.

23. **Lauhon, C. T. and R. Kambampati**. 2000. The *iscS* gene in *Escherichia coli* is required for the biosynthesis of 4-thiouridine, thiamin, and NAD. J.Biol.Chem. **275**:20096-20103.

24. **Mueller, E. G., C. J. Buck, P. M. Palenchar, L. E. Barnhart, and J. L. Paulson**. 1998. Identification of a gene involved in the generation of 4-thiouridine in tRNA. Nucleic.Acids.Res. **26**:2606-2610.

25. **Kambampati, R. and C. T. Lauhon**. 1999. IscS is a sulfurtransferase for the in vitro biosynthesis of 4-thiouridine in *Escherichia coli* tRNA. Biochemistry **38**:16561-16568.

26. **Lauhon, C. T.** 2002. Requirement for IscS in biosynthesis of all thionucleosides in *Escherichia coli*. J.Bacteriol. **184**:6820-6829.

27. **Cupp-Vickery, J. R., H. Urbina, and L. E. Vickery**. 2003. Crystal structure of IscS, a cysteine desulfurase from *Escherichia coli*. J.Mol Biol. **330**:1049-1059.

28. **Fujii, T., M. Maeda, H. Mihara, T. Kurihara, N. Esaki, and Y. Hata**. 2000. Structure of a NifS homologue: X-ray structure analysis of CsdB, an *Escherichia coli* counterpart of mammalian selenocysteine lyase. Biochemistry **39**:1263-1273.

29. **Lima, C. D.** 2002. Analysis of the *E. coli* NifS CsdB protein at 2.0 Å reveals the structural basis for perselenide and persulfide intermediate formation. J.Mol.Biol. **315**:1199-1208.

30. **Kaiser, J. T., T. Clausen, G. P. Bourenkow, H. D. Bartunik, S. Steinbacher, and R. Huber**. 2000. Crystal structure of a NifS-like protein from *Thermotoga maritima*: implications for iron sulphur cluster assembly. J.Mol.Biol. **297**:451-464.

31. **Loiseau, L., S. Ollagnier-de-Choudens, L. Nachin, M. Fontecave, and F. Barras**. 2003. Biogenesis of Fe-S cluster by the bacterial Suf system : SufS and SufE form a new type of cysteine desulfurase. J.Biol.Chem. **278**:38352-38359.

32. **Outten, F. W., M. J. Wood, F. M. Munoz, and G. Storz**. 2003. The SufE protein and the SufBCD complex enhance SufS cysteine desulfurase activity as part of a sulfur transfer pathway for Fe-S cluster assembly in *E. coli*. J.Biol.Chem. **278**:45713-45719.

33. **Cooper, A. J.** 1983. Biochemistry of sulfur-containing amino acids. Annu.Rev.Biochem **52:187-222**:187-222.

34. **Bordo, D. and P. Bork**. 2002. The rhodanese/Cdc25 phosphatase superfamily: Sequence-structure-function relations. EMBO Rep. **3**:741-746.

35. **Bordo, D., D. Deriu, R. Colnaghi, A. Carpen, S. Pagani, and M. Bolognesi**. 2000. The crystal structure of a sulfurtransferase from *Azotobacter vinelandii* highlights the evolutionary relationship between the rhodanese and phosphatase enzyme families. J.Mol.Biol. **298**:691-704.

36. **Vennesland, B., P. A. Castric, E. E. Conn, L. P. Solomonson, M. Volini, and J. Westley**. 1982. Cyanide metabolism. Fed.Proc. **41**:2639-2648.

37. **Fauman, E. B., J. P. Cogswell, B. Lovejoy, W. J. Rocque, W. Holmes, V. G. Montana, H. Piwnica-Worms, M. J. Rink, and M. A. Saper**. 1998. Crystal structure of the catalytic domain of the human cell cycle control phosphatase, Cdc25A. Cell **93**:617-625.

38. **Bordo, D., F. Forlani, A. Spallarossa, R. Colnaghi, A. Carpen, M. Bolognesi, and S. Pagani**. 2001. A persulfurated cysteine promotes active site reactivity in *Azotobacter vinelandii* rhodanese. Biol.Chem. **382**:1245-1252.

39. **Spallarossa, A., J. L. Donahue, T. J. Larson, M. Bolognesi, and D. Bordo**. 2001. *Escherichia coli* GlpE is a prototype for single-domain sulfurtransferase (rhodanese) homology superfamily. Structure **9**:1117-1125.

40. **Westley, J.** 1981. Thiosulfate: cyanide sulfurtransferase (rhodanese). Methods Enzymol. **77**:285-291.

41. **Westley, J., H. Adler, L. Westley, and C. Nishida**. 1983. The sulfurtransferases. Fundam.Appl.Toxicol. **3**:377-382.

42. **Ploegman, J. H., G. Drent, K. H. Kalk, and W. G. Hol**. 1979. The structure of bovine liver rhodanese. II. The active site in the sulfur-substituted and the sulfur-free enzyme. J.Mol.Biol. **127**:149-162.

43. **Ploegman, J. H., G. Drent, K. H. Kalk, and W. G. Hol**. 1978. Structure of bovine liver rhodanese. I. Structure determination at 2.5 Å resolution and a comparison of the conformation and sequence of its two domains. J.Mol.Biol. **123**:557-594.

44. **Gliubich, F., M. Gazerro, G. Zanotti, S. Delbono, G. Bombieri, and R. Berni**. 1996. Active site structural features for chemically modified forms of rhodanese. J.Biol.Chem. **271**:21054-21061.

45. **Horowitz, P. M. and S. Bowman**. 1989. Oxidative inactivation of rhodanese by hydrogen peroxide produces states that show differential reactivation. J.Biol.Chem. **264**:3311-3316.

46. **Pagani, S., G. Sessa, F. Sessa, and R. Colnaghi**. 1993. Properties of *Azotobacter vinelandii* rhodanese. Biochem Mol.Biol.Int. **29**:595-604.

47. **Lijk, L. J., C. A. Torfs, K. H. Kalk, De Maeyer M.C., and W. G. Hol**. 1984. Differences in the binding of sulfate, selenate and thiosulfate ions to bovine liver rhodanese, and a description of a binding site for ammonium and sodium ions. An X-ray diffraction study. Eur.J.Biochem **142**:399-408.

48. **Adams, H., W. Teertstra, M. Koster, and J. Tommassen**. 2002. PspE (phage-shock protein E) of *Escherichia coli* is a rhodanese. FEBS Lett. **518**:173-176.

49. **Wolfe, M. D., F. Ahmed, G. M. Lacourciere, T. C. Stadtman, C. T. Lauhon, and T. J. Larson**. 2004. Functional diversity of the rhodanese homology domain: *Escherichia coli* YbbB is a selenophosphate-dependent tRNA 2-selenouridine synthase. J.Biol.Chem. **279**:1801-1809.

50. **Palenchar, P. M., C. J. Buck, H. Cheng, T. J. Larson, and E. G. Mueller**. 2000. Evidence that ThiI, an enzyme shared between thiamin and 4-thiouridine biosynthesis, may be a sulfurtransferase that proceeds through a persulfide intermediate. J.Biol.Chem. **275**:8283-8286.

51. **Matthies, A., K. V. Rajagopalan, R. R. Mendel, and S. Leimkuhler**. 2004. Evidence for the physiological role of a rhodanese-like protein for the biosynthesis of the molybdenum cofactor in humans. Proc.Natl.Acad.Sci.U.S.A **101**:5946-5951.

52. **Spallarossa, A., A. Carpen, F. Forlani, S. Pagani, M. Bolognesi, and D. Bordo**. 2003. SseA, a 3-mercaptopyruvate sulfurtransferase from *Escherichia coli*: crystallization and preliminary crystallographic data. Acta Crystallogr.D.Biol.Crystallogr. **59**:168-170.

53. **Spallarossa, A., F. Forlani, A. Carpen, A. Armirotti, S. Pagani, M. Bolognesi, and D. Bordo**. 2004. The "rhodanese" fold and catalytic mechanism of 3-mercaptopyruvate sulfurtransferases: crystal structure of SseA from *Escherichia coli*. J.Mol.Biol. **335**:583-593.

54. **Nagahara, N., T. Okazaki, and T. Nishino**. 1995. Cytosolic mercaptopyruvate sulfurtransferase is evolutionarily related to mitochondrial rhodanese. Striking similarity in active site amino acid sequence and the increase in the mercaptopyruvate sulfurtransferase activity of rhodanese by site-directed mutagenesis. J.Biol.Chem. **270**:16230-16235.

55. **Papenbrock, J. and A. Schmidt**. 2000. Characterization of two sulfurtransferase isozymes from *Arabidopsis thaliana*. Eur.J.Biochem **267**:5571-5579.

56. **Colnaghi, R., G. Cassinelli, M. Drummond, F. Forlani, and S. Pagani**. 2001. Properties of the *Escherichia coli* rhodanese-like protein SseA: contribution of the active-site residue Ser240 to sulfur donor recognition. FEBS Lett. **500**:153-156.

57. **Alphey, M. S., R. A. M. Williams, J. C. Mottram, G. H. Coombs, and W. N. Hunter**. 2003. The crystal structure of *Leishmania major* 3-mercaptopyruvate sulfurtransferase; a three-domain architecture with a serine protease-like triad at the active site. J.Biol.Chem. **278**:48219-48227.

58. **Williams, R. A. M., S. M. Kelly, J. C. Mottram, and G. H. Coombs**. 2003. 3-Mercaptopyruvate sulfurtransferase of *Leishmania* contains an unusual C-terminal extension and is involved in thioredoxin and antioxidant metabolism. J.Biol.Chem. **278**:1480-1486.

59. **Nagahara, N., T. Ito, and M. Minami**. 1999. Mercaptopyruvate sulfurtransferase as a defense against cyanide toxication: molecular properties and mode of detoxification. Histol.Histopathol. **14**:1277-1286.

60. **Nagahara, N. and T. Nishino**. 1996. Role of amino acid residues in the active site of rat liver mercaptopyruvate sulfurtransferase. cDNA cloning, overexpression, and site-directed mutagenesis. J.Biol.Chem. **271**:27395-27401.

61. **Kiley, P. J. and H. Beinert**. 2003. The role of Fe-S proteins in sensing and regulation in bacteria. Curr.Opin.Microbiol. **6**:181-185.

62. **Takahashi, Y. and U. Tokumoto**. 2002. A third bacterial system for the assembly of iron-sulfur clusters with homologs in archaea and plastids. J.Biol.Chem. **277**:28380-28383.

63. **Yuvaniyama, P., J. N. Agar, V. L. Cash, M. K. Johnson, and D. R. Dean**. 2000. NifS-directed assembly of a transient [2Fe-2S] cluster within the NifU protein. Proc.Natl.Acad.Sci.U.S.A **97**:599-604.

64. **Agar, J. N., P. Yuvaniyama, R. F. Jack, V. L. Cash, A. D. Smith, D. R. Dean, and M. K. Johnson**. 2000. Modular organization and identification of a mononuclear iron-binding site within the NifU protein. J.Biol.Inorg.Chem. **5**:167-177.

65. **Dos Santos, P. C., A. D. Smith, J. Frazzon, V. L. Cash, M. K. Johnson, and D. R. Dean**. 2004. Iron-sulfur cluster assembly: NifU-directed activation of the nitrogenase Fe protein. J.Biol.Chem. **279**:19705-19711.

66. **Tong, W. H., G. N. L. Jameson, B. H. Huynh, and T. A. Rouault**. 2003. Subcellular compartmentalization of human Nfu, an iron-sulfur cluster scaffold protein, and its ability to assemble a [4Fe-4S] cluster. Proc.Natl.Acad.Sci.USA **100**:9762-9767.

67. **Nishio, K. and M. Nakai**. 2000. Transfer of Iron-Sulfur Cluster from NifU to Apoferredoxin. J.Biol.Chem. **275**:22615-22618.

68. **Takahashi, Y. and M. Nakamura**. 1999. Functional assignment of the *ORF2-iscS-iscU-iscA-hscB-hscA-fdx-ORF3* gene cluster involved in the assembly of Fe-S clusters in *Escherichia coli*. J.Biochem.(Tokyo) **126**:917-926.

69. **Schwartz, C. J., O. Djaman, J. A. Imlay, and P. J. Kiley**. 2000. The cysteine desulfurase, IscS, has a major role in in vivo Fe-S cluster formation in *Escherichia coli*. Proc.Natl.Acad.Sci.U.S.A **97**:9009-9014.

70. **Tokumoto, U. and Y. Takahashi**. 2001. Genetic analysis of the *isc* operon in *Escherichia coli* involved in the biogenesis of cellular iron-sulfur proteins. J.Biochem.(Tokyo) **130**:63-71.

71. **Urbina, H. D., J. J. Silberg, K. G. Hoff, and L. E. Vickery**. 2001. Transfer of Sulfur from IscS to IscU during Fe/S cluster assembly. J.Biol.Chem. **276**:44521-44526.

72. **Ollagnier-de-Choudens, S., T. Mattioli, Y. Takahashi, and M. Fontecave**. 2001. Iron-sulfur cluster assembly. Characterization of IscA and evidence for a specific and functional complex with ferredoxin. J.Biol.Chem. **276**:22604-22607.

73. **Ding, H., R. J. Clark, and B. Ding**. 2004. IscA mediates iron delivery for assembly of iron-sulfur clusters in IscU under the limited accessible free iron conditions. J.Biol.Chem. **279**:ahead of print.

74. **Hoff, K. G., D. T. Ta, T. L. Tapley, J. J. Silberg, and L. E. Vickery**. 2002. Hsc66 substrate specificity is directed toward a discrete region of the iron-sulfur cluster template protein IscU. J.Biol.Chem. **277**:27353-27359.

75. **Hoff, K. G., J. J. Silberg, and L. E. Vickery**. 2000. Interaction of the iron-sulfur cluster assembly protein IscU with the Hsc66/Hsc20 molecular chaperone system of *Escherichia coli*. Proc.Natl.Acad.Sci.U.S.A **97**:7790-7795.

76. **Silberg, J. J., K. G. Hoff, T. L. Tapley, and L. E. Vickery**. 2001. The Fe/S assembly protein IscU behaves as a substrate for the molecular chaperone Hsc66 from *Escherichia coli*. J.Biol.Chem. **276**:1696-1700.

77. **Schwartz, C. J., J. L. Giel, T. Patschkowski, C. Luther, F. J. Ruzicka, H. Beinert, and P. J. Kiley**. 2001. IscR, an Fe-S cluster-containing transcription factor, represses expression of *Escherichia coli* genes encoding Fe-S cluster assembly proteins. Proc.Natl.Acad.Sci.USA 14895-14900.

78. **Pilon-Smits, E. A. H., G. F. Garifullina, S. Abdel-Ghany, S. I. Kato, H. Mihara, K. L. Hale, J. L. Burkhead, N. Esaki, T. Kurihara, and M. Pilon**. 2002. Characterization of a NifS-Like chloroplast protein from *Arabidopsis*. Implications for its role in sulfur and selenium metabolism. Plant Physiol. **130**:1309-1318.

79. **Leon, S., B. Touraine, J. F. Briat, and S. Lobreaux**. 2002. The AtNFS2 gene from *Arabidopsis thaliana* encodes a NifS-like plastildial cysteine desulphurase. Biochemical Journal **366**:557-564.

80. **Xu, X. M. and S. G. Moller**. 2004. AtNAP7 is a plastidic SufC-like ATP-binding cassette/ATPase essential for *Arabidopsis* embryogenesis. Proc.Natl.Acad.Sci.U.S.A **101**:9143-9148.

81. **Zheng, M., X. Wang, L. J. Templeton, D. R. Smulski, R. A. LaRossa, and G. Storz**. 2001. DNA microarray-mediated transcriptional profiling of the *Escherichia coli* response to hydrogen peroxide. J.Bacteriol. **183**:4562-4570.

82. **Patzer, S. I. and K. Hantke**. 1999. SufS is a NifS-like protein, and SufD is necessary for stability of the [2Fe-2S] FhuF protein in *Escherichia coli*. J.Bacteriol. **181**:3307-3309.

83. **Outten, F. W., O. Djaman, and G. Storz**. 2004. A *suf* operon requirement for Fe-S cluster assembly during iron starvation in *Escherichia coli*. Mol.Microbiol. **52**:861-872.

84. **Ollagnier-de-Choudens, S., D. Lascoux, L. Loiseau, F. Barras, E. Forest, and M. Fontecave**. 2003. Mechanistic studies of the SufS-SufE cysteine desulfurase: evidence for sulfur transfer from SufS to SufE. FEBS Lett. **555**:263-267.

85. **Kambampati, R. and C. T. Lauhon**. 2000. Evidence for the transfer of sulfane sulfur from IscS to ThiI during the in vitro biosynthesis of 4-thiouridine in *Escherichia coli* tRNA. J.Biol.Chem. **275**:10727-10730.

86. **Eitenmiller, R. R. and W. O. Landen, Jr.** 1999. Vitamin Analysis for the Health and Food Sciences. CRC Press, Boca Raton, Florida.

87. **Begley, T. P., D. M. Downs, S. E. Ealick, F. W. McLafferty, L. A. Van, S. Taylor, N. Campobasso, H. J. Chiu, C. Kinsland, J. J. Reddick, and J. Xi**. 1999. Thiamin biosynthesis in prokaryotes. Arch.Microbiol. **171**:293-300.

88. **Taylor, S. V., N. L. Kelleher, C. Kinsland, H. J. Chiu, C. A. Costello, A. D. Backstrom, F. W. McLafferty, and T. P. Begley**. 1998. Thiamin biosynthesis in *Escherichia coli*. Identification of ThiS thiocarboxylate as the immediate sulfur donor in the thiazole formation. J.Biol.Chem. **273**:16555-16560.

89. **Leonardi, R. and P. L. Roach**. 2004. Thiamine biosynthesis in *Escherichia coli*: in vitro reconstitution of the thiazole synthase activity. J.Biol.Chem. **279**:17054-17062.

90. **Park, J. H., P. C. Dorrestein, H. Zhai, C. Kinsland, F. W. McLafferty, and T. P. Begley**. 2003. Biosynthesis of the thiazole moiety of thiamin pyrophosphate (vitamin B1). Biochemistry **42**:12430-12438.

91. **Wuebbens, M. M. and K. V. Rajagopalan**. 2003. Mechanistic and mutational studies of *Escherichia coli* molybdopterin synthase clarify the final step of molybdopterin biosynthesis. J.Biol.Chem. **278**:14523-14532.

92. **Guse, A., C. E. Stevenson, J. Kuper, G. Buchanan, G. Schwarz, G. Giordano, A. Magalon, R. R. Mendel, D. M. Lawson, and T. Palmer**. 2003. Biochemical and structural analysis of the molybdenum cofactor biosynthesis protein MobA. J.Biol.Chem. **278**:25302-25307.

93. **Reiss, J., C. Dorche, B. Stallmeyer, R. R. Mendel, N. Cohen, and M. T. Zabot**. 1999. Human molybdopterin synthase gene: genomic structure and mutations in molybdenum cofactor deficiency type B. Am.J.Hum.Genet. **64**:706-711.

94. **Mendel, R. R. and G. Schwarz**. 2002. Biosynthesis and molecular biology of the molybdenum cofactor (Moco). Met.Ions Biol.Syst. **39**:317-368.

95. **Leimkuhler, S. and K. V. Rajagopalan**. 2001. A sulfurtransferase is required in the transfer of cysteine sulfur in the in vitro synthesis of molybdopterin from precursor Z in *Escherichia coli*. J.Biol.Chem. **276**:22024-22031.

96. **Leimkuhler, S., A. Freuer, J. A. S. Araujo, K. V. Rajagopalan, and R. R. Mendel**. 2003. Mechanistic studies of human molybdopterin synthase reaction and characterization of mutants identified in group B patients of molybdenum cofactor deficiency. J.Biol.Chem. **278**:26127-26134.

97. **Cortese, M. S., A. B. Caplan, and R. L. Crawford**. 2002. Structural, functional, and evolutionary analysis of *moeZ*, a gene encoding an enzyme required for the synthesis of the *Pseudomonas* metabolite, pyridine-2,6-bis(thiocarboxylic acid). BMC.Evol.Biol. **2**:8.

98. **Bjork, G. R.** 1995. Genetic dissection of synthesis and function of modified nucleosides in bacterial transfer RNA. Prog.Nucleic Acid Res.Mol.Biol. **50**:263-338.

99. **Wright, C. M., P. M. Palenchar, and E. G. Mueller**. 2002. A paradigm for biological sulfur transfers via persulfide groups: a persulfide-disulfide-thiol cycle in 4-thiouridine biosynthesis. Chem.Comm. **2002**:2708-2709.

100. **Nilsson, K., H. K. Lundgren, T. G. Hagervall, and G. R. Bjork**. 2002. The cysteine desulfurase IscS is required for synthesis of all five thiolated nucleosides present in tRNA from *Salmonella enterica* serovar Typhimurium. J.Bacteriol. **184**:6830-6835.

101. **Mueller, E. G., P. M. Palenchar, and C. J. Buck**. 2001. The role of the cysteine residues of ThiI in the generation of 4-thiouridine in tRNA. J.Biol.Chem. **276**:33588-33595.

102. **Lauhon, C. T., W. M. Erwin, and G. N. Ton**. 2004. Substrate specificity for 4-thiouridine modification in *Escherichia coli*. J.Biol.Chem. **279**:23022-23029.

103. **Vold, B. S., M. E. Longmire, and D. E. Keith, Jr.** 1981. Thiolation and 2-methylthio- modification of *Bacillus subtilis* transfer ribonucleic acids. J.Bacteriol. **148**:869-876.

104. **Dakshinamurti, K., C. Lorraire, and R. P. Bhullar**. 1985. Requirements for biotin and the function of biotin in cells in culture, p. 38-55. *In* K. Dakshinamurti and H. N. Bhagavan (eds.), Annals of the New York Academy of Sciences: Biotin. New York Academy of Sciences, New York.

105. **Whitehead, C. C.** 1985. Assessment of biotin deficiency in animals, p. 86-96. *In* K. Dakshinamurti and H. N. Bhagavan (eds.), Annals of the New York Academy of Sciences: Biotin. New York Academy of Sciences, New York.

106. **Nyhan, W. L.** 1985. Clinical problems related to biotin, p. 222-224. *In* K. Dakshinamurti and H. N. Bhagavan (eds.), Annals of the New York Academy of Sciences: Biotin. New York Academy of Sciences, New York.

107. **Berkovitch, F., Y. Nicolet, J. T. Wan, J. T. Jarrett, and C. L. Drennan**. 2004. Crystal structure of biotin synthase, an *S*-adenosylmethionine-dependent radical enzyme. Science **303**:76-79.

108. **Tse Sum, B. B., R. Benda, V. Schunemann, D. Florentin, A. X. Trautwein, and A. Marquet**. 2003. Fate of the (2Fe-2S)(2+) cluster of *Escherichia coli* biotin synthase during reaction: a Mossbauer characterization. Biochemistry **42**:8791-8798.

109. **Cosper, M. M., G. N. Jameson, H. L. Hernandez, C. Krebs, B. H. Huynh, and M. K. Johnson**. 2004. Characterization of the cofactor composition of *Escherichia coli* biotin synthase. Biochemistry **43**:2007-2021.

110. **Ugulava, N. B., K. K. Frederick, and J. T. Jarrett**. 2003. Control of adenosylmethionine-dependent radical generation in biotin synthase: a kinetic and thermodynamic analysis of substrate binding to active and inactive forms of BioB. Biochemistry **42**:2708-2719.

111. **Ollagnier-de-Choudens, S., E. Mulliez, and M. Fontecave**. 2002. The PLP-dependent biotin synthase from *Escherichia coli*: mechanistic studies. FEBS Lett. **532**:465-468.

112. **Ugulava, N. B., C. J. Sacanell, and J. T. Jarrett**. 2001. Spectroscopic changes during a single turnover of biotin synthase: destruction of a [2Fe-2S] cluster accompanies sulfur insertion. Biochemistry **40**:8352-8358.

113. **Ollagnier-de-Choudens, S., E. Mulliez, K. S. Hewitson, and M. Fontecave**. 2002. Biotin synthase is a pyridoxal phosphate-dependent cysteine desulfurase. Biochemistry **41**:9145-9152.

114. **Jameson, G. N., M. M. Cosper, H. L. Hernandez, M. K. Johnson, and B. H. Huynh**. 2004. Role of the [2Fe-2S] cluster in recombinant *Escherichia coli* biotin synthase. Biochemistry **43**:2022-2031.

115. **Kiyasu, T., A. Asakura, Y. Nagahashi, and T. Hoshino**. 2002. Biotin synthase of *Bacillus subtilis* shows less reactivity than that of *Escherichia coli* in in vitro reaction systems. Arch.Microbiol. **179**:26-32.

116. **Picciocchi, A., R. Douce, and C. Alban**. 2003. The plant biotin synthase reaction. Identification and characterization of essential mitochondrial accessory protein components. J.Biol.Chem. **278**:24966-24975.

117. **Marquet, A., B. T. Bui, and D. Florentin**. 2001. Biosynthesis of biotin and lipoic acid. Vitam.Horm. **61**:51-101.

118. **Booker, S. J.** 2004. Unraveling the pathway of lipoic acid biosynthesis. Chem.Biol. **11**:10-12.

119. **Cicchillo, R. M., D. F. Iwig, A. D. Jones, N. M. Nesbitt, C. Baleanu-Gogonea, M. G. Souder, L. Tu, and S. J. Booker**. 2004. Lipoyl synthase requires two equivalents of S-adenosyl-L-methionine to synthesize one equivalent of lipoic acid. Biochemistry **43**:6378-6386.

120. **Smith, A. R., S. V. Shenvi, M. Widlansky, J. H. Suh, and T. M. Hagen**. 2004. Lipoic acid as a potential therapy for chronic diseases associated with oxidative stress. Curr.Med.Chem. **11**:1135-1146.

121. **Zhao, X., J. R. Miller, Y. Jiang, M. A. Marletta, and J. E. Cronan**. 2003. Assembly of the covalent linkage between lipoic acid and its cognate enzymes. Chem.Biol. **10**:1293-1302.

122. **Mueller, E. G. and P. M. Palenchar**. 1999. Using genomic information to investigate the function of ThiI, an enzyme shared between thiamin and 4-thiouridine biosynthesis. Protein Sci. **8**:2424-2427.

123. **Aravind, L. and E. V. Koonin**. 2001. THUMP - a predicted RNA-binding domain shared by 4-thiouridine, pseudouridine synthetases and RNA methylases. Trends Biochem.Sci. **26**:215-217.

124. **Appleyard, M. V., J. Sloan, Kana, I. S. Heck, J. R. Kinghorn, and S. E. Unkles**. 1998. The *Aspergillus nidulans cnxF* gene and its involvement in molybdopterin biosynthesis. Molecular characterization and analysis of in vivo generated mutants. J.Biol.Chem. **273**:14869-14876.

125. **Lewis, T. A., M. S. Cortese, J. L. Sebat, T. L. Green, C. H. Lee, and R. L. Crawford**. 2000. A *Pseudomonas stutzeri* gene cluster encoding the biosynthesis of the CCl4-dechlorination agent pyridine-2,6-bis(thiocarboxylic acid). Environ.Microbiol. **2**:407-416.

126. **Katoh, E., T. Hatta, H. Shindo, Y. Ishii, H. Yamada, T. Mizuno, and T. Yamazaki**. 2000. High precision NMR structure of YhhP, a novel *Escherichia coli* protein implicated in cell division. J.Mol.Biol. **304**:219-229.

127. **Yee, A., X. Chang, A. Pineda-Lucena, B. Wu, A. Semesi, B. Le, T. Ramelot, G. M. Lee, S. Bhattacharyya, P. Gutierrez, A. Denisov, C. H. Lee, J. R. Cort, G. Kozlov, J. Liao, G. Finak, L. Chen, D. Wishart, W. Lee, L. P. McIntosh, K. Gehring, M. A. Kennedy, A. M. Edwards, and C. H. Arrowsmith**. 2002. An NMR approach to structural proteomics. Proc.Natl.Acad.Sci.USA **99**:1825-1830.

128. **Ishii, Y., H. Yamada, T. Yamashino, K. Ohashi, E. Katoh, H. Shindo, T. Yamazaki, and T. Mizuno**. 2000. Deletion of the *yhhP* gene results in filamentous cell morphology in *Escherichia coli*. Biosci.Biotechnol.Biochem **64**:799-807.

129. **Garcia, C., P. L. Fortier, S. Blanquet, J. Y. Lallemand, and F. Dardel**. 1995. Solution structure of the ribosome-binding domain of *E. coli* translation initiation factor IF3. Homology with the U1A protein of the eukaryotic spliceosome. J.Mol.Biol. **254**:247-259.

130. **Liss, L. R.** 1987. New M13 host, DH5αF' competent cells. Focus **3**:13-14.

131. **Lutz, R. and H. Bujard**. 1997. Independent and tight regulation of transcriptional units in *Escherichia coli* via the LacR/O, the TetR/O and AraC/I_1-I_2 regulatory elements. Nucleic Acids Res. **25**:1203-1210.

132. **Studier, F. W. and B. A. Moffatt**. 1986. Use of bacteriophage T7 RNA polymerase to direct selective high-level expression of cloned genes. J.Mol.Biol. **189**:113-130.

133. **Popham, D. L. and P. Setlow**. 1996. Phenotypes of *Bacillus subtilis* mutants lacking multiple class A high-molecular-weight penicillin-binding proteins. J.Bacteriol. **178**:2079-2085.

134. **Tabor, S. and C. C. Richardson**. 1985. A bacteriophage T7 RNA polymerase/promoter system for controlled exclusive expression of specific genes. Proc.Natl.Acad.Sci.U.S.A. **82**:1074-1078.

135. **Guerout-Fleury, A. M., K. Shazand, N. Frandsen, and P. Stragier**. 1995. Antibiotic-resistance cassettes for *Bacillus subtilis*. Gene **167**:335-336.

136. **Sambrook, J., E. F. Fritsch, and T. Maniatis**. 1989. Molecular Cloning. A Laboratory Manual, p. A1-A2. Cold Spring Harbor Laboratory, Cold Spring Harbor, NY.

137. **Leighton, T. J. and R. H. Doi**. 1971. The stability of messenger ribonucleic acid during sporulation in *Bacillus subtilis*. J.Biol.Chem. **246**:3189-3195.

138. **Spizizen, J**. Transformation of biochemical strains of *Bacillus subtilis* by deoxyribonucleate. Proc.Natl.Acad.Sci.USA 44, 1072-1078. 1958.

139. **Young, F. E. and J. Spizizen**. 1961. Physiological and genetic factors affecting transformation of *Bacillus subtilis*. J.Bacteriol. **81**:823-829.

140. **Young, F. E. and J. Spizizen**. 1963. Incorporation of deoxyribonucleic acid in the *Bacillus subtilis* transformation system. J.Bacteriol. **86**:392-400.

141. **Bradford, M. M.** 1976. A rapid and sensitive method for the quantitation of microgram quantities of protein utilizing the principle of protein-dye binding. Anal.Biochem. **72**:248-254.

142. **Laemmli, U.** 1970. Cleavage of structural proteins during the assembly of the head of bacteriophage T4. Nature **227**:680-685.

143. **Bhattacharjee, H. and B. P. Rosen**. 1996. Spatial proximity of Cys113, Cys172, and Cys422 in the metalloactivation domain of the ArsA ATPase. J.Biol.Chem. **271**:24465-24470.

144. **Wong, M. D., Y. F. Lin, and B. P. Rosen**. 2002. The soft metal ion binding sites in the *Staphylococcus aureus* pI258 CadC Cd(II)/Pb(II)/Zn(II)-responsive repressor are formed between subunits of the homodimer. J.Biol.Chem. **277**:40930-40936.

145. **Miller, S., M. D. Edwards, C. Ozdemir, and I. R. Booth**. 2003. The closed structure of the MscS mechanosensitive channel: Cross-linking of single cysteine mutants. J.Biol.Chem. **278**:32246-32250.

146. **Samanta, S., T. Ayvaz, M. Reyes, H. A. Shuman, J. Chen, and A. L. Davidson**. 2003. Disulfide cross-linking reveals a site of stable interaction between C-terminal regulatory domains of the two MalK subunits in the maltose transport complex. J.Biol.Chem. **278**:35265-35271.

147. **Higgins, D. G., J. D. Thompson, and T. J. Gibson**. 1996. Using CLUSTAL for multiple sequence alignments. Methods Enzymol. **266**:383-402.

148. **Smith, R. F., B. A. Wiese, M. K. Wojzynski, D. B. Davison, and K. C. Worley**. 1996. BCM Search Launcher--an integrated interface to molecular biology data base search and analysis services available on the World Wide Web. Genome Res. **6**:454-462.

149. **Sali, A. and T. L. Blundell**. 1993. Comparative protein modelling by satisfaction of spatial restraints. J.Mol.Biol. **234**:779-815.

150. **Marti-Renom, M. A., A. C. Stuart, A. Fiser, R. Sanchez, F. Melo, and A. Sali**. 2000. Comparative protein structure modeling of genes and genomes. Annu.Rev.Biophys.Biomol.Struct. **29**:291-325.

151. **Weiner, S. J., P. A. Kollman, D. T. Nguyen, and D. A. Case**. 1986. An all atom force-field for simulations of proteins and nucleic-acids. J.Comput.Chem. **7**:230-252.

152. **Ponder, J. W. and D. A. Case**. 2003. Force fields for protein simulations. Adv.Protein Chem. **66**:27-85.

153. **Humphrey, W., A. Dalke, and K. Schulten**. 1996. VMD: visual molecular dynamics. J.Mol.Graph. **14**:33-38.

154. **Kunst, F., N. Ogasawara, I. Moszer, A. M. Albertini, G. Alloni, V. Azevedo, M. G. Bertero, P. Bessieres, A. Bolotin, S. Borchert, R. Borriss, L. Boursier, A. Brans, M. Braun, S. C. Brignell, S. Bron, S. Brouillet, C. V. Bruschi, B. Caldwell, V. Capuano, N. M. Carter, S. K. Choi, J. J. Codani, I. F. Connerton, and A. Danchin**. 1997. The complete genome sequence of the gram-positive bacterium *Bacillus subtilis*. Nature **390**:249-256.

155. **Cheng, H.** 2003. **M.S. Thesis**. **Virginia Polytechnic Institute and State University**. Characterization of PspE, a secreted sulfurtransferase of *Escherichia coli*.

156. **Cereda, A., F. Forlani, S. Iametti, R. Bernhardt, P. Ferranti, G. Picariello, S. Pagani, and F. Bonomi**. 2003. Molecular recognition between *Azotobacter vinelandii* rhodanese and a sulfur acceptor protein. Biol.Chem. **384**:1473-1481.

157. **Westley, J. and D. Heyse**. 1971. Mechanisms of sulfur transfer catalysis. Sulfhydryl-catalyzed transfer of thiosulfonate sulfur. J.Biol.Chem. **246**:1468-1474.

158. **Wang, S. F. and M. Volini**. 1973. The interdependence of substrate and protein transformations in rhodanese catalysis. I. Enzyme interactions with substrate, product, and inhibitor anions. J.Biol.Chem. **248**:7376-7385.

159. **Alexander, K. and M. Volini**. 1987. Properties of an *Escherichia coli* rhodanese. J.Biol.Chem. **262**:6595-6604.

160. **Bordo, D., T. J. Larson, J. L. Donahue, A. Spallarossa, and M. Bolognesi**. 2000. Crystals of GlpE, a 12 kDa sulfurtransferase from *Escherichia coli*, display 1.06 Å resolution diffraction: a preliminary report. Acta Crystallogr.D.Biol.Crystallogr. **56**:1691-1693.

161. **Glaser, P., A. Danchin, F. Kunst, P. Zuber, and M. M. Nakano**. 1995. Identification and isolation of a gene required for nitrate assimilation and anaerobic growth of Bacillus subtilis. J.Bacteriol. **177**:1112-1115.

162. **Nakano, M. M. and P. Zuber**. 1998. Anaerobic growth of a "strict aerobe" (*Bacillus subtilis*). Annu.Rev.Microbiol. **52**:165-190.

163. **Clemedson, C. J., H. I. Hultman, and B. Sörbo**. 1955. A combination of rhodanese and ethanethiosulfonate as an antidote in experimental cyanide poisoning. Acta Physiol Scand. **35**:31-35.

164. **Pagani, S., F. Bonomi, and P. Cerletti**. 1984. Enzymic synthesis of the iron-sulfur cluster of spinach ferredoxin. Eur.J.Biochem **142**:361-366.

165. **Ogata, K. and M. Volini**. 1990. Mitochondrial rhodanese: membrane-bound and complexed activity. J.Biol.Chem. **265**:8087-8093.

166. **Pagani, S. and Y. M. Galante**. 1983. Interaction of rhodanese with mitochondrial NADH dehydrogenase. Biochim.Biophys.Acta **742**:278-284.

167. **Nishino, T., C. Usami, and K. Tsushima**. 1983. Reversible interconversion between sulfo and desulfo xanthine oxidase in a system containing rhodanese, thiosulfate, and sulfhydryl reagent. Proc.Natl.Acad.Sci.U.S.A. **80**:1826-1829.

168. **Yang, S. H., T. Berberich, A. Miyazaki, H. Sano, and T. Kusano**. 2003. Ntdin, a tobacco senescence-associated gene, is involved in molybdenum cofactor biosynthesis. Plant Cell Physiol. **44**:1037-1044.

169. **Tatusov, R. L., D. A. Natale, I. V. Garkavtsev, T. A. Tatusova, U. T. Shankavaram, B. S. Rao, B. Kiryutin, M. Y. Galperin, N. D. Fedorova, and E. V. Koonin**. 2001. The COG database: new developments in phylogenetic classification of proteins from complete genomes. Nucleic Acids Res. **29**:22-28.

170. **Liepinsh, E., A. Leonchiks, A. Sharipo, L. Guignard, and G. Otting**. 2003. Solution structure of the R3H domain from human Smubp-2. J.Mol.Biol. **326**:217-223.

171. **Petersohn, A., M. Brigulla, S. Haas, J. D. Hoheisel, U. Volker, and M. Hecker**. 2001. Global analysis of the general stress response of *Bacillus subtilis*. J.Bacteriol. **183**:5617-5631.

172. **Mostertz, J., C. Scharf, M. Hecker, and G. Homuth**. 2004. Transcriptome and proteome analysis of *Bacillus subtilis* gene expression in response to superoxide and peroxide stress. Microbiology **150**:497-512.

173. **Leichert, L. I. O., C. Scharf, and M. Hecker**. 2003. Global characterization of disulfide stress in *Bacillus subtilis*. J.Bacteriol. **185** :1967-1975.

174. **Yamanishi, T. and S. Tuboi**. 1981. The mechanism of the L-cystine cleavage reaction catalyzed by rat liver γ-cystathionase. J.Biochem.(Tokyo) **89**:1913-1921.

175. **Fasano, M., M. Orsale, S. Melino, E. Nicolai, F. Forlani, N. Rosato, D. Cicero, S. Pagani, and M. Paci**. 2003. Surface changes and role of buried water molecules during the sulfane sulfur transfer in rhodanese from *Azotobacter vinelandii*: a fluorescence quenching and nuclear magnetic relaxation dispersion spectroscopic study. Biochemistry **42**:8550-8557.

176. **Miller-Martini, D. M., S. Hua, and P. M. Horowitz**. 1994. Cysteine 254 can cooperate with active site cysteine 247 in reactivation of 5,5'-dithiobis(2-nitrobenzoic acid)-inactivated rhodanese as determined by site-directed mutagenesis. J.Biol.Chem. **269**:12414-12418.

177. **Scharf, C., S. Riethdorf, H. Ernst, S. Engelmann, U. Volker, and M. Hecker**. 1998. Thioredoxin is an essential protein induced by multiple stresses in *Bacillus subtilis*. J.Bacteriol. **180**:1869-1877.

VITAE

Jeremy Hunt

Engel Hall, Virginia Tech

Blacksburg 24061

(540)-231-3477

jehunt1@vt.edu

Education	**M. S. Biochemistry** 2003 - 2004 Virginia Polytechnic Institute and State University **B. S. Biochemistry** 2000 - 2003 Virginia Polytechnic Institute and State University
Publications	Hunt, Jeremy P., Donahue, J. L, Ray, W. K, and Larson, T. J. Genetic and Biochemical Characterization of YrkF, a Novel Two-Domain Sulfurtransferase in *Bacillus subtilis*. (manuscript under preparation)
Awards	William E. Newton Award – Distinguished Undergraduate Researcher in Biochemistry Dept. 2002 Sigma Xi, The Scientific Research Society – Undergraduate Research Award 2003 Pratt Nutrition Senior Research Scholarship – Virginia Tech, College of Agriculture and Life Sciences 2002 – 03 Cyrus H. McCormick Scholarship – Virginia Tech, Biochemistry 2002 – 03
Presentations	Virginia Academy of Science 80th meeting, Hampton, Virginia May 22 – 24, 2002. Poster presentation. American Society for Microbiology 103rd general meeting, Washington D.C., May 18 – 22, 2003. Poster presentation